

อนุพันธ์พอลิ(3,4-เอทิลีนไดออกซีไทโอฟีน) ลอกแบบโมเลกุลจากปฏิกิริยาพอลิเมอไรเซชัน
ในสถานะของแข็ง



นางสาวภัศราภรณ์ อังกรรัมย์

จุฬาลงกรณ์มหาวิทยาลัย

CHULALONGKORN UNIVERSITY

บทคัดย่อและแฟ้มข้อมูลฉบับเต็มของวิทยานิพนธ์ตั้งแต่ปีการศึกษา 2554 ที่ให้บริการในคลังปัญญาจุฬาฯ (CUIR)
เป็นแฟ้มข้อมูลของนิสิตเจ้าของวิทยานิพนธ์ ที่ส่งผ่านทางบัณฑิตวิทยาลัย

The abstract and full text of theses from the academic year 2011 in Chulalongkorn University Intellectual Repository (CUIR)
are the thesis authors' files submitted through the University Graduate School.

วิทยานิพนธ์นี้เป็นส่วนหนึ่งของการศึกษาตามหลักสูตรปริญญาวิทยาศาสตรมหาบัณฑิต

สาขาวิชาเคมี ภาควิชาเคมี

คณะวิทยาศาสตร์ จุฬาลงกรณ์มหาวิทยาลัย

ปีการศึกษา 2558

ลิขสิทธิ์ของจุฬาลงกรณ์มหาวิทยาลัย

MOLECULARLY IMPRINTED POLY(3,4-ETHYLENEDIOXYTHIOPHENE) DERIVATIVES
FROM SOLID STATE POLYMERIZATION

Miss Phatsaraporn Angkornram



A Thesis Submitted in Partial Fulfillment of the Requirements
for the Degree of Master of Science Program in Chemistry

Department of Chemistry

Faculty of Science

Chulalongkorn University

Academic Year 2015

Copyright of Chulalongkorn University

Thesis Title	MOLECULARLY IMPRINTED POLY(3,4-ETHYLENEDIOXYTHIOPHENE) DERIVATIVES FROM SOLID STATE POLYMERIZATION
By	Miss Phatsaraporn Angkornram
Field of Study	Chemistry
Thesis Advisor	Assistant Professor Yongsak Sritana-anant, Ph.D.

Accepted by the Faculty of Science, Chulalongkorn University in Partial Fulfillment of the Requirements for the Master's Degree

..... Dean of the Faculty of Science
(Associate Professor Polkit Sangvanich, Ph.D.)

THESIS COMMITTEE

..... Chairman
(Associate Professor Vudhichai Parasuk, Ph.D.)

..... Thesis Advisor
(Assistant Professor Yongsak Sritana-anant, Ph.D.)

..... Examiner
(Panuwat Padungros, Ph.D.)

..... External Examiner
(Associate Professor Siritron Samosorn, Ph.D.)

ภัสราภรณ์ อังกรรัมย์ : อนุพันธ์พอลิ(3,4-เอทิลีนไดออกซีไทโอเฟน) ลอกแบบโมเลกุลจากปฏิกิริยาพอลิเมอไรเซชันในสถานะของแข็ง (MOLECULARLY IMPRINTED POLY(3,4-ETHYLENEDIOXYTHIOPHENE) DERIVATIVES FROM SOLID STATE POLYMERIZATION) อ.ที่ปรึกษาวิทยานิพนธ์หลัก: ผศ. ดร.ยงศักดิ์ ศรีธนาอนันต์, 111 หน้า.

พอลิเมอร์ลอกแบบโมเลกุลของพอลิ(3,4-เอทิลีนไดออกซีไทโอเฟน) สังเคราะห์ได้จากมอนอเมอร์ 2,5-ไดโบรโม-3,4-เอทิลีนไดออกซีไทโอเฟน ด้วยปฏิกิริยาพอลิเมอไรเซชันในสถานะของแข็งที่มีโมเลกุลแม่แบบคือ พาราไนโตรฟินอล 2,4-ไดไนโตรฟินอล 2,4,6-ไตรไนโตรฟินอล หรือไพรีน จากการติดตามด้วยเทคนิคยูวี-วิสิเบิล สเปกโทรสโกปี พอลิเมอร์ลอกแบบโมเลกุลนี้สามารถจดจำโมเลกุลแม่แบบที่เติมกลับลงไปในกลุ่มของไนโตรฟินอลเหล่านี้ได้ทุกชนิดอย่างจำเพาะ เมื่อเปรียบเทียบกับพอลิเมอร์ที่ไม่ถูกลอกแบบ ในทางตรงกันข้าม พอลิเมอร์ลอกแบบโมเลกุลที่มีโมเลกุลแม่แบบคือไพรีน แสดงให้เห็นความแตกต่างในการยึดจับโมเลกุลแม่แบบที่ไม่มีขั้วนี้เพียงเล็กน้อย เมื่อเปรียบเทียบกับพอลิเมอร์ที่ไม่ถูกลอกแบบ

ในทำนองเดียวกัน โคพอลิเมอร์ลอกแบบโมเลกุลของพอลิ(3,4-เอทิลีนไดออกซีไทโอเฟน) และพอลิ(3,4-เอทิลีนไดออกซีไทโอเฟน เมทานอล) เตรียมได้โดยใช้โมเลกุลแม่แบบคือ พาราไนโตรฟินอล ซึ่งโคพอลิเมอร์ลอกแบบโมเลกุลที่มีสัดส่วนของพอลิ(3,4-เอทิลีนไดออกซีไทโอเฟน เมทานอล) มากขึ้น จะสามารถจดจำโมเลกุลพาราไนโตรฟินอลได้ดีขึ้น เมื่อเทียบกับพอลิเมอร์ที่ไม่ถูกลอกแบบ และพอลิเมอร์ลอกแบบโมเลกุลที่ไม่มีพอลิ(3,4-เอทิลีนไดออกซีไทโอเฟน เมทานอล) รวมอยู่ และมีความสามารถในการยึดจับพาราไนโตรฟินอลในเชิงปริมาณที่คำนวณได้มีผลที่ดีขึ้นเช่นเดียวกัน ผลการศึกษาเหล่านี้ชี้ให้เห็นว่า การมีหมู่ฟังก์ชันมีขั้วบนโครงสร้างของแต่ละหน่วยมอนอเมอร์ในพอลิเมอร์ลอกแบบโมเลกุล และบนโมเลกุลแม่แบบ เป็นส่วนสำคัญในการชักนำให้เกิดสมบัติการลอกแบบอย่างมีประสิทธิภาพ ความสำเร็จเหล่านี้นำไปสู่ความเป็นไปได้ในการพัฒนากลุ่มของพอลิเมอร์ลอกแบบโมเลกุลจากอนุพันธ์ของพอลิ(3,4-เอทิลีนไดออกซีไทโอเฟน) เพื่อใช้ในการตรวจวัดทางเคมีที่จำเพาะสำหรับสารบางชนิดได้

ภาควิชา เคมี

ลายมือชื่อนิสิต

สาขาวิชา เคมี

ลายมือชื่อ อ.ที่ปรึกษาหลัก

ปีการศึกษา 2558

5672048023 : MAJOR CHEMISTRY

KEYWORDS: MOLECULARLY IMPRINTED POLYMER / SOLID STATE POLYMERIZATION / PEDOT / 3,4-ETHYLENEDIOXYTHIOPHENE METHANOL (EDTM)

PHATSARAPORN ANGKORNRAM: MOLECULARLY IMPRINTED POLY(3,4-ETHYLENEDIOXYTHIOPHENE) DERIVATIVES FROM SOLID STATE POLYMERIZATION. ADVISOR: ASSIST. PROF. YONGSAK SRITANA-ANANT, Ph.D., 111 pp.

Molecularly imprinted polymers (MIPs) based on poly(3,4-ethylenedioxythiophene) (PEDOT) were prepared via solid state polymerization (SSP) of 2,5-dibromo-3,4-ethylenedioxythiophene in the presence of template molecules such as *p*-nitrophenol (PNP), 2,4-dinitrophenol (DNP), 2,4,6-trinitrophenol (TNP) or pyrene. The conjugated MIPs exhibited the distinctive recognition of all of the externally added nitrophenol templates compared to the non-imprinted polymers (NIPs) prepared in parallel in the rebinding experiments, monitored by UV-Vis absorption. In contrast, the similarly prepared MIP using pyrene as the template showed only small difference in rebinding the nonpolar pyrene in comparison to its NIP.

Similarly, molecularly imprinted copolymers (coMIPs) based on PEDOT and poly(3,4-ethylenedioxythiophene methanol) (PEDTM) were prepared using PNP as the template molecule. The resulted conjugated coMIPs with higher percentage of PEDTM showed much better recognition of externally added PNP molecules compared to the non-imprinted copolymers (coNIPs) and MIP without PEDTM. The same trend was also observed with the calculated rebinding capacities of the co-MIPs. These results indicated that the presences of polar functional groups on both template molecule and monomeric units of the MIP contribute significantly on the induced imprinting property. These accomplishments suggest a strong possibility to develop the family of PEDOT derivatives as highly specific MIP-based sensors.

Department: Chemistry

Student's Signature

Field of Study: Chemistry

Advisor's Signature

Academic Year: 2015

ACKNOWLEDGEMENTS

My utmost gratitude goes to my thesis advisor, Assist. Prof. Dr. Yongsak Sritana-anant, whose expertise, understanding, generous guidance and advocacy made it possible for me to accomplish the course research that was of great interest to me. It was a great privilege working with him.

I am highly indebted and thoroughly grateful to the members of the committee, Assoc. Prof. Dr. Vudhichai Parasuk, Dr. Panuwat Padungros and Assoc. Prof. Dr. Siritron Samosorn, for providing their valuable comments and suggestions regarding the topic of research.

I would like to gratefully acknowledge the members of YS-research group on the fourteenth floor, Mahamakut building for their support, encouragement and camaraderie, I have grown and developed myself in research.

Finally, I would like to take this opportunity to express my sincere appreciation and gratitude to my family and Faculty of Science, Chulalongkorn University for partial support on funding and laboratory.

CONTENTS

	Page
THAI ABSTRACT	iv
ENGLISH ABSTRACT	v
ACKNOWLEDGEMENTS	vi
CONTENTS	vii
LIST OF FIGURES	xi
LIST OF SCHEMES	xiii
LIST OF TABLES	xiv
LIST OF ABBREVIATIONS	xv
CHAPTER I INTRODUCTION.....	1
1.1 A Brief History of Molecularly Imprinted Polymers.....	1
1.2 Fundamental Principle of Molecularly Imprinting Technique	1
1.3 Approach for Selective Binding Sites.....	3
1.3.1 Covalent Imprinting Approach	3
1.3.2 Non-covalent Imprinting Approach	4
1.3.2.1 Functional Monomer	5
1.3.2.2 Cross-linkers.....	6
1.3.2.3 Solvents.....	7
1.4 Applications of the Molecularly Imprinted Polymers.....	8
1.5 Polythiophene derivative	10
1.5.1 Poly(3,4-ethylenedioxythiophene) (PEDOT)	11
1.5.2 Poly(3,4-ethylenedioxythiophene methanol) (PEDTM).....	12
1.6 Solid State Polymerization (SSP) of thiophene derivatives	12

	Page
1.7 Literature Reviews.....	14
1.8 Objectives.....	19
CHAPTER II EXPERIMENTS.....	20
2.1 Chemicals.....	20
2.2 Instruments and equipment.....	21
2.3 Monomer synthesis.....	21
2.3.1 Ethyl chloroacetate.....	21
2.3.2 Diethyl thiodiglycolate (1).....	22
2.3.3 Diethyl 3,4-dihydroxythiophene-2,5-dicarboxylate (2).....	22
2.3.4 Butyl chloroacetate.....	23
2.3.5 Dibutyl thiodiglycolate (3).....	23
2.3.6 Dibutyl 3,4-dihydroxythiophene-2,5-dicarboxylate (4).....	24
2.3.7 Diethyl 2-(hydroxymethyl)-2,3-dihydrothieno[3,4- <i>b</i>]-1,4-dioxine-5,7- dicarboxylate (5).....	24
2.3.8 Diethyl 2-vinyl-2,3-dihydrothieno[3,4- <i>b</i>][1,4]dioxine-5,7-dicarboxylate (6).....	25
2.3.9 2-(hydroxymethyl)-2,3-dihydrothieno[3,4- <i>b</i>][1,4]dioxine-5,7- dicarboxylic.....	26
2.3.10 2-vinyl-2,3-dihydrothieno[3,4- <i>b</i>][1,4]dioxine-5,7-dicarboxylic acid (8).....	26
2.3.11 3,4-ethylenedioxythiophene methanol (EDTM).....	27
2.3.12 2-vinyl-2,3-dihydrothieno[3,4- <i>b</i>][1,4]dioxine (9).....	28
2.3.13 α -Brominations of thiophene derivatives.....	28
2.3.13.1 2,5-Dibromo-3,4-ethylenedioxythiophene (10).....	29
2.3.14.2 2,5-Dibromo[3,4- <i>b</i>]-1,4-dioxin-2-yl methanol (11).....	29

	Page
2.3.13.3 5,7-dibromo-3-vinyl-2,3,4a,5-tetrahydrothieno[3,4- b][1,4]dioxine (12).....	30
2.4 Preparation of template molecules.....	30
2.4.1 2,4-Dinitrophenol (DNP).....	30
2.4.2 2,4,6-Trinitrophenol (TNP).....	31
2.5 Preparation of molecularly imprinted polymers (MIPs).....	31
2.5.1 Molecularly imprinted polymer of PEDOT.....	31
2.5.2 Molecularly imprinted copolymer of PEDOT+ PEDTM.....	33
2.6 Binding experiments.....	33
CHAPTER III RESULTS AND DISCUSSION.....	35
3.1 Monomer Synthesis.....	35
3.1.1 Synthesis of Diethyl 3,4-dihydroxythiophene-2,5-dicarboxylate (3).....	35
3.1.2 Synthesis of dibutyl 3,4-dihydroxythiophene-2,5-dicarboxylate (4).....	37
3.1.3 (2,3-Dihydrothieno[3,4- <i>b</i>][1,4]dioxin-2-yl)methanol (EDTM).....	38
3.1.4 2-Vinyl-2,3-dihydrothieno[3,4- <i>b</i>][1,4]dioxine (9).....	40
3.1.5 Bromination of thiophene derivatives.....	42
3.2 Preparations of template molecules: 2,4-dinitrophenol (DNP) and 2,4,6- trinitrophenol (TNP).....	44
3.3 Preparation of molecularly imprinted polymer (MIPs).....	45
3.3.1 Pyrene-molecularly imprinted polymers (Pyrene-MIPs).....	46
3.3.2 <i>p</i> -Nitrophenol molecularly imprinted polymers (PNP-MIPs).....	49
3.3.3 2,4-Dinitrophenol molecularly imprinted polymers (DNP-MIPs).....	52
3.3.4 2,4,6-Trinitrophenol molecularly imprinted polymers (TNP-MIPs).....	54
3.3.5 <i>p</i> -Nitrophenol molecularly imprinted copolymers (PNP-coMIPs).....	55

	Page
CHAPTER IV CONCLUSION.....	59
REFERENCES	64
APPENDIX A.....	71
APPENDIX B.....	98
VITA.....	111



LIST OF FIGURES

Figure	Page
1.1 Schematic illustration of the imprinting process	2
1.2 Structures of the most common monomers employed for imprinting.....	5
1.3 Structures of the most common cross-linkers employed for molecular imprinting.....	7
1.4 The structure of poly(3,4-ethylenedioxythiophene) (PEDOT)	11
1.5 The structure of poly(3,4-ethylenedioxythiophene methanol) (PEDTM).....	12
1.6 Solid-state polymerization to PEDOT	13
1.7 Synthesis of PEDOT through acid-assisted polycondensation	14
3.1 The concentrations of pyrene at various sampling times during binding process in the presence of pyrene-MIPs and NIPs, using EtOAc extraction off the template.....	48
3.2 The concentrations of pyrene at various sampling times during binding process in the presence of pyrene-MIPs and NIPs, using MeOH extraction off the template.....	48
3.3 The concentrations of PNP at various sampling times during binding process in the presence of PNP-MIPs and NIPs, using EtOAc extraction off the template.....	50
3.4 The concentrations of PNP at various sampling times during binding process in the presence of PNP-MIPs and NIPs, using MeOH extraction off the template.....	51
3.5 The concentrations of DNP at various sampling times during binding process in the presence of DNP-MIPs and NIPs, using EtOAc extraction off the template.....	53

3.6 The concentrations of DNP at various sampling times during binding process in the presence of DNP-MIPs and NIPs, using MeOH extraction off the template.....	53
3.7 The concentrations of TNP at various sampling times during binding process in the presence of TNP-MIPs and NIPs.....	55
3.8 The concentrations of PNP at various sampling times during binding process in the presence of PNP-coMIPs and coNIPs.....	57
3.9 The concentrations of PNP at various sampling times during binding process in the presence of PNP-coMIPs and coNIPs.....	58



LIST OF SCHEMES

Scheme	Page
2.1 Imprinting template molecules through SSP process.....	32
3.1 Synthesis of Diethyl 3,4-dihydroxythiophene-2,5-dicarboxylate 2	35
3.2 Mechanism of Hinsberg reaction	36
3.3 Synthesis of dibutyl 3,4-dihydroxythiophene-2,5-dicarboxylate 4	37
3.4 Synthesis of (2,3-dihydrothieno[3,4-b][1,4]dioxin-2-yl)methanol (EDTM).....	38
3.5 Mechanism of the substitutions on epichlorohydrin	39
3.6 Synthesis of compound 9	41
3.7 Synthesis of compound 10	42
3.8 Synthesis of DNP and TNP	44
3.9 Synthesis of MIPs with pyrene as the template molecule.....	46
3.10 Synthesis of MIPs with a template molecule.....	49
3.11 Synthesis of coMIPs with PNP as a template molecule.....	56
4.1 Synthesis of compound 2	59
4.2 Synthesis of compound 4	60
4.3 Synthesis of compound 11	61
4.4 Synthesis of compound 12	61

LIST OF TABLES

Table	Page
3.1 Conditions for the synthesis of compound 5	39
3.2 Dibromination results of 3,4-dialkoxythiophene derivatives	43
4.1 The specific adsorption values (ΔQ) of MIPs and NIPs	62
4.2 The rebinding capacities of MIPs and NIPs.....	62
4.3 the specific adsorption values (ΔQ) for PNP-MIPs and coMIPs.....	63
4.4 The rebinding capacities of PNP-MIPs and coMIPs.	63



LIST OF ABBREVIATIONS

BuOH	: Butanol
cm ⁻¹	: Unit of wavenumber (IR)
¹³ C NMR	: Carbon-13 nuclear magnetic resonance spectroscopy
°C	: Degree Celsius
CDCl ₃	: Deuterated chloroform
coMIPs	: Molecularly imprinted copolymers
coNIPs	: Non-imprinted copolymers
d	: Doublet (NMR)
DBEDOT	: 2,5-dibromo-3,4-ethylenedioxythiophene
DBEDTM	: 2,5-dibromo-3,4-ethylenedioxythiophene methanol
DBU	: 1,8-diazabicycloundec-7-ene
DMA	: <i>N,N</i> -dimethylacetamide
DMSO- <i>d</i> ₆	: Hexadeuterated dimethyl sulfoxide
DMAP	: 4-(dimethylamino)pyridine
DNP	: 2,4-dinitrophenol
EDOT	: 3,4-ethylenedioxythiophene
EDTM	: 3,4-ethylenedioxythiophene methanol
Equiv	: Equivalent
EtOAc	: Ethyl acetate
FeCl ₃	: Ferric chloride
g	: Gram
¹ H NMR	: Proton nuclear magnetic resonance spectroscopy
h	: Hour
Hz	: Hertz
IR	: Infrared spectroscopy
<i>J</i>	: Coupling constant
K ₂ CO ₃	: Potassium carbonate
m	: Multiplet (NMR)

min	: Minute
mg	: Milligram
mL	: Milliliter
M	: Molar
mM	: Millimolar
mmol	: Millimole
m.p.	: Melting point
MeOH	: Methanol
MgSO ₄	: Magnesium sulfate
MIPs	: Molecularly imprinted polymers
MS	: Mass spectrometry
m/z	: mass per charge ratio
NIPs	: Non-imprinted polymers
nm	: Nanometer
NBS	: <i>N</i> -bromosuccinimide
PEDOT	: Poly(3,4-ethylenedioxythiophene)
PEDTM	: Poly(3,4-ethylenedioxythiophene methanol)
PNP	: <i>p</i> -nitrophenol
ppm	: Parts per million
Q	: The amount of template molecules bound to polymers
Q _e	: the initial amount of template molecules in solution used to prepare MIPs before the binding experiment
Q _i	: the amount of template molecules in solution obtained from exhaustive extraction at the end of the binding process
Q _{MIPs}	: The amount of template molecules bound to imprinted polymers
Q _{NIPs}	: The amount of template molecules bound to non-imprinted polymers
q	: Quartet (NMR)
RT.or rt	: Room temperature
SSP	: Solid-state polymerization

s	: Singlet (NMR)
st	: Stretching vibration
t	: Triplet (NMR)
TLC	: Thin layer chromatography
TNP	: 2,4,6-trinitrophenol
UV-Vis	: Ultra-violet and visible spectroscopy
V	: Volume
μmol	: Micromole
δ	: Chemical shift
λ_{max}	: Maximum wavelength absorption



CHAPTER I

INTRODUCTION

1.1 A Brief History of Molecularly Imprinted Polymers

Over recent years, molecularly imprinted polymers (MIPs) have shown great potential in numerous applications in pharmaceuticals, biological technology, sensor technology and so forth. Although there has been substantial research during the past years, increased motivation to assess the true potential of molecularly imprinted polymers is still in demand for modern chemistry.

From Wulff's seminal work [1] in 1972, the notion of molecularly imprinted polymers was developed and intensively studied. They were among the early group to synthesize molecularly imprinted polymers, employing a covalent approach for resolving the racemic mixture of glyceric acid. Elsewhere, Mosbach and coworkers [2] were the first group to introduce molecularly imprinted polymers using a non-covalent approach in order to mimic antibody combining sites. The simplicity of their method allowed it to be vastly used to create the later-generation of imprinted polymers.

1.2 Fundamental Principle of Molecularly Imprinting Technique

Molecularly imprinted polymers have experienced much attention due to their versatile synthetic approach for preparing highly cross-linked polymer matrix with recognition sites that are solely specific to certain templates e.g. an atom, ion, molecule, complex or a molecular, ionic or a molecular assembly, including micro-organisms.[3] The preparation of molecularly imprinted polymers commences with the assembling of functional monomers surrounding our interest templates. This process is analogous to a theory originating in biochemistry which is called lock-and-key mechanism, explaining the interaction between enzyme and substrate.[4]

Subsequently, the recognition site with high selectivity is formed during the interaction between functional groups on the template and monomer through a polymerization process. Then the template is removed from the site by a certain

condition, leaving it with a cavity that resembles both size and shape of the template. The obtained cavity, which occurs inside the synthetic polymer, demonstrates an excellent sensitivity and selectivity toward specific template molecule.[5, 6] (Figure 1.1)

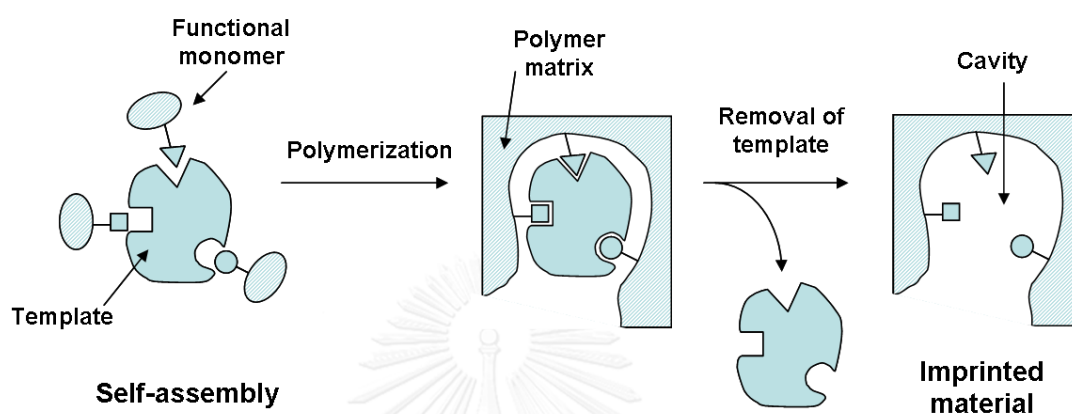


Figure 1.1 Schematic illustration of the imprinting process

The classification of molecularly imprinted polymers depends on several factors, but the interactions between templates and functional monomers are one-way to indicate the types of molecularly imprinted polymers. As mentioned earlier, there are two approaches which have been commonly employed: covalent (including metal-coordination) and non-covalent bond. Nonetheless, the more popular approach, which was extensively used for synthesizing molecularly imprinted polymers, is the non-covalent method due to these reasons: [4, 7]

- The interactions between functional monomers and templates are easy to design and obtain.
- Extraction procedure of templates requires unsophisticated technique, normally accomplished by exhaustive extraction.
- Greater possibility of various functional groups can be employed to interact with the templates in the molecularly imprinted polymer.

- Molecularly imprinted polymer can be retained for years without degrading its efficiency.

1.3 Approach for Selective Binding Sites

1.3.1 Covalent Imprinting Approach

Covalent imprinting was the first strategies that were employed in the molecularly imprinted polymer. The covalent imprinting approach is discriminated by mean of which one or more functional units and the templates are attached through covalent bonds in order to form a template-monomer by a chemical step independent of polymer formation. After polymerization process, the templates are extracted from the imprinted polymer matrix, leaving the unpaired functional groups in the binding sites and these sites are capable of binding specific target molecule by re-establishment of the covalent bond. The classical methods of covalent imprinting implicate readily reversible condensation reactions such as ketal/acetal, boronate ester and Schiff's base formation to prepare template-monomers [3, 5].

The boronic acids, which are somewhat suitable for covalent binding with diol-containing templates, are often employed as binding sites, and their formation and dissociation process are swift and facile. Boronic acids consist of five-membered cyclic structures in which the rigidity is sufficient to fix the covalent linkages for a desired conformation. The latter procedure involves hydrolysis of boronate ester groups to remove the template. Thus, the linkages of boronic groups inside the recognition site are arranged orderly for guest binding. The boronic esters approach has been the most successful reversible covalent methods, especially for imprinting of carbohydrate derivatives. The template molecules employed include [5, 7] glyceric acid, derivatives of mannose, galactose, fructose, sialic acid, castasterone and nucleotides. Furthermore, the boronate esters have also been consolidated in molecularly imprinted polymers for fluorescent sensing.

Ketal/acetal formation between a diol and a carbonyl compound has been employed for molecular imprinting protocols. After the extraction of templates, the

rebinding process took place by carbonyl chloride with an alcohol reaction or by the displacement of bromide by a carboxylate anion. However, carboxylic acids have limited capability when employed in the fully covalent method owing to their slow rebinding kinetics and the need for activate intermediates. Shea and coworkers [6], who employed a polymerizable diol as the binding group, have been intensively studied mono- and di- ketone templates in particular.

The Schiff's bases are a beneficial approach for the imprinting of either primary amine or carbonyl compound by condensation. The derivatives of amino acid have been prosperously imprinted via this approach, but the rebinding procedure with the resultant enantioselective polymers take a considerable amount of time for many potential applications, such as chromatographic separation [8].

The advantage of the covalent imprinting approach is that the functional group residues are only found in the recognition sites associated with a template, which perhaps useful to lower non-specific interactions. However, the disadvantages of the covalent approach are the need for a sophisticated technique of synthetic chemistry to be fulfilled on the template before the polymerization process and a chemical treatment on the polymer to release the template.

1.3.2 Non-covalent Imprinting Approach

The formation of non-covalent imprinting interactions between functional monomer and template during polymerization are similar to those interactions between polymer and template in the rebinding process. The interactions are based on typical non-covalent forces such as hydrogen bonding, ionic interactions, electrostatic interactions, van der Waals forces and hydrophobic forces [9]. This approach has been vastly employed because it provides more flexibility in terms of the functionalities on a desirable template. Additionally, the synthesis process requires much less complicated procedure than the pre-synthesis of covalent adducts. On the other hand, those imprinted polymers, which employed the covalent approach, were obtained in situ simply by conglomerating the functional monomers and templates in

the form of polymerization mixtures while the non-covalent imprinting was spontaneously formed. After the polymerization, the removal of the template can be facilely done by simple extraction of polymer with suitable solvents.

1.3.2.1 Functional Monomer

The selected monomer is a crucial factor in order to synthesize unique recognition sites designed for a specific template. A wide variety of commercially available functional monomers enables researchers to take advantage of distinct kinds of intermolecular interactions. Typical functional monomers (**Figure 1.2**) [10] are carboxylic acids (acrylic acid, methacrylic acid, vinylbenzoic acid), sulphonic acids (2-acrylamido-2-methylpropane sulphonic acid), heteroaromatic bases (vinylpyridine, vinylimidazole)

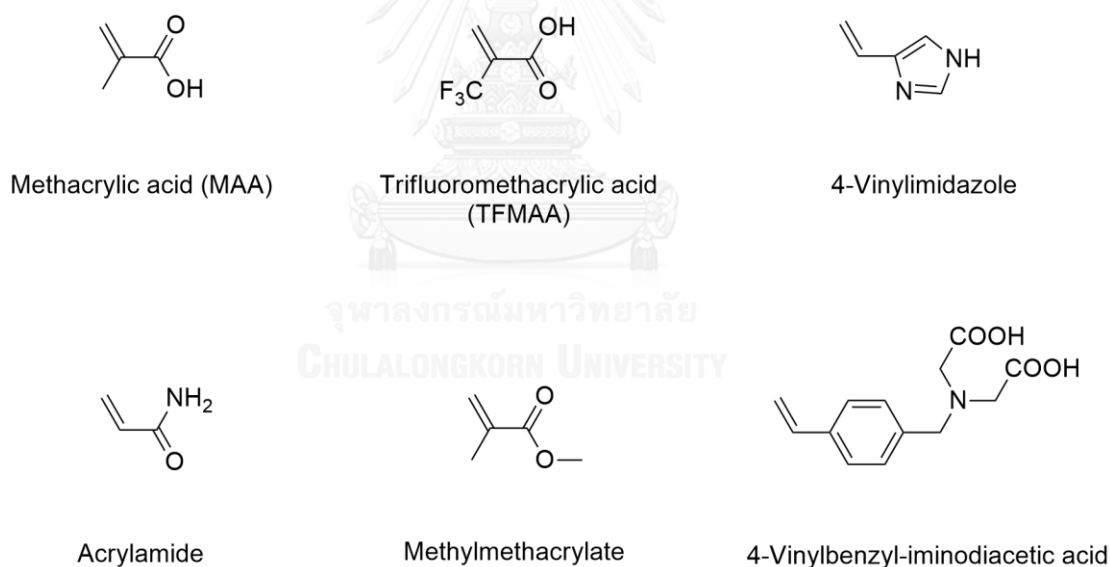


Figure 1.2 Structures of the most common monomers employed for imprinting

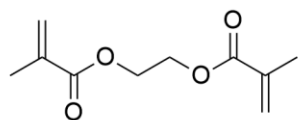
In general, the selected monomer carry functional groups that must complement to those found on the template molecule. For instance, if our interested template consists of either carboxylic or sulfonic acid groups, the possibility of selected functional monomer should contain an amine group. The reason is that they can both

form strong ionic interactions between one another. In addition, functional monomers are selected considering strength and nature between template and monomer.

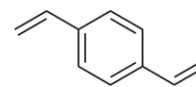
Methacrylic acid (MAA) [11] has been extensively used as the most common functional monomer for the variety of template molecules such as nucleotides, drugs, peptides, herbicides, biologically active substance, environmental contamination and so forth. Furthermore, methacrylic acid, consisting of carboxyl group that act both as hydrogen bond donor and acceptor, has the capability to interact with a basic functional group on a template molecule. Recently, new functional monomers, trifluoromethacrylic acid (TFMAA), have been developed. Because it is a stronger acid due to the effect of electronegativity. Thus, trifluoromethacrylic acid is competent in forming stronger ionic interactions. The function monomers, consisting of amidine and urea, have been developed for the purpose of the stoichiometrically imprinted polymeric receptor of β -lactam antibiotics, abating non-specific adsorption [12]

1.3.2.2 Cross-linkers

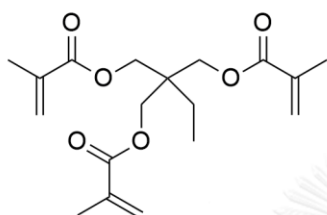
In imprinted polymer synthesis, cross-linker also implements vital functions, for instance, controlling the morphology of the polymer matrix, stabilizing the imprinted binding sites and imparting mechanical stability to the polymer matrix in order to maintain its molecular recognition capability [10, 13]. Varieties of cross-linkers have been employed as shown in **Figure 1.3** [10].



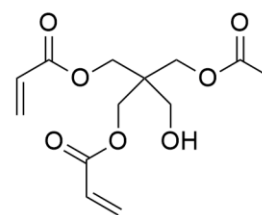
Ethyleneglycol dimethacrylate (EDMA)



Divinylbenzene (DVB)



Trimethoxypropane trimethacrylate (TRIM)



Pentaerythritol triacrylate (PETRA)

Figure 1.3 Structures of the most common cross-linkers employed for molecular imprinting

High cross-link ratios are normally employed in order to access permanently porous (macroporous) materials with a sufficient mechanical stability. The most widely utilizable cross-linkers are ethylene glycol dimethacrylate (EGDMA) and trimethoxypropane trimethacrylate (TRIM). Furthermore, the capability of cross-linkers also depends on the templates and solvent in the reaction mixtures. Trimethoxypropane trimethacrylate as a cross-linker provides more rigidity, structure order and effective binding sites in comparison with ethylene glycol dimethacrylate.

1.3.2.3 Solvents

Selecting a suitable solvent has been a crucial factor in achieving a satisfactory imprinting and successful rebinding results. Commonly, the solvents generally employed for molecularly imprinted polymers synthesis are toluene, chloroform, dichloromethane or acetonitrile. The solvent serves as aiding substance in order to bring all the components (monomer, template, initiator and cross-linker) into a single

phase in the polymerization process and responsible for creating pores within a macroporous polymer. Large size of pores will assure good flow through the resultant molecularly imprinted polymer. The choice of solvents depends on its role toward which type of imprinting approach. The selection of solvents for the non-covalent imprinting approach is more significant in order to promote the formation of non-covalent interactions among the functional monomer and template and, therefore, enhance the imprinting efficiency [14].

Generally, the non-covalent imprinting approach is less complicated to achieve and applicable to a variety of template molecules than the covalent imprinting approach. During the polymerization process, the covalent linkage between template and monomer is needless and the condition of polymerization has to be cautiously chosen to maximize the formation of non-covalent interaction in the mixture. Additionally, the removal of template molecules can be facilely occurred from the polymer matrix by exhaustive extraction with appropriate solvents due to its weakly interact by non-covalent linkages. On the contrary, the covalent imprinting interaction between template and monomer requires stability and specific geometry. In some condition, the imprinting effect is decreased in the extraction procedure, which requires rather severe conditions for cleavage of covalent linkages. Selection of the imprinting approach in accordance with a desirable selectivity for the analyzed template molecules should be carefully considered.

1.4 Applications of the Molecularly Imprinted Polymers

The unique properties of molecularly imprinted polymers have made them an intriguing method for variety of applications including:

- Molecularly imprinting chromatographic techniques

One of the most traditional applications is the molecularly imprinting chromatography, particularly for liquid chromatography (LC) using molecularly imprinted polymers. They are employed as a stationary phase for the separation, which

were generally synthesized through bulk polymerization, ground, sieved mechanically and subsequently packed into a chromatographic column. Furthermore, the focused analysis is mainly the separation of template molecules with closely related structures such as different kinds of steroids, various herbicides, and structures that are not amino acid derivatives.

- Solid-phase extraction and by-product removal

Another important field of molecularly imprinted polymers in analytical chemistry is solid-phase extraction (SPE). In this case, molecular imprinting polymer particles, employed as selective sorbent materials, are packed in a high-performance liquid chromatography (HPLC) column for separating and purifying analyzed molecules from the complex matrices. This application has been adapted to extract several compounds in different sample matrices, for instance, clinical samples, environmental samples, food analysis and so forth.

- Molecularly imprinted polymers as chemical sensors and biosensors

The applications of molecularly imprinted polymers, based on sensing, are capable of identifying and binding target molecules with related specificity and selectivity to their natural analogues. Recently, there has been prosperously employed with different kinds of transducers, for instance, the integration of molecularly imprinted polymers with sensors using either a photochemical or thermal initiator, and by surface grafting with chemical or UV initiation. The latter approach has a possibility to control modification of inert electrode surfaces with thin films of specific polymers which are an advantage comparing to the previous approach. In addition, the molecularly imprinted polymer can be electropolymerized on the surface of transduction platform.

- Molecularly imprinted polymers in catalysis and drug delivery

The usage of molecularly imprinted polymer for catalytic purposes is an important aspect of modern chemistry because they have the ability to mimic the

selectivity and stereospecificity of the binding domains of antibodies and enzymes which are normally utilized as catalysts in some reactions [10]. Molecularly imprinted polymers for drug delivery applications have been considered a great challenge over the past few years owing to unique characteristics: the polymer matrix should be stable to maintain the conformation in the absence of the template; they should be capable of resisting enzymatic, chemical interference and mechanical stress that can be found in biological fluids.

1.5 Polythiophene derivative

Polythiophenes (PTs) are polymerized thiophenes, a sulfur heterocycle. They can become conducting when electrons are added or removed from the conjugated π -orbitals via doping. The most notable property of these materials, electrical conductivity, results from the delocalization of electrons along the polymer backbone. However, conductivity is not the only interesting property resulting from electron delocalization. The optical properties of these materials respond to environmental stimuli, with dramatic color shifts in response to changes in solvent, temperature, applied potential, and binding to other molecules. Both color changes and conductivity changes are induced by the same mechanism-twisting of the polymer backbone, disrupting conjugation-making conjugated polymers attractive as sensors that can provide a range of optical and electronic responses. [11-13]

Originally, this polymer was prepared by employing either standard oxidative chemical or electrochemical polymerization methods. Since the preparation of a coated-polymer was conducted on the anode surface during electrochemical polymerization, the obtained polymers are not easily processed after the formation of polymers. The yields of prepared polymers from this method are relatively low, and the polymers often do not have a stable structure.

In addition, the traditional oxidative polymerization with FeCl_3 in organic solvents provides relatively high yields in comparison with the electrochemical polymerization method and the final product, which the researchers obtain, has a

characteristic of an insoluble blue-black doped polymer powder, the use of a water-soluble electrolyte polystyrene sulfonic acid (PSS) as a charge-balancing dopant during polymerization, gives a polymer solution which is capable of processing and forms semitransparent conducting films upon spin-casting. In order to obtain the neutral polymer, a nickel (0) complex-promoted polycondensation of 2,5-dihalo-3,4-ethylenedioxythiophenes has been employed [15] However, the limitations of this method can cause a severe problem for poly(3,4-ethylenedioxythiophene) applications as well as for in depth investigation of molecular order in this conducting polymer. In truth, there is no possibility to obtain a well-defined polymer structure, except the synthesis of conducting polymers is conducted via pure chemical polymerization ways, without the addition of catalysts.

1.5.1 Poly(3,4-ethylenedioxythiophene) (PEDOT)

Polythiophene derivative, poly(3,4-ethylenedioxythiophene) (PEDOT), has been one of the most industrially essential conjugated polymer owing to its excellent electronic properties and remarkable stability. The backbone structure of this polymer is shown in **Figure 1.4** [16]

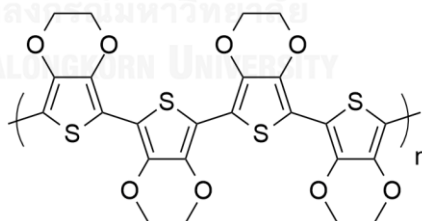


Figure 1.4 The structure of poly(3,4-ethylenedioxythiophene) (PEDOT)

Poly(3,4-ethylenedioxythiophene) had attracted considerable interests attribute to its low band gap, high electrical conductivity, stable morphology, and excellent optical transparency in the visible region; additionally, it also possesses many practical applications, for instance, all-organic light-emitting diodes, polymer field-effect transistors and so forth. The ether groups at the position of β and β' in poly(3,4-ethylenedioxythiophene) help avoiding the formation of α - β' linkages defect during

the polymerization. Therefore, the thiophene ring, which acquires from other substituents such as polyether or alkoxy groups at the β positions, has the possibility of higher solubility and better physical and chemical properties.

1.5.2 Poly(3,4-ethylenedioxythiophene methanol) (PEDTM)

Poly(3,4-ethylenedioxythiophene methanol) (PEDTM) having the backbone structure shown in **Figure 1.5**. PEDTM was prepared from 3,4-ethylenedioxythiophene methanol (EDTM), the presence of the hydroxyl groups added many useful properties such as increasing polarity, hydrogen bond ability, and functionalizability.[16-18]

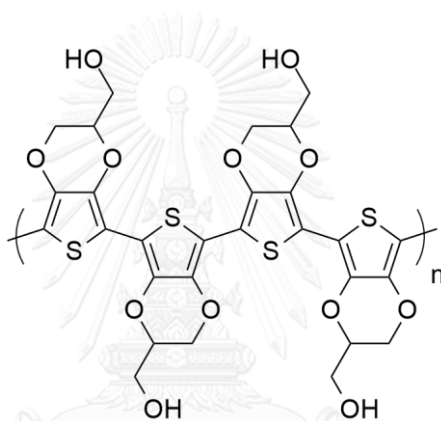


Figure 1.5 The structure of poly(3,4-ethylenedioxythiophene methanol) (PEDTM)

1.6 Solid State Polymerization (SSP) of thiophene derivatives

A reasonable solution for the problems of methods for preparing poly(3,4-ethylenedioxythiophene) lies in a solid-state polymerization of a structurally pre-organized crystalline dibromo monomer. The notion of solid-state polymerization was first realized in the 1960s and 1970s with polydiacetylenes. Subsequently, this technique has attracted a substantial group of research due to several advantages, including low operating temperatures, which control byproducts and thermal degradation of the reaction, inexpensive equipment, less complicate procedures, and environmental-friendly process.

Meng and co-workers [15] have discovered by coincidence that as prolonged storage (2 years) of the dibromo derivatives of EDOT at room temperature or heated approximately 50-80°C has led to the solid-state polymerization to PEDOT (**Figure 1.6**).

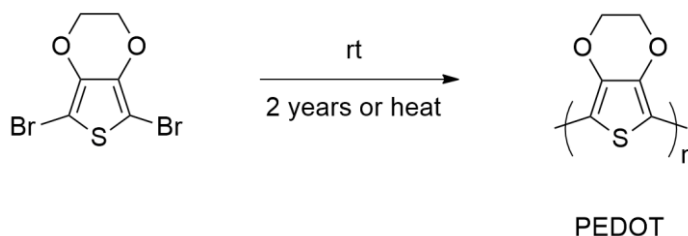


Figure 1.6 Solid-state polymerization to PEDOT

Time is an important factor which influences the transformation of colorless crystalline precursor into black blue substance without evident change of morphology. Astonishingly, the conductivity of this decomposition product seemed to be very high for an organic solid, approximately up to 80 S/cm. Furthermore, the reaction time can be reduced by increasing the temperature to the melting point.

The solid-state polymerizations at the lowest temperature and longest duration of the reaction time provides the highest conductivity, which perhaps reflects the achievement of a higher degree of order. It is apparent that heating monomer above its melting point results in a significant decreased of conductivity by 0.1 S/cm, which increased to 5.8 S/cm after doping with iodine, approaching the value of a FeCl₃-synthesized PEDOT (7.6 S/cm). Not very significant, but a certain rise in conductivity of SSP-PEDOT about 2 times was found on exposing a sample to iodine vapor.

Gulprasertrat and coworkers [17] have studied the solid state polymerization of 2,5-dibromo-3,4-ethylenedioxythiophene methanol which are another thiophene derivatives that can be prepared by SSP. They found that the dibromo derivative is liquid at room temperature and the solution of the compound changed color while being concentrated at high temperature. They decided to heat the liquid sample of the precursor under usual SSP procedure and obtained the dark blue insoluble solid PEDTM, having the conductivity at 44.5 S/cm after doping by iodine vapor.

Yin and coworkers [19] have conducted a synthesis of poly(3,4-ethylenedioxythiophene) (PEDOT) by acid-assisted polycondensation based on 2-bromo-3,4-ethylenedioxy thiophene (BEDOT). Under the exposure to ambient atmosphere, the formation of poly(3,4-ethylenedioxythiophene) is in a doped state to some extent, revealing a lack of conductivity at 10^{-6} S/cm while improved to 0.3 S/cm along with further iodine doping. Such discovering provides an alternative way for the synthesis of conjugated polymers by simple acid-assisted polycondensation due to the formation of a neutral polymer (**Figure 1.7**).

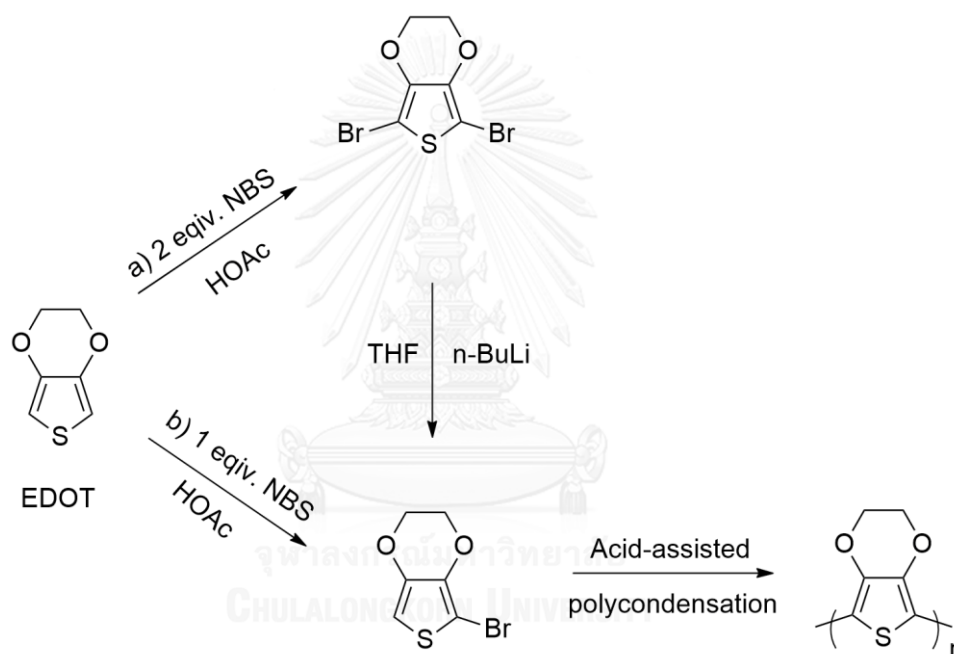


Figure 1.7 Synthesis of PEDOT through acid-assisted polycondensation

1.7 Literature Reviews

Kubo and coworkers [20] have prepared a cyclobarbital-selective molecularly imprinted polymer using 2-acrylamidoquinoline as a fluorescent functional monomer. This molecular imprinting polymer was polymerized through self-assembly of template molecules with functional monomers followed by co-polymerization with a cross-linker. The resultant imprinted polymer exhibited an improvement in fluorescence intensity when target compounds were bound. This sensing approach employing

fluorescent imprinted polymers as signaling receptors would be beneficial for the quantitation of non-fluorescent analytes.

Pardieu and coworkers [21] have prepared an electrochemical sensor that consolidates the selectivity demonstrated by molecular imprinting polymers, with the sensitivity and the immediate detection offered by the use of an electrochemical transduction. Furthermore, it is capable of recognizing pesticide molecules, atrazine. The poly(3,4-ethylenedioxythiophene-co-thiophene-acetic acid), poly(EDOT-co-AAT), has been fabricated, in the presence of atrazine, on a platinum electrode by electrochemical polymerization. From this research, the AAT monomers are capable of interact with atrazine through hydrogen bonds in which EDOT monomers are polymerized in order to stabilize and homogenize the film. The further extracting process of atrazine creates highly specific recognition sites towards newly added atrazine. In addition, the sensor showed promising results: selectivity towards triazinic groups, a large range of detection 10^{-9} mol L⁻¹ to 1.5×10^{-2} mol L⁻¹ in atrazine and low detection limit (LOD) at 10^{-7} mol L⁻¹.

Ho and coworkers [22] have deposited poly(3,4-ethylenedioxythiophene) on an indium tin oxide electrode (ITO) for the amperometric detection of morphine which this electrode displays a satisfied electrocatalyst for morphine oxidation. Furthermore, the MIP-PEDOT modified electrode is prepared through electropolymerized 3,4-ethylenedioxythiophene (EDOT) onto an indium tin oxide electrode (ITO) in an electrolytic solution containing morphine. By applying a fixed potential to the MIP-PEDOT modified electrode at 0.75 V, a satisfied linear relationship between the current density and morphine concentration, ranging from 0.1 to 1 mM, was achieved. Additionally, a sensitivity of 91.86 $\mu\text{A}/\text{cm}^2$ per mM morphine is obtained and the detection limit was calculated as 0.2 mM (57.0 $\mu\text{g}/\text{mL}$) at a signal-to-noise ratio of 3. As a result, the researcher is able to fabricate a modified electrode which exhibits satisfied sensitivity, selectivity, and reproducibility for morphine detection.

Chen and coworkers [23] have successfully prepared a conductive polymer of poly(3,4-ethylenedioxythiophene) by solid-state polymerization and used as a counter electrode in the liquid dye-sensitized solar cell. The experiment results shown that the performance of poly(3,4-ethylenedioxythiophene) is comparable with traditional Pt in a dye-sensitized solar cell when it employed as the counter electrode. This indicates that solid-state polymerization is a versatile preparation method owing to its ease preparation, simple coating, and heating processes; additionally, this method may have more advantages over other traditional methods of the large scale fabrication of poly(3,4-ethylenedioxythiophene) counter electrode for dye-sensitized solar cell.

Tiu and coworkers [24] have prepared pyrene-imprinted polythiophene nanofilm by electrochemical deposition and used for highly sensitive detection of pyrene and its analogues. Using a molecular imprinting technique, pyrene-specific recognition sites are formed throughout the oligo/polythiophene film deposited onto a gold surface. These pyrene “imprints” possess complimentary geometric features to the analyte and are capable of forming π -donor and hydrogen bonding interactions with pyrene. Upon exposure to pyrene, the functionalized nanosurface produces specific fluorescence emission whose response is linearly proportional to its concentration range between 0.01 and 1.0 M with good stability and reproducibility. The nanofilm sensor can also discriminate pyrene from its structural analogues in ultra-trace levels by shifting the fluorescence detection. Based on theoretical modeling studies, the strong polar hydrogen (Hp)- π interaction between the polythiophene film and pyrene, which generate fluorescent emission, was determined to be within -15 to -25 kJ/mol, a range close or even larger than common hydrogen bonds. The SH groups of the thiophene moieties act as the Hp- π interaction donors while the aromatic ring of pyrene functions as an Hp- π acceptor. These interactions as combined with the size and shape of the pyrene binding sites lead to a highly sensitive and specific detection of pyrene. The nanofilm MIP sensor may have advantages in environmental monitoring of pyrene and other polycyclic aromatic hydrocarbons (PAHs) in aquatic, marine and air samples.

Roy and coworkers [25] have prepared a conducting polymer based molecularly imprinted *p*-nitrophenol (PNP) sensor. A water pollutant, PNP is

electrochemically imprinted with polyvinyl sulphonic acid (PVSA) doped polyaniline onto indium tin oxide (ITO) glass substrate. The response studies of PNP imprinted electrode (PNPI-PANIPVSA/ITO) carried out using differential pulse voltammetry (DPV) reveal a lower detection limit of 1×10^{-3} mM, improved sensitivity as 1.5×10^{-3} A mM⁻¹ and stability of 45 days. The PNPI-PANI-PVSA/ITO electrode shows good precision with relative standard deviation of 2.1% and good reproducibility with standard deviation of 3.78%.

Jing and coworkers [26] have developed an electrochemical method to determine 2,4-dinitrophenol (DNP) in surface water samples, using hydrophilic molecularly imprinted polymers (MIPs) as the recognition element and nickel (Ni) fiber as the catalytic element. Hydrophilic MIPs were synthesized using DNP as the template, acrylamide as the monomer, glycidylmethacrylate as the pro-hydrophilic co-monomer and acetonitrile as the solvent. Hydrophilic modification could enhance the accessibility of DNP to the imprinted cavities and improve the selective recognition properties of traditional MIPs in water medium. Subsequently, hydrophilic MIPs/Ni fiber electrode was prepared to determine trace DNP by cyclic voltammetry. The parameters affecting the analytical performance were investigated. Under optimized conditions, the linear range was 0.7–30 $\mu\text{g L}^{-1}$ and the detection limit was 0.1 $\mu\text{g L}^{-1}$. Finally, the proposed method was applied to measure DNP in surface water samples. The spiked recoveries were changed from 91.3% to 102.6% and the RSD was not higher than 5.1%. There was no statistically significant difference between the results obtained by the proposed method and the traditional chromatographic method.

Guo and coworkers [27] have successfully coupled molecularly imprinted polymers (MIPs) with electrochemical sensor based on gold nanoparticles (AuNPs), to form a microporous-metal-organic film (MMOF), in order to improve selectivity. The MMOF was deposited on a gold electrode by electropolymerization of *p*-aminothiophenol (PATP) functionalized-AuNPs in the presence of TNT as a template. [28] This sensor provided a minimal detection limit of TNT that equals to 0.04 fM which

was obtained from a calibration curve of TNT, within the range of 4.4 fM–44 nM. To conclude, the MIP-hybrid sensor has provided many advantages such as highly sensitive, inexpensive and facile for onsite detection of TNT.

Xu and coworkers [29] have designed the MIPs with trinitrophenol (TNP) as a dummy template molecule capped with CdTe quantum dots (QDs) using 3-aminopropyl-triethoxy silane (APTES) and tetraethoxysilane (TEOS) as the functional monomer and the cross linker, respectively, for the preparation of a high-affinity DMIP@QDs by a sol–gel process for the recognition and sensing of TNT. The developed DMIP@QDs could highly selectively rebind TNT and quickly quench the fluorescence of the QDs. The obtained result was successfully applied to develop sensors for the rapid recognition and determination of hazardous materials from complex matrices.

Sukrakarn [30] have studied molecularly imprinted polymers (MIPs) based on PEDOT were prepared by solid state polymerization (SSP) in the presence of templates molecules: 2,4,6-trinitrophenol (TNP) or 2,4,6-trinitrotoluene (TNT). The resulting conjugated MIPs exhibited the recognition of its template molecules compared to non-imprinted polymers (NIPs) in the binding experiments monitored by UV-Vis spectroscopy. The result was found that the specific adsorption values (ΔQ) of TNP and TNT molecules bound to the MIPs were 128.41 and 103.63 $\mu\text{mol/g}$, respectively. The rebinding capacities of the TNP-MIPs were 38.64% for TNP-MIPs and 28.63% for TNT-MIPs. Cross binding experiments confirmed the selectivity of the MIPs only towards their template molecules. These results showed that PEDOT could be imprinted and developed to be sensors for specific detection of selected template compounds.

In conclusion, the molecular imprinting technology can be applied to create recognition sites that determined selectivity properties. The molecularly imprinted polymers are obtained through polymerization in the presence of a template molecule. The solid-state polymerization could also result in another stable polymer structures without adding any catalysts. Therefore, highly specific cavities are generated in the polymeric matrix. After the extraction of target molecules, molecularly imprinted

polymers display interesting recognition properties towards the template, originating from a shape and chemical functionality considerations in the cavities present in the polymer matrix. Hence, the objective of high specificity together with high sensitivity can be realized by combining the concept of molecularly imprinted polymers with the use of conducting polymers.

1.8 Objectives

The objective of this research are to employ the solid-state polymerization of PEDOT derivatives surrounding selected template molecules, to provide imprinted PEDOT derivatives and PEDOT copolymer. The resulting molecular imprinted conjugated PEDOT derivatives and PEDOT copolymer would consist of cavities that have selectivity and specificity towards the template molecules, in which the binding property of the imprinted polymer was monitored by the altered concentration of the template solution in comparison to the non-imprinted polymers.

CHAPTER II

EXPERIMENTS

2.1 Chemicals

Thin layer Chromatography (TLC) was performed on aluminum sheets precoated with silica gel (Merck Kieselgel 60 F₂₅₄, Merck KGaA, Darmstadt, Germany). Column chromatography was performed using 0.063-0.200 mm or 70-230 mesh ASTM silica gel 60 (Merck Kieselgel 60 G, Merck KGaA, Darmstadt, Germany). Solvents used in synthesis were reagent or analytical grades. Solvents used in column chromatography were distilled from commercial grade prior to use. Other reagents were purchased from the following vendors:

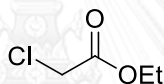
- RCI Labscan (Bangkok, Thailand): acetone, acetonitrile, dichloromethane, nitric acid (HNO₃), dimethylsulfoxide (DMSO), dimethylformamide (DMF), sodium hydrogen carbonate (NaHCO₃)
- AcrÖs Organics (New Jersey, USA): quinoline, *N*-bromosuccinimide (NBS)
- Carlo Erba (Milan, Italy): triethylamine (TEA), fuming nitric acid
- Fluka Chemical (Buchs, Switzerland): cuprous oxide (Cu₂O), sodium metal, potassium carbonate (K₂CO₃), *N,N*-dimethylacetamide (DMA)
- Merck Co. (Darmstadt, Germany): chloroacetyl chloride, sodium hydroxide (NaOH), ethanol absolute (EtOH), diethyl ether (Et₂O), concentrated hydrochloric acid, concentrated sulfuric acid, acetic acid (AcOH), epichlorohydrin, *p*-nitrophenol (PNP)
- Ajax Finechem Pty (Auckland, New Zealand): calcium chloride
- Cambridge Isotope Laboratories (USA): deuterium oxide (D₂O), deuterated chloroform (CDCl₃), deuterated dimethylsulfoxide (DMSO-*d*₆)
- Aldrich (USA): ethyl chloroacetate, diethyl oxalate (CO₂Et)₂, 3,4-ethylene dioxothiophene (EDOT), pyrene, diazabicycloundecene (DBU)
- Panreac (Spain) anhydrous magnesium sulfate (MgSO₄)

2.2 Instruments and equipment

Melting points were determined with a Stuart Scientific Melting Point SMP10 (Bibby Sterlin Ltd., Staffordshire, UK). The FT-IR spectra were recorded on a Nicolet 6700 FT-IR spectrometer. The ^1H and ^{13}C NMR spectra were obtained in deuterated chloroform (CDCl_3), deuterated dimethylsulfoxide ($\text{DMSO-}d_6$) or deuterium oxide (D_2O) using Varian Mercury NMR spectrometer operated at 400.00 MHz for ^1H and 100.00 MHz for ^{13}C nuclei (Varian Company, USA). The mass spectra were recorded on Waters Micromass Quattro micro API ESCi (Waters, USA). Samples were dissolved in EtOAc, MeOH, acetone or water. The UV-Vis absorption spectra were recorded on an Agilent 8453E UV-Visible spectroscopy.

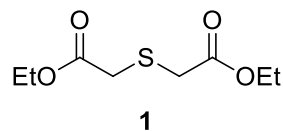
2.3 Monomer synthesis

2.3.1 Ethyl chloroacetate



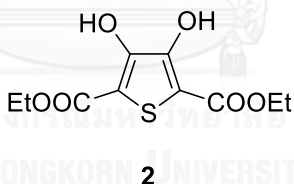
50 mL (56.510 g, 0.50 mol) of chloroacetyl chloride was slowly dropped into 32 mL (25.4 g, 0.55 mol) of EtOH over period of 30 min. The reaction mixture was stirred at 0 °C and then allowed to warm to room temperature for another 3 h. The mixture was added 120 mL of 2 M NaOH and extracted with diethyl ether three times. The combined organic layers were dried over anhydrous MgSO_4 . The solvent was removed using rotary evaporator to give an almost quantitative yield of the product as colorless liquid (55 mL, which was used without further purification). ^1H NMR (400 MHz, CDCl_3): δ (ppm) 4.24 (q, $J = 7.2$ Hz, 2H), 4.04 (s, 2H), 1.29 (t, $J = 7.2$ Hz, 3H) (**Figure A.1, Appendix A**). ^{13}C NMR (100 MHz, CDCl_3): δ (ppm) 167.3, 62.2, 40.9, 14.0 (**Figure A.2, Appendix A**).

2.3.2 Diethyl thiodiglycolate (1)



A solution of sodium sulfide nonahydrate ($\text{Na}_2\text{S}\cdot 9\text{H}_2\text{O}$, 12.0 g, 50 mmol) in water (30 mL) was added dropwise to the solution of ethyl chloroacetate (13.24 g, 55 mmol) in acetone (50 mL). Then the reaction was refluxed under nitrogen atmosphere for approximately 3 h. The cooled reaction mixture was extracted by diethyl ether three times. The separated organic layer was dried over anhydrous MgSO_4 and was evaporated by a rotary evaporator to give compound **1** as yellow liquid (5.741 g, which was used without further purification). ^1H NMR (400 MHz, CDCl_3): δ (ppm) 4.19 (q, $J = 7.1$ Hz, 4H), 3.37 (s, 4H), 1.28 (t, $J = 7.2$ Hz, 6H) (Figure A.3, Appendix A). ^{13}C NMR (100 MHz, CDCl_3): δ (ppm) 169.5, 61.1, 33.3, 13.9 (Figure A.4, Appendix A). MS: $[\text{M}+\text{Na}]^+$ $m/z = 229.05$ (Figure A.5, Appendix A). [31]

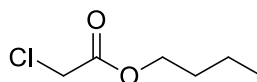
2.3.3 Diethyl 3,4-dihydroxythiophene-2,5-dicarboxylate (2)



Sodium metal (2.4 g, 0.21 mol) was dissolved in ethanol (75 mL). Subsequently, this solution was added dropwise to a mixture of compound **1** (2.00 g, 0.010 mol) and diethyl oxalate (4.5 g, 0.03 mol) for 30 min in an ice bath. Then the reaction was refluxed under nitrogen atmosphere for additional 3 h. After the refluxed process, the reaction was cooled to room temperature, poured distilled water (400 mL) to dissolve the remaining residues, and acidified by concentrated hydrochloric acid (15 mL) to obtain a yellow precipitate. The filtered solid was recrystallized from methanol, resulted in white needle crystals of compound **2** (1.242 g, 61%), m.p. 134-135 °C. ^1H NMR (400 MHz, CDCl_3): δ (ppm) 9.36 (s, 2H), 4.39 (q, $J = 7.1$ Hz, 4H), 1.38 (t, $J = 7.1$ Hz, 6H) (Figure A.6, Appendix A). ^{13}C NMR (100 MHz, CDCl_3): δ (ppm) 165.5, 151.6, 107.1,

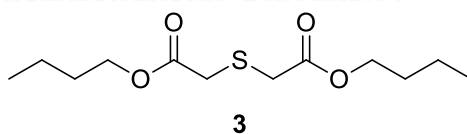
61.7, 14.0 (Figure A.7, Appendix A). IR (ATR, cm^{-1}): 3305 (-OH st), 2981 (-CH st), 1690 (C=O st), 1663 (C=C st) (Figure A.8, Appendix A). MS: $[\text{M}+\text{H}]^+$ $m/z = 250.20$ (Figure A.9, Appendix A). [32]

2.3.4 Butyl chloroacetate



50 mL (56.510 g, 0.50 mol) of chloroacetyl chloride was slowly dropped into 32 mL (25.9 g, 0.35 mol) of *n*-BuOH over period of 30 min. The reaction mixture was stirred at 0 °C and then warmed to room temperature for another 4 h. The mixture was added 120 mL of 2 M NaOH and extracted with diethyl ether three times. The combined organic layers were dried over anhydrous MgSO_4 . The solvent was removed using rotary evaporator to give the product as colorless liquid (36.4 g, which was used without further purification). ^1H NMR (400 MHz, CDCl_3): δ (ppm) 4.14 (t, $J = 6.7$ Hz, 2H), 4.03 (d, $J = 7.9$ Hz, 2H), 1.60 (dt, $J = 14.6, 6.7$ Hz, 2H), 1.34 (dq, $J = 14.7, 7.4$ Hz, 2H), 0.89 (t, $J = 7.4$ Hz, 3H) (Figure A.10, Appendix A) ^{13}C NMR (100 MHz, CDCl_3): δ (ppm) 167.3, 64.3, 40.5, 30.2, 19.0, 13.9 (Figure A.11, Appendix A). [40]

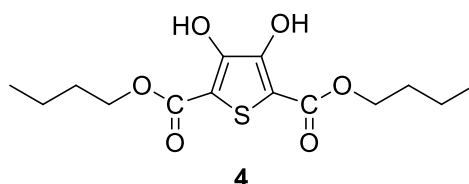
2.3.5 Dibutyl thiodiglycolate (3)



A solution of sodium sulfide nonahydrate ($\text{Na}_2\text{S}\cdot 9\text{H}_2\text{O}$, 12.0 g, 50 mmol) in water (30 mL) was added dropwise to the solution of butyl chloroacetate (8.28 g, 55 mmol) in acetone (50 mL). Then the reaction was refluxed under nitrogen atmosphere for approximately 4 h. The cooled reaction mixture was extracted by diethyl ether three times. The separated organic layer was dried over anhydrous MgSO_4 and was evaporated by a rotary evaporator to give compound **2** as yellow liquid (1.940 g, which was used without further purification). ^1H NMR (400 MHz, CDCl_3): δ (ppm) 4.02 (t, $J = 6.7$ Hz, 4H), 3.27 (s, 4H), 1.53 (m, 4H), 1.27 (dq, $J = 14.6, 7.3$ Hz, 4H), 0.82 (t, $J = 7.5$ Hz,

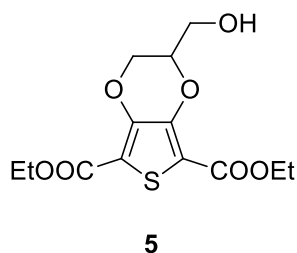
6H) (Figure A.12, Appendix A). ^{13}C NMR (100 MHz, CDCl_3): δ (ppm) 210.8, 62.2, 34.8, 31.3, 18.9, 14.0 (Figure A.13 Appendix A). [41]

2.3.6 Dibutyl 3,4-dihydroxythiophene-2,5-dicarboxylate (4)



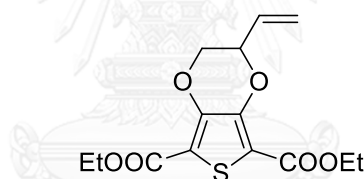
Sodium metal (3.5 g, 0.3 mol) was dissolved in *n*-butanol (50 mL). Subsequently, this solution was added dropwise to a mixture of compound **2** (1.311 g, 5.0 mmol) and diethyl oxalate (1.0 g, 6.3 mmol) for 30 min in an ice bath. Then the reaction was refluxed under nitrogen atmosphere for additional 3 h. After the refluxed process, the reaction was cooled to room temperature, poured distilled water (400 mL) to dissolve the remaining residues, and acidified by concentrated hydrochloric acid (15 mL). The reaction mixture was extracted by diethyl ether three times. The separated organic layer was dried over anhydrous MgSO_4 and was evaporated by a rotary evaporator to give compound **4** as brown liquid (0.470 g, which was used without further purification). ^1H NMR (400 MHz, CDCl_3): δ (ppm) 4.32-4.23 (m, 4H), 1.75-1.66 (m, 4H), 1.40 (dt, $J = 13.8, 7.0$ Hz, 4H), 0.98-0.87 (m, 6H) (Figure A.14, Appendix A). ^{13}C NMR (100 MHz, CDCl_3): δ (ppm) 158.8, 128.1, 110.1, 66.7, 31.9, 19.1, 13.9 (Figure A.15, Appendix A). [42]

2.3.7 Diethyl 2-(hydroxymethyl)-2,3-dihydrothieno[3,4-*b*]-1,4-dioxine-5,7-dicarboxylate (5)



Compound **3** (0.260 g, 1.0 mmol), epichlorohydrin (0.47 mL, 6.0 mmol) and K_2CO_3 (0.28 g, 2.0 mmol) were mixed in EtOH (20 mL). The reaction was stirred and refluxed for 72 h under nitrogen atmosphere. The reaction mixture was quenched by 10% hydrochloric acid solution and then extracted twice with chloroform. The combined organic layers were washed by 2 M NaOH, dried over anhydrous $MgSO_4$, and evaporated using rotary evaporator to get yellow solid. The crude mixture was purified by passing through a silica gel column, eluted with hexane : ethyl acetate (2:1) to yield a white solid (0.091 g, 28.4%). 1H NMR (400 MHz, $CDCl_3$): δ (ppm) 4.47 (m, 2H), 4.36 (m, 1H), 4.27 (m, 2H), 3.94 (q, $J = 12.5$, 4H), 1.36 (s, 1H), 1.33 (td, $J = 7.1$, 1.2 Hz, 6H) (**Figure A.16, Appendix A**). ^{13}C NMR (100 MHz, $CDCl_3$): δ (ppm) 161.0, 160.8, 145.3, 144.7, 112.0, 111.3, 74.8, 74.5, 66.0, 61.4, 60.9, 14.2 (**Figure A.17, Appendix A**). IR (ATR, cm^{-1}): 3539 (-OH st), 2987, 2934 (-CH st), 1702 (C=O st) (**Figure A.18, Appendix A**). [33]

2.3.8 Diethyl 2-vinyl-2,3-dihydrothieno[3,4-b][1,4]dioxine-5,7-dicarboxylate (**6**)

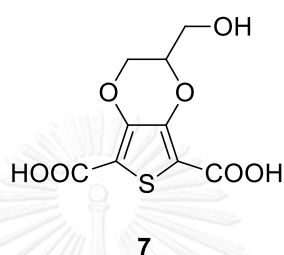


6

Compound **3** (0.260 g, 1.0 mmol), *trans*-1,4-dibromo-2-butene (0.320 g, 1.50 mmol), 4-dimethylaminopyridine (0.012 g, 0.10 mmol) and potassium carbonate (0.414 g, 3.00 mmol) in dimethyl formamide (10 mL) were allowed to mix. The reaction mixture was stirred and refluxed for 1 h under nitrogen atmosphere, cooled to 0-5°C and added cold water (20 mL). The mixture was extracted with ethyl acetate. The combined organic layers were washed by 1 M NaOH, water, and dried over anhydrous $MgSO_4$, filtered and distilled under reduced pressure. The product was purified by column chromatography using hexane: ethyl acetate (4:1) to yield compound **6** as white needle crystal (0.166 g, 53%) 1H NMR (400 MHz, $CDCl_3$): δ (ppm) 5.87 (m, 1H), 5.54 (d, $J = 17.3$ Hz, 1H), 5.39 (d, $J = 10.7$ Hz, 1H), 4.76 (m, 1H), 4.37 (m, 1H), 4.29 (q, $J = 7.1$ Hz, 4H), 4.04 (m, 1H), 1.32 (t, $J = 7.1$ Hz, 6H) (**Figure A.19, Appendix A**). ^{13}C NMR

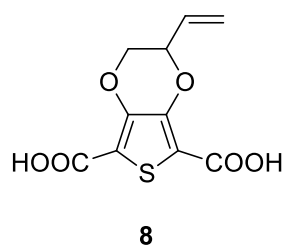
(100 MHz, CDCl₃): δ (ppm) 160.7, 146.7, 144.7, 130.5, 120.4, 111.8, 111.6, 74.2, 67.8, 61.3, 61.2, 14.2 (Figure A.20, Appendix A). IR (ATR, cm⁻¹): 2983 (-CH st), 1702 (C=O st), 1502, 1453 (C=C st), 1268 (C(O)-O st) (Figure A.21, Appendix A). MS: [M+Na]⁺ m/z = 335.27 (Figure A.22, Appendix A).

2.3.9 2-(hydroxymethyl)-2,3-dihydrothieno[3,4-*b*][1,4]dioxine-5,7-dicarboxylic acid (7)



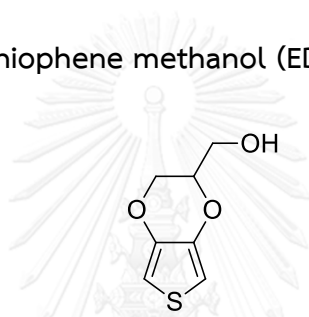
Compound **5** (0.33 g, 1.0 mmol) was mixed with 1 mL EtOH and 10 mL of 1M NaOH. The reaction was stirred and refluxed for 3 h under nitrogen atmosphere and then cooled to room temperature. The precipitate was collected by filtration and washed with water to obtain compound **7** as a white solid (0.243 g, 90 %). ¹H NMR (400 MHz, DMSO-*d*₆): δ (ppm) 13.15 (m, 1H), 5.15 (s, 1H), 4.41 (d, *J* = 11.8 Hz, 1H), 4.29 (s, 1H), 4.15 (dd, *J* = 11.7 Hz, 1H), 3.65 (m, 2H) (Figure A.23, Appendix A). ¹³C NMR (100 MHz, DMSO-*d*₆): δ (ppm) 161.6, 144.7, 144.5, 111.4, 74.17, 65.4, 64.2, 59.3 (Figure A.24, Appendix A). IR (ATR, cm⁻¹): 3553 (-OH st), 2938 (-CH st), 1652 (C=O st), 1079 (-C-O st) (Figure A.25, Appendix A).

2.3.10 2-vinyl-2,3-dihydrothieno[3,4-*b*][1,4]dioxine-5,7-dicarboxylic acid (8)



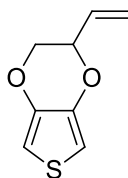
Compound **6** (0.312 g, 1.0 mmol) was mixed with 1 mL EtOH and 10 mL of 1M NaOH. The reaction was stirred and refluxed for 3 h under nitrogen atmosphere, cooled to room temperature. The precipitate was collected by filtration and washed with water to obtain compound **8** as a pale yellow powder (0.243 g, 90 %). ^1H NMR (400 MHz, $\text{DMSO-}d_6$): δ (ppm) 5.91 (m, 1H), 5.48 (d, $J = 17.3$ Hz, 1H), 5.31 (d, $J = 10.7$ Hz, 1H), 4.80 (m, 1H), 4.38 (m, 1H), 4.04 (m, 1H) (**Figure A.26, Appendix A**). ^{13}C NMR (100 MHz, $\text{DMSO-}d_6$): δ (ppm) 161.1, 144.5, 144.0, 132.4, 122.4, 119.4, 112.8, 74.1, 67.3 (**Figure A.27, Appendix A**) IR (ATR, cm^{-1}): 3455 (broad, O-H st), 1664 (C=O st) (**Figure A.28, Appendix A**).[34]

2.3.11 3,4-ethylenedioxythiophene methanol (EDTM)



A mixture of compound **7** (0.254 g, 1.0 mmol) and diazobicycloundecane (DBU) (1.2 mL, 8.0 mmol) in dimethylacetamide (DMA) (2 mL) was heated in sealed vessel in a microwave reactor 150°C, 200 W for 1 h. After cooling to room temperature, the mixture was added by 10% hydrochloric acid solution (10 mL) and then extracted twice with EtOAc. The combined organic layers were dried over anhydrous MgSO_4 . The crude mixture was purified by column chromatography using hexane: ethyl acetate (3: 2) as eluent to yield the product as yellow oil (0.066 g, 38%). ^1H NMR (400 MHz, CDCl_3): δ (ppm) 6.27 (s, 2H), 4.15 (m, 2H), 4.02 (m, 1H), 3.77 (m, 2H), 1.94 (s, 1H) (**Figure A.29, Appendix A**). ^{13}C NMR (100 MHz, CDCl_3) δ (ppm): 141.4, 100.2, 99.8, 74.1, 65.7, 61.6 (**Figure A.30, Appendix A**). IR (ATR, cm^{-1}): 3386 (-OH st), 3114 (-CH st), 2923, 1485 (C=C st), 1183 (-C-O st) (**Figure A.31, Appendix A**).[35]

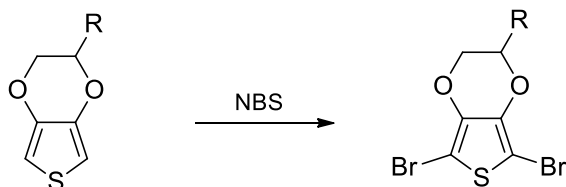
2.3.12 2-vinyl-2,3-dihydrothieno[3,4-*b*][1,4]dioxine (9)



9

A mixture of compound **8** (0.256 g, 1.0 mmol), cuprous oxide (Cu_2O) (0.025 g, 0.17 mmol), 10 mL quinoline and 8 mL DMSO was stirred and refluxed for 6 h under nitrogen atmosphere. After cooling to room temperature, the mixture was filtered and poured into an excess of 10% hydrochloric acid solution. The product was extracted with ethyl acetate, washed with 10% hydrochloric acid and water. The solvent was removed under reduced pressure after drying the organic layer over anhydrous MgSO_4 . The product was purified by column chromatography using dichloromethane: hexane (1: 4) as eluent to give compound **9** as pale yellow oil (0.043 g, 26%). ^1H NMR (400 MHz, CDCl_3): δ (ppm) 6.35 (s, 1H), 6.33 (s, 1H), 5.88 (m, 1H), 5.54 (d, $J = 17.3$ Hz, 1H), 5.40 (d, $J = 10.7$ Hz, 1H), 4.63 (m, 1H), 4.20 (m, 1H), 3.90 (m, 1H) (**Figure A.32, Appendix A**). ^{13}C NMR (100 MHz, CDCl_3) δ (ppm): 141.7, 141.4, 131.9, 119.5, 99.7, 74.1, 67.9 (**Figure A.33, Appendix A**). IR (ATR, cm^{-1}): 2915 (-CH st), 1478 (C=C st), 1179 (C-O st) (**Figure A.34, Appendix A**).[34]

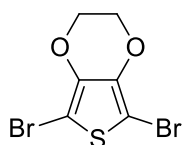
2.3.13 α -Brominations of thiophene derivatives



General procedure: 2.5 equivalents of *N*-bromosuccinimide (NBS) were added to a stirred solution of thiophene precursor (1.0 mmol) in dichloromethane (10 mL) at room temperature. After completion, the reaction mixture was quenched by adding saturated NaHCO_3 solution. The organic layer was separated and the aqueous layer

was extracted with dichloromethane three times. Then the combined organic layers were washed with 2 M NaOH three times. After drying over anhydrous MgSO_4 , the solution was evaporated using rotary evaporator and then purified by column chromatography to obtain the corresponding dibromothiophene.[35]

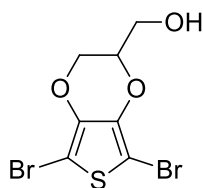
2.3.13.1 2,5-Dibromo-3,4-ethylenedioxythiophene (10)



10

Following the general procedure; 3,4-ethylenedioxythiophene (EDOT) (0.142 g, 1.0 mmol) and NBS (0.445 g, 2.5 mmol) in dichloromethane (10 mL) were mixed for 2 min. The crude mixture was purified by column chromatography, eluted with 3: 2 mixture of hexane and ethyl acetate to get a light yellow solid of product (0.290 g, 98%). mp. 96-97 °C; ^1H NMR (400 MHz, CDCl_3): δ (ppm) 4.27 (s, 4H) (**Figure A.35, Appendix A**). ^{13}C NMR (100 MHz, CDCl_3): δ (ppm) 139.7, 85.5, 64.9 (**Figure A.36, Appendix A**). IR (ATR, cm^{-1}): 2923 (CH st), 1505 (C=O st), 1080 (C-O st) (**Figure A.37, Appendix A**). MS: $[\text{M}+\text{H}]^+$ m/z = 299.20 (**Figure A.38, Appendix A**).[15]

2.3.14.2 2,5-Dibromo[3,4-b]-1,4-dioxin-2-yl methanol (11)

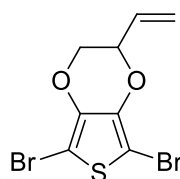


11

Following the general procedure; EDTM (0.172 g, 1.0 mmol) and NBS (0.4450 g, 2.5 mmol) in dichloromethane (10 mL) were mixed for 2 min. The crude mixture was purified by column chromatography, eluted with ethyl acetate to get a pale yellow liquid of product (0.30 g, 90%). ^1H NMR (400 MHz, CDCl_3): δ (ppm) 4.24 (m, 2H), 4.10

(m, 1H), 3.84 (m, 2H), 1.99 (s, 1H) (Figure A.39, Appendix A). ^{13}C NMR (100 MHz, CDCl_3): δ (ppm) 139.5, 85.6, 85.5, 74.6 65.1, 61.4 (Figure A.40, Appendix A). MS: $[\text{M}+\text{H}]^+$ m/z = 329.09 (Figure A.41, Appendix A).[17]

2.3.13.3 5,7-dibromo-3-vinyl-2,3,4a,5-tetrahydrothieno[3,4-*b*][1,4]dioxine (12)

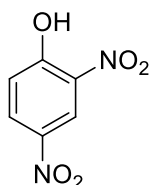


12

Following the general procedure; compound **9** (0.172 g, 1.0 mmol) and NBS (0.445 g, 2.5 mmol) in dichloromethane (10 mL) were mixed for 5 min. The crude mixture was purified by column chromatography, eluted with ethyl acetate to get a pale yellow liquid of product (0.250 g, 77%). ^1H NMR (400 MHz, CDCl_3): δ (ppm) 5.93-5.82 (m, 1H), 5.55 (d, J = 17.4 Hz, 1H), 5.44 (d, J = 10.7 Hz, 1H), 4.67 (s, 1H), 4.26 (d, J = 12.2 Hz, 1H), 4.00-3.92 (m, 1H) (Figure A.42, Appendix A). ^{13}C NMR (100 MHz, CDCl_3): δ (ppm) 139.6, 130.7, 120.4, 85.5, 85.4, 74.6, 68.1 (Figure A.43, Appendix A). IR (ATR, cm^{-1}): 2913 (-CH st), 1499, 1406, 1305 (C=C st), 1060 (C-O st) (Figure A.44, Appendix A).[35]

2.4 Preparation of template molecules

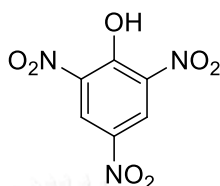
2.4.1 2,4-Dinitrophenol (DNP)



p-Nitrophenol (PNP, 1.000 g, 0.007 mol) was added into concentrated nitric acid (8 mL) at $-5\text{ }^\circ\text{C}$ in ice-salt bath and stirred the mixture for 30 min. The reaction was allowed to warm and stir at room temperature for 5 h. It was quenched by adding 10

mL saturated NaHCO_3 solution. The obtained yellow precipitate was filtered and washed with water to obtain a yellow solid product (1.288 g, 92%). mp. 108-109°C; ^1H NMR (400 MHz, CDCl_3): δ (ppm) 7.18 (d, 1H), 8.75 (d, 1H), 9.02 (s, 1H), 11.02 (s, 1H) (Figure A.45, Appendix A) UV: $\lambda_{\text{max}} = 262$ nm (Figure A.46, Appendix A).[36].

2.4.2 2,4,6-Trinitrophenol (TNP)



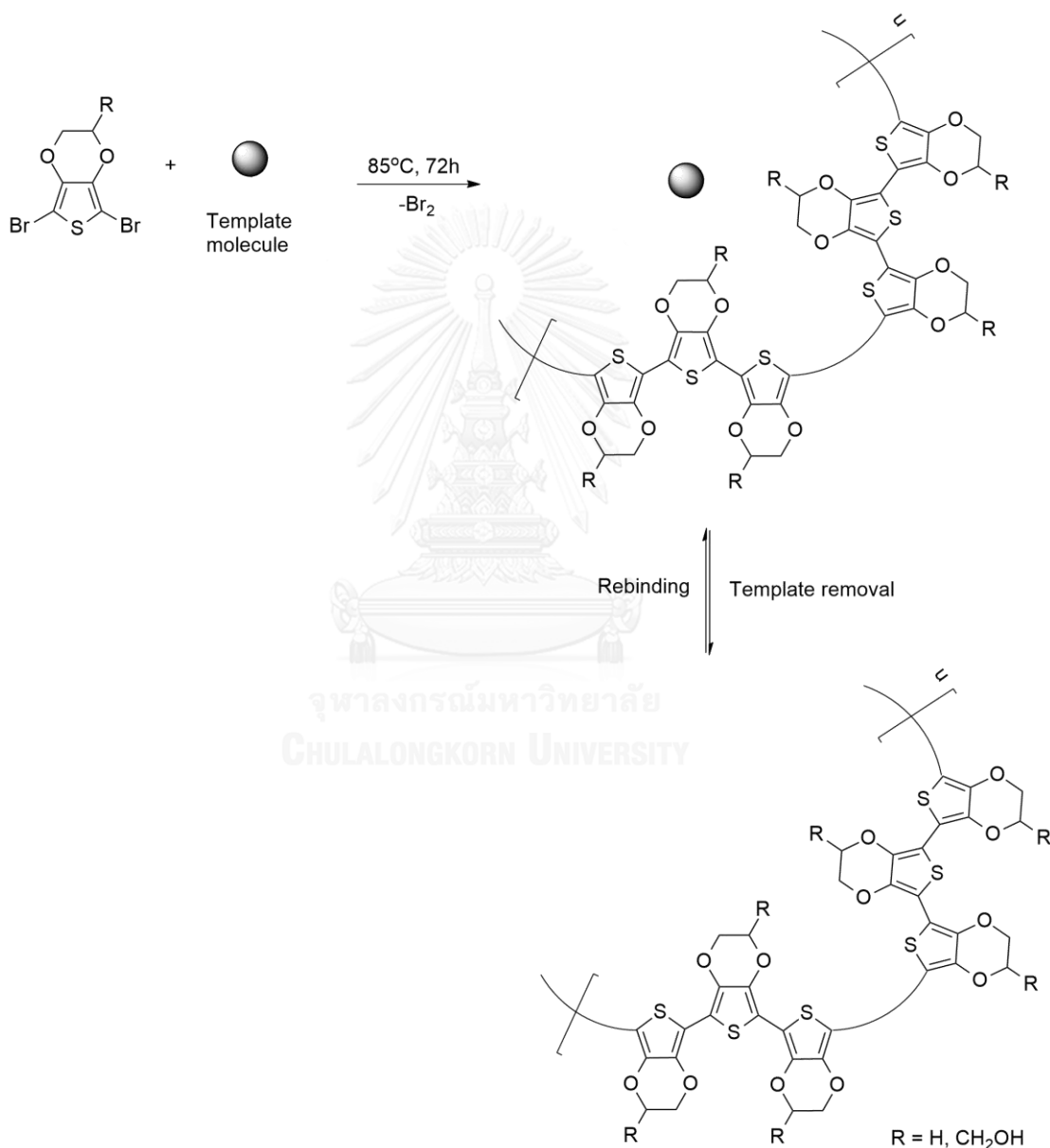
DNP (1.000 g, 0.005 mol) was added into concentrated nitric acid (8 mL) at room temperature and stirred the mixture for 48 h. It was quenched by adding 10 mL saturated NaHCO_3 solution. The obtained yellow precipitate was filtered and washed with water to obtain a yellow crystalline solid product (1.097 g, 67%). mp. 122-123°C; ^1H NMR (400 MHz, CDCl_3): δ (ppm) 9.21 (s, 2H), 11.91 (s, 1H) (Figure A.47, Appendix A) UV: $\lambda_{\text{max}} = 254$ nm (Figure A.48, Appendix A) [36].

2.5 Preparation of molecularly imprinted polymers (MIPs)

2.5.1 Molecularly imprinted polymer of PEDOT

The selected template molecule 1000 ppm {PNP (0.010 g, 0.071 mmol), DNP (0.010 g, 0.054 μmol), TNP (0.010 g, 0.043 mmol) or pyrene (0.010 g, 0.049 mmol)} was added to 10 mL ethyl acetate solution of DBEDOT (0.299 g, 1.0 mmol). The rotary evaporator was used to remove solvent from the homogeneous mixture, resulting in a white solid substance. Subsequently, the obtained product was heated at 85°C for 72 h. During the heating process, the solid turned into dark blue with slight appearance of brown bromine vapor. After the heating, the resulting dark blue solid was allowed to cool to room temperature in a desiccator as the molecularly imprinted polymers of the template. In order to measure the specific binding abilities of MIPs, non-imprinted polymers (NIPs) were prepared similarly to MIPs in parallel, but in the absence of the template molecules. After the polymerization processes, both MIPs

and NIPs samples were exhaustively extracted by soxhlet extraction with ethyl acetate or methanol for approximately 16 h or until no template molecules and leftover monomers were detected by TLC and UV-Vis spectroscopy. The template-vacant polymer samples were kept dry in desiccator overnight. The dried polymers were characterized by IR (Figure A.49, Appendix A) and UV (Figure A.50, Appendix A).



Scheme 2.1 Imprinting template molecules through SSP process

2.5.2 Molecularly imprinted copolymer of PEDOT+ PEDTM

The template molecule, PNP (0.010 g, 0.071 mmol) was added to 10 mL ethyl acetate solution of the mixture of **11** (0.066 g, 0.2 mmol) and **10** (0.239 g, 0.8 mmol). The rotary evaporator was used to remove solvent from the homogeneous mixture, resulting in a yellow solid substance. Subsequently, the obtained product was heated at 85 °C for 72 h. After the heating, the resulting dark blue solid was allowed to cool to room temperature in a desiccator as the PNP imprinted 20:80 PEDTM:PEDOT copolymers (20% coMIP). The process was repeated with the mixture of **11** (0.132 g, 0.4 mmol) and **10** (0.179 g, 0.6 mmol) to obtain PNP imprinted 40:60 PEDTM:PEDOT copolymer (40% coMIP). Non-imprinted copolymers (coNIPs) were also prepared similarly to coMIPs in parallel, but in the absence of PNP. After the polymerization processes, all coMIPs and coNIPs samples were exhaustively extracted by soxhlet extraction with methanol (250 mL) for approximately 16 h or until no template molecules and leftover monomers were detected by TLC and UV-Vis spectroscopy. The template-vacant polymer samples were kept dry in desiccator overnight. The dried polymers were characterized by IR (**Figure A.51, Appendix A**) and UV (**Figure A.52, Appendix A**).

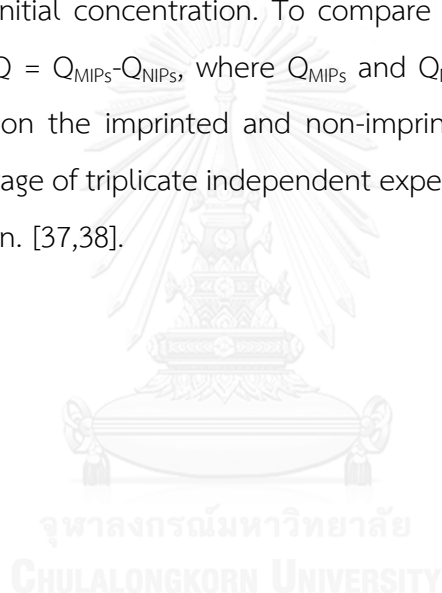
2.6 Binding experiments

Five exact concentrations of the template solutions in the range of 800-1000 ppm were prepared and measured their UV-Visible absorption to obtain a calibration curve of the template. In particular, the binding processes are monitored by UV-Vis spectroscopy, measuring at the λ_{\max} of 306, 262, 254 and 273 nm for PNP, DNP, TNP and pyrene templates, respectively (**Figure A.53** for PNP, **A.46** for DNP, **A.48** for TNP and **A.54** for pyrene, **Appendix A**). Calibration curves of all templates were prepared and measured by plotting a graph between absorbances and concentrations of template solutions. (**Figure B.1-B.4, Appendix B**) Linear relationships were obtained and employed for subsequent calculations of ΔQ , Q_{MIPs} , and Q_{NIPs} values.

Then 50 mL of 1000 ppm of the template solution was added to each of the corresponding MIP and NIP samples. These mixtures were stirred at room temperature.

At every hour, 20 μL from each solution was drawn and diluted to a suitable concentration before being measured the absorbance of the template. The measurements of template absorbance were done until the value reached the equilibrium and remained relatively constant (approximately 8-15 h). The amount of binding capacities of the MIP was examined by extracting out the bound template molecules from the equilibrated MIP and NIP samples by soxhlet extraction with methanol for 8 h.

The amount of template molecules bound to the imprinted polymer (Q) was calculated by subtracting the average concentration of unbound substrate obtained at equilibrium from its initial concentration. To compare imprinting effect, the specific adsorption values: $\Delta Q = Q_{\text{MIPs}} - Q_{\text{NIPs}}$, where Q_{MIPs} and Q_{NIPs} are the amount of bound template molecules on the imprinted and non-imprinted polymers at equilibrium, respectively. The average of triplicate independent experiments was employed for the analysis and discussion. [37,38].

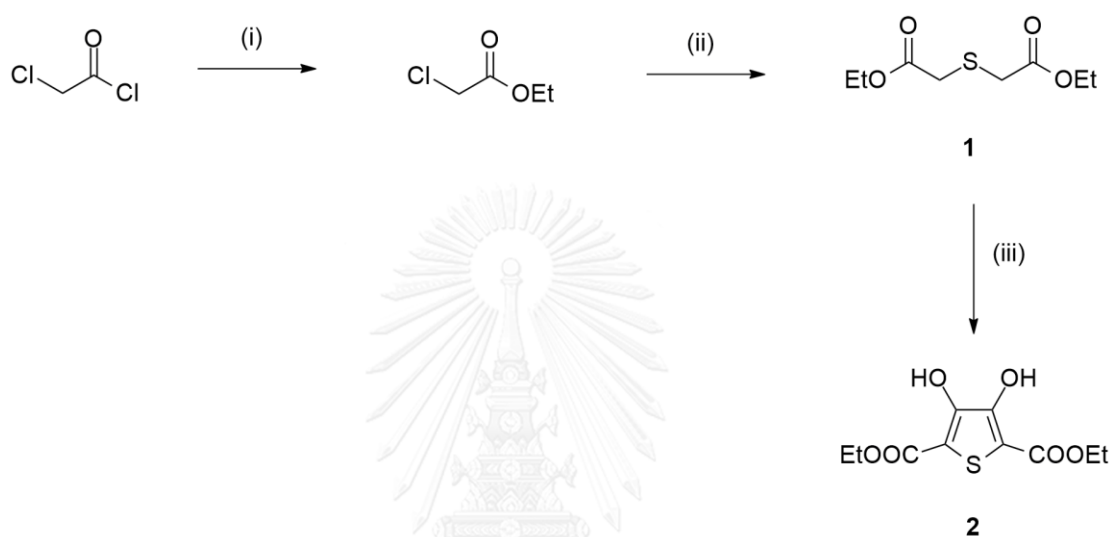


CHAPTER III

RESULTS AND DISCUSSION

3.1 Monomer Synthesis

3.1.1 Synthesis of Diethyl 3,4-dihydroxythiophene-2,5-dicarboxylate (3)



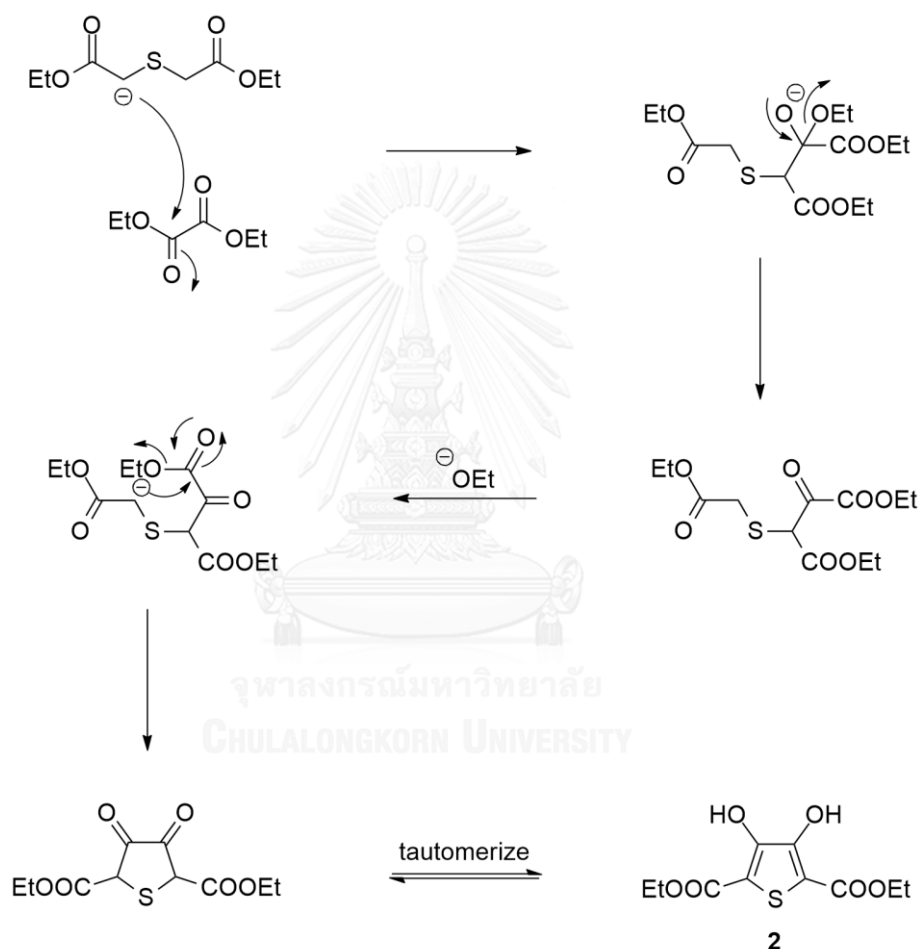
Reagents and conditions: (i) absolute EtOH, rt; (ii) Na₂S.9H₂O, acetone, reflux, 3h;
(iii) NaOEt, 0.5 h, (CO₂Et)₂, reflux 3 h.

Scheme 3.1 Synthesis of Diethyl 3,4-dihydroxythiophene-2,5-dicarboxylate 2

The reaction of chloroacetyl chloride and EtOH obtained an almost quantitative yield of ethyl chloroacetate as colorless liquid. This reaction underwent the bimolecular nucleophilic acyl substitution. The presence of quartet and triplet signals of the newly added ethyl group appeared at 4.24 and 1.29 ppm in the ¹H NMR spectrum (Figure A.1, Appendix A) and 62.2 and 14.0 ppm in the ¹³C NMR spectrum (Figure A.2, Appendix A). The solution of ethyl chloroacetate in acetone was treated via double S_N2 reaction with sodium sulfide, resulting in the formation of compound 1, as yellow liquid substance in 56% yield. The ¹H NMR spectrum exhibited methylene peak at 3.37 ppm, and the quartet and triplet signals of the ethyl groups at 4.19 and 1.28 ppm, respectively (Figure A.3, Appendix A). The ¹³C NMR spectrum showed the carbonyl carbon at 169.5 ppm (Figure A.4, Appendix A). Finally, the formation of

compound **1** was supported by the mass value from MS in the positive mode at 229.05 amu $[M+Na]^+$. (Figure A.5, Appendix A). [31]

Hinsberg reaction [32], which is a condensation of **1** with diethyl oxalate under basic condition, was next carried out. The mechanism is the consecutive Claisen condensation reactions to produce a diketone intermediate, which readily tautomerizes to the corresponding dihydroxythiophene (Scheme 3.2).

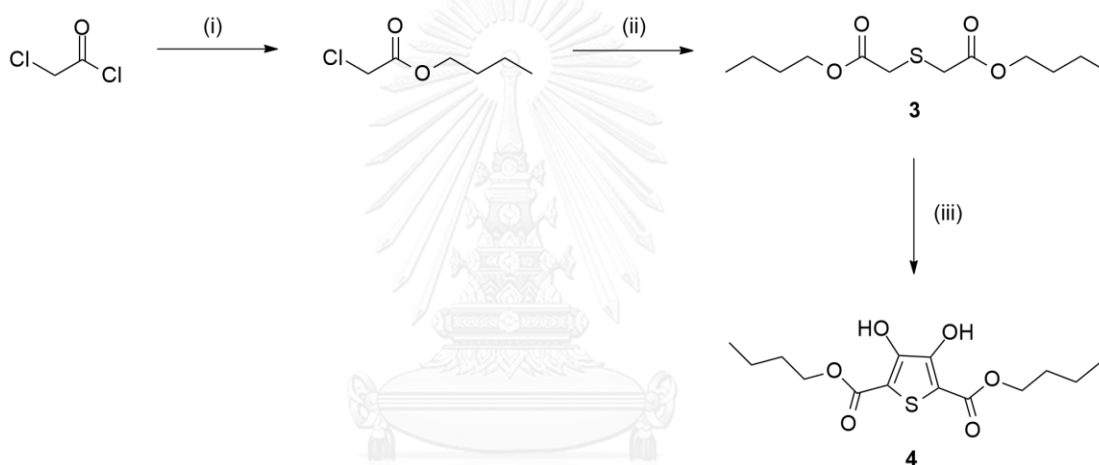


Scheme 3.2 Mechanism of Hinsberg reaction

The physical appearance of the obtained compound **2** was white needle crystals with 61% yield after recrystallization in methanol. The ^1H NMR displayed a broad singlet $-\text{OH}$ peak at 9.36 ppm (Figure A.6, Appendix A). The ^{13}C NMR spectrum showed a peak of the carbonyl carbon at 165.5 ppm, and the two carbons of the thiophene ring appeared at 107.1 and 151.6 ppm (Figure A.7, Appendix A).

Additionally, the IR spectrum exhibited a significantly strong broad $-OH$ stretching at 3305 cm^{-1} , and the aromatic double bond region at 1690 and 1663 cm^{-1} (**Figure A.8, Appendix A**). The mass spectrum of compound **2** showed at $[M+H]^+$ $m/z = 250.20$. (**Figure A.9, Appendix A**) This intermediate **2** was originally planned to be used in a subsequent 3-step synthesis of 3,4-ethylenedioxythiophene (EDOT). However, due to the time limit, the planned synthesis has never been carried out. Instead, the commercially available EDOT was used for further reactions and preparations of the derived polymers in the rest of this work.

3.1.2 Synthesis of dibutyl 3,4-dihydroxythiophene-2,5-dicarboxylate (**4**)



Reagents and conditions: (i) *n*-BuOH, rt; (ii) $\text{Na}_2\text{S}\cdot 9\text{H}_2\text{O}$, acetone, reflux, 4h; (iii) $\text{NaO-}n\text{-Bu}$, 0.5 h, $(\text{COOEt})_2$, reflux 4 h.

Scheme 3.3 Synthesis of dibutyl 3,4-dihydroxythiophene-2,5-dicarboxylate **4**

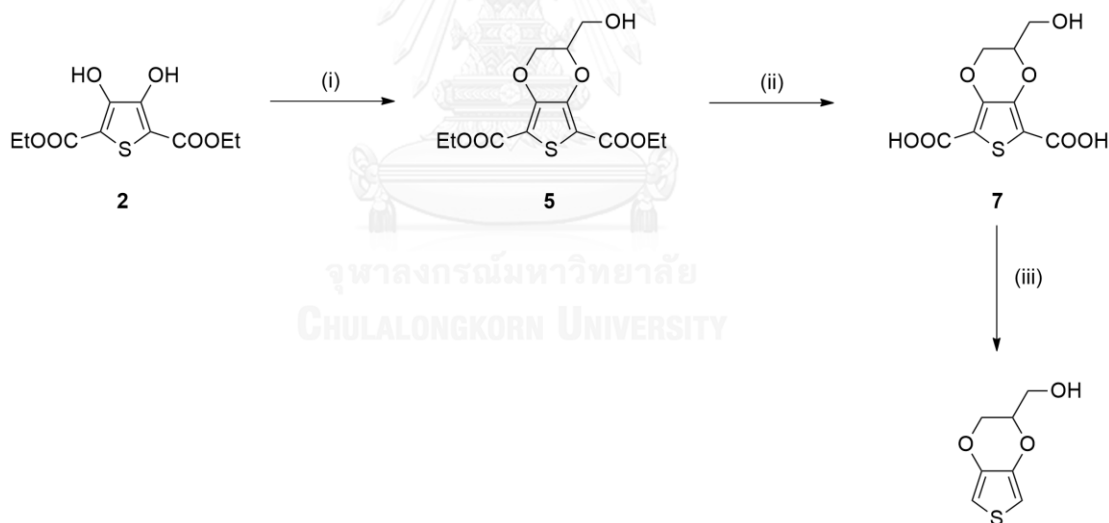
Similar to ethyl chloroacetate, the reaction of chloroacetyl chloride and *n*-BuOH obtained 69% yield of butyl chloroacetate as colorless liquid. The singlet signal of methylene peak at 4.14 ppm, and the butyl groups at 4.03, 1.60, 1.34 and 0.89 ppm, were present in the ^1H NMR spectrum (**Figure A.10, Appendix A**) ^{13}C NMR spectrum matched well with the structure and that from literature (**Figure A.11, Appendix A**). [40]

The solution of butyl chloroacetate in acetone was treated with sodium sulfide [41], resulting in the formation of compound **3**, as yellow liquid in 46% yield. The ^1H

NMR and ^{13}C NMR spectra of the product were similar to those of the starting material except the signals of methylene peak appeared at 3.27 ppm (**Figure A.12** for ^1H NMR and **A.13** for ^{13}C NMR, **Appendix A**).

Dibutyl 3,4-dihydroxythiophene-2,5-dicarboxylate **4** was planned to replace compound **2** with an expectation of better solubility in organic solvent. It was also made from Claisen condensation of **3** and diethyl oxalate as crude brown liquid. The ^1H NMR and ^{13}C NMR spectra displayed quite complicate signals of the unpure product. (**Figure A.14** for ^1H NMR and **Figure A.15** for ^{13}C NMR, **Appendix A**). Due to the solubility of compound **2** was badly in organic solvent then side chain added of butyl derivatives. Unfortunately, the purification of compound **4** is very difficult and yield of the product was expected to be relatively low. Further synthetic improvement and use of this intermediate were then abandoned.

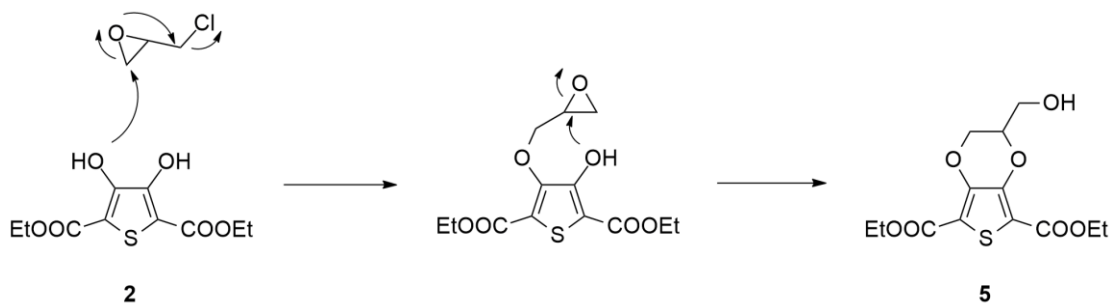
3.1.3 (2,3-Dihydrothieno[3,4-*b*][1,4]dioxin-2-yl)methanol (EDTM)



Reagents and conditions: (i) epichlorohydrin, K_2CO_3 , EtOH, MW 120°C 1.5 h; (ii) 1M NaOH, EtOH, reflux 4 h; (iii) DBU, DMA, MW 150°C 1 h.

Scheme 3.4 Synthesis of (2,3-dihydrothieno[3,4-*b*][1,4]dioxin-2-yl)methanol (EDTM)

To prepare compound **5**, **2** was reacted with slightly excess epichlorohydrin via double S_N2 mechanism as shown in **Scheme 3.5**. The synthesis of compound **5** was optimized in various conditions as shown in **Table 3.1**.



Scheme 3.5 Mechanism of the substitutions on epichlorohydrin

Table 3.1 Conditions for the synthesis of compound **5**

Entry	Epichlorohydrin (equiv)	Base (equiv)	Heating method	Time (h)	Yield (%)
1	3.5	K ₂ CO ₃ (2.0)	Reflux	72	10
2	3.5	K ₂ CO ₃ (2.0)	MW	1.5	28
3	0.5	K ₂ CO ₃ (1.0)	Reflux	72	-
4	0.5	C ₂ H ₅ ONa (1.0)	Reflux	3	3

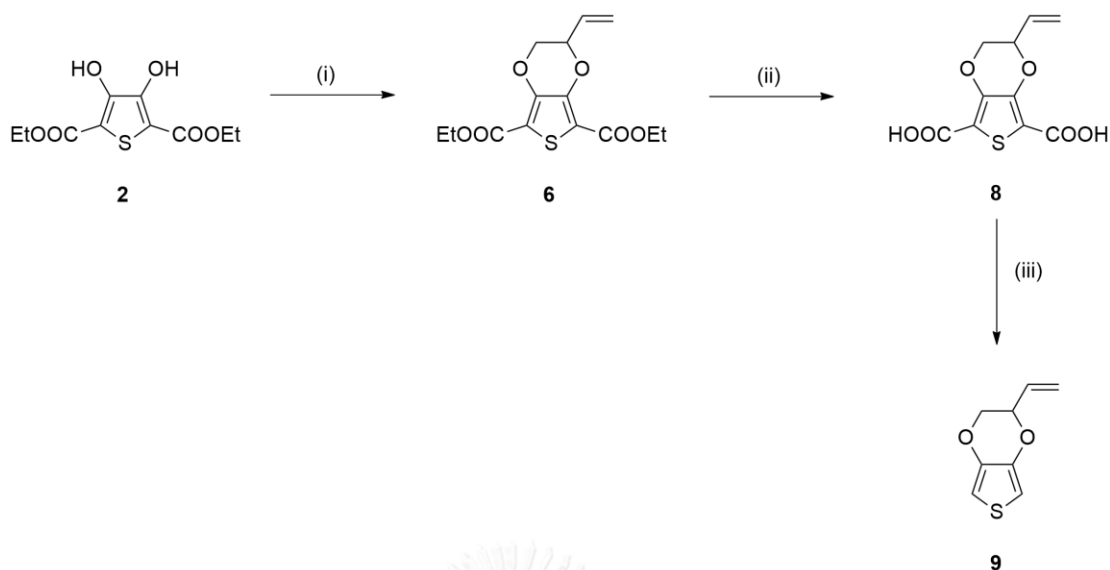
The best heating method appeared to be using MW, giving the product in 28% yield. Prolong reflux was assumed to convert **5** to other by-products by further reactions with excess epichlorohydrin. Lower amount of the reagent didn't solve the problem, but instead rendered the reaction to incompleteness (**Entries 3-4, Table 3.1**). The signal in ¹H NMR spectrum at 9.36 ppm which corresponds to hydrogen signal of -OH groups of **2** was absent and new multiplet signals appeared at 4.47, 4.36 and 4.27 ppm. (**Figure A.16, Appendix A**). The ¹³C NMR spectrum matched well with the structure and that from literature (**Figure A.17, Appendix A**). IR spectra and the results matched well with those reported in the literature (**Figure A.18, Appendix A**).[33, 39].

Compound **7** was synthesized from hydrolysis of diethyl ester **5** in 90% yield with no chromatographic purification needed. The ^1H NMR and ^{13}C NMR spectra of the product were similar to those of the starting material except the absence of the signals of the ethyl groups (**Figure A.23 and A.24, Appendix A**). IR spectrum showed the characteristic strong carbonyl C=O stretching peak at 1652 cm^{-1} and the strong broad band of carboxylic O-H stretching peak (**Figure A.25, Appendix A**).

EDTM was finally synthesized by decarboxylation of dicarboxylic acid precursor **7**. The mixture of compound **7** and DBU in DMA was heated in a sealed vessel in a microwave reactor to obtain the product as pale yellow liquid in 38% yield. [39] Some insoluble dark-blue solid was observed which was assumed to be the polymer PEDTM, probably resulted from self-polymerization. The ^1H NMR, ^{13}C NMR and IR spectra of the product matched well with those reported in the literature (**Figure A.29-A.31, Appendix A**). [39]

3.1.4 2-Vinyl-2,3-dihydrothieno[3,4-*b*][1,4]dioxine (**9**)

Compound **6** was synthesized in good yield through double nucleophilic substitutions from compound **2**, *trans*-1,4-dibromo-2-butene and base. The ^1H NMR spectrum displayed a multiplet signal at 5.87 ppm and the doublet signals at 5.54 and 5.39 ppm assigned to the vinyl group (**Figure A.19, Appendix A**). The vinyl carbons appeared at 130.5 and 120.4 ppm in ^{13}C NMR spectrum (**Figure A.20, Appendix A**). IR spectrum showed no strong broad band of -OH group at 3293 cm^{-1} (**Figure A.21, Appendix A**). The mass spectrum of compound **6** showed the molecular ion peak $[\text{M}+\text{Na}]^+$ at m/z 335.27 (**Figure A.22, Appendix A**).



Reagents and conditions: (i) 1.5 equiv. *trans*-1,4-dibromo-2-butene, 0.1 equiv. DMAP, K_2CO_3 , DMF reflux 1 h; (ii) 1M NaOH, EtOH, reflux 3 h; (iii) 0.17 equiv. Cu_2O , quinoline, DMSO, reflux 6 h.

Scheme 3.6 Synthesis of compound 9

Compound **8** was synthesized from hydrolysis of diethyl ester **6** in 90% yield. The 1H NMR and ^{13}C NMR spectra of the product were quite similar to those of the starting material except the absence of the signals of the ethyl groups (**Figure A.26 and A.27, Appendix A**). IR spectra showed the characteristic strong carbonyl $C=O$ stretching peak at 1664 cm^{-1} and strong broad band of carboxylic O-H stretching peak (**Figure A.28, Appendix A**). [34]

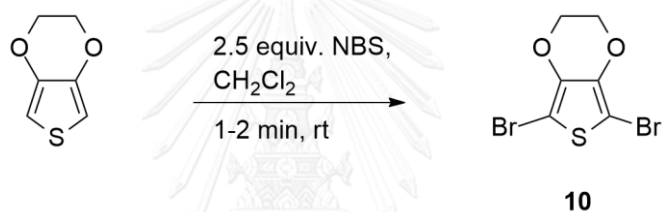
The decarboxylation procedure was modified from the existing protocols to minimize the amount of quinoline solvent, that was very hard to be removed from the obtained product [34]. Compound **9** was prepared in 59.5% yield through this procedure on compound **8** using copper(I) oxide and 1.5% quinoline in DMSO. It was assumed that part of compound **9** may be lost during the repeated aqueous washes of the leftover DMSO solvent and column chromatography purification.

Compound **9** was structurally confirmed by the presence of the singlet of α -protons of thiophene ring at 6.35 and 6.33 ppm in 1H NMR spectrum and also the disappearance of the carboxyl functional group signals from both 1H NMR and ^{13}C NMR

spectra (Figure A.32 and A.33, Appendix A). The carbonyl stretching peaks were no longer observed in its IR spectrum (Figure A.34, Appendix A). The presence of the vinyl group was expected to allow many useful modifications to add more functions to the polymer derived from this monomer.

3.1.5 Bromination of thiophene derivatives

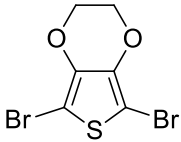
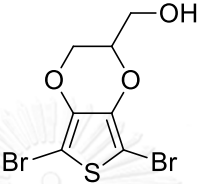
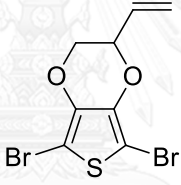
Commonly, the α -positions of thiophene ring are reactive towards electrophiles or radicals, particularly those of the electron-rich thiophenes. 3,4-Ethylenedioxythiophene (EDOT) was efficiently brominated at room temperature employing *N*-bromosuccinimide (NBS), resulting in the formation of compound **10**, which required only 1-2 min in accordance with the Scheme 3.7. [17]



Scheme 3.7 Synthesis of compound **10**

This method of treating with NBS in a halogenated solvent (CH₂Cl₂) at room temperature and ambient atmosphere provided the most promising yields of most electron-rich thiophene brominations in excellent yields (Table 3.2). The extended time of this reaction was found to result in degrading of the product and lower yields were obtained [35,17].

Table 3.2 Dibromination results of 3,4-dialkoxythiophene derivatives

Entry	Product	Yield (%)
1	 10	98
2	 11	90
3	 12	77

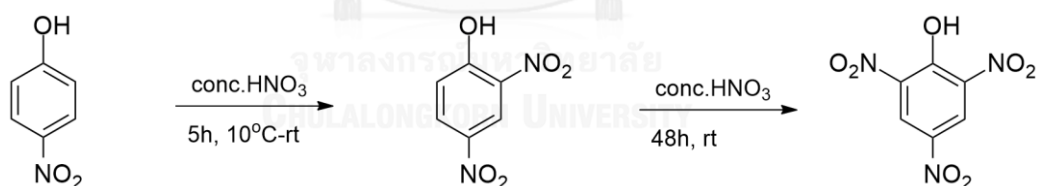
The product **10** was characterized by ^1H NMR and ^{13}C NMR spectrum with the absence of the signal at δ 6.32 ppm, which corresponds to the α -hydrogen signal of the precursor. (Figure A.35-A.36, Appendix A) IR spectra of product matched well with those of previous report. (Figure A.37, Appendix A) [30] The mass spectrum of compound **10** showed the molecular ion peak $[\text{M}+\text{H}]^+$ at m/z 299.20. (Figure A.38, Appendix A)

Similar results were obtained for compound **11** and **12**. The ^1H NMR and ^{13}C NMR spectra of compound **11** were quite similar to those of the starting material except the absence of the α -hydrogen signals on the thiophene ring (Figure A.39 and A.40, Appendix A). The mass spectrum of compound **11** showed the molecular ion peak $[\text{M}+\text{H}]^+$ at m/z 329.09 (Figure A.41, Appendix A). [17]

The structure of compound **12** was confirmed by NMR spectroscopy. In ^1H NMR, the α -hydrogen signals on the thiophene ring at 6.35 and 6.33 ppm were absent after bromination (Figure A.42, Appendix A). ^{13}C NMR spectrum matched well with the product structure (Figure A.43, Appendix A). The carbonyl stretching peaks were no longer observed in its IR spectrum. (Figure A.44, Appendix A) [35] For compound **12** however, it was observed that increasing the reaction time to 10 minutes was necessary to complete the reaction and give higher yields. Slightly longer time was required probably due to less reactivity of the precursor.

3.2 Preparations of template molecules: 2,4-dinitrophenol (DNP) and 2,4,6-trinitrophenol (TNP)

p-Nitrophenol was readily nitrated with concentrated nitric acid in ice-salt bath at ambient atmosphere (Scheme 3.8) to give DNP as yellow solid in 92% yield [36]. The ^1H NMR spectrum of DNP showed the two doublet signals and singlet signal of aromatic protons at 7.18, 8.75 and 9.02 ppm, respectively. The signal of -OH group appeared at 11.02 ppm. (Figure A.45, Appendix A) $\lambda_{\text{max}} = 262 \text{ nm}$ (Figure A.46, Appendix A)



Scheme 3.8 Synthesis of DNP and TNP

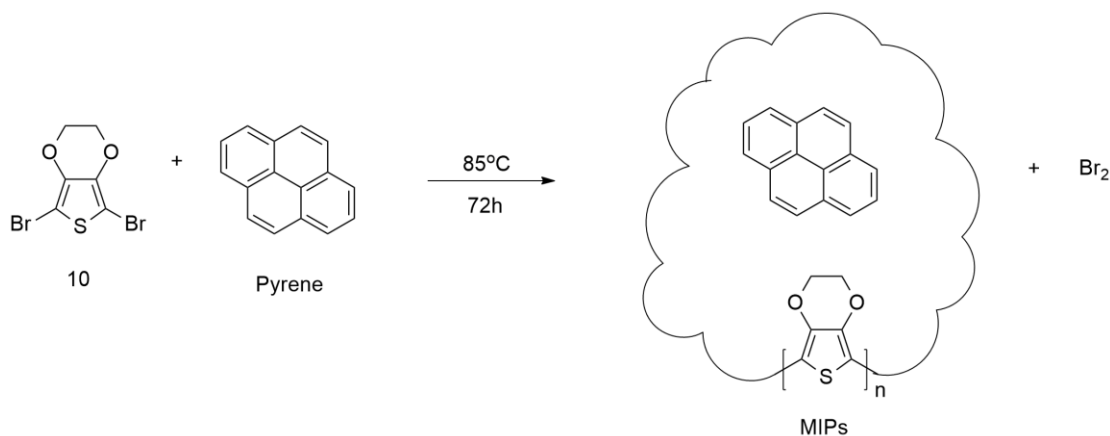
DNP was nitrated with concentrated nitric acid at room temperature. (Scheme 3.8) After completion, the product TNP as yellow solid was obtained in 67% yield [36]. The ^1H NMR spectrum of TNP showed the singlet signal of aromatic protons and the broad signal of -OH group at 9.21 and 11.91 ppm, respectively (Figure A.47, Appendix A) $\lambda_{\text{max}} = 254 \text{ nm}$ (Figure A.48, Appendix A)

3.3 Preparation of molecularly imprinted polymer (MIPs)

Solid state polymerization (SSP) method reported by Meng and coworkers [15] provided readily-doped PEDOT, from heating of the corresponding dibromo derivatives of EDOT monomer. Among the prepared brominated compounds, only **10** is a solid at room temperature and have sufficiently high melting points to be used as the precursor for solid state polymerization to give polymer PEDOT. Nevertheless, the liquid **11** was also successfully turned into the corresponding polymer PEDTM under the same polymerization condition. Unfortunately, the liquid **12** did not turn into polymer after being heated. Therefore, compound **12** was not used in preparing any polymers.

The resulted insoluble SSP-PEDOT and PEDTM, became an ideal framework for molecular imprinting. Theoretically, suitable template molecules were surrounded by the monomer molecules and formed specific cavities that were proper to the trapped templates during the SSP approach. After the templating process, the template molecules were extracted off by exhaustive soxhlet extraction with either ethyl acetate or methanol, resulting in a porous polymer with supposedly vacant specific cavities imprinted by the removed template. As a solid, the SSP method was expected to stabilize and retain the arrangements of the cavities in the polymeric matrices. Then the MIPs were dried and immersed again in template solution to test the specific rebinding process which was monitored by UV-Vis absorption of the template. Non-imprinted polymers (NIPs), which were prepared in parallel following the preceding experiment without the template molecules, were employed in similar experiments for direct comparison to their corresponding MIPs. The amount of template molecules that were bound to the polymers provided the specific absorption values (ΔQ), at various sampling times of MIPs and NIPs, which could be calculated to compare any differential imprinting effects between them.

3.3.1 Pyrene-molecularly imprinted polymers (Pyrene-MIPs)



Scheme 3.9 Synthesis of MIPs with pyrene as the template molecule

Pyrene was chosen to represent a relatively non-polar template. Its MIPs was prepared from SSP of **10** and pyrene blended together in the solid mixture (**Scheme 3.9**).

To quantitatively compare the imprinting effect, we defined the specific adsorption values as:

$$\Delta Q = Q_{MIPs} - Q_{NIPs} \quad (1)$$

$$Q \left(\frac{\mu\text{mol}}{\text{g}} \right) = \left(\frac{C_i - C_e}{W \times MW} \right) \times V \quad (2)$$

Where C_i , the initially measured concentration, and C_e , the equilibrium concentration, can be acquired from the binding experiment. V (mL) is the volume of the solution and W (g) is the weight of the dried polymer, MIPs or NIPs, and MW stands for the molecular weight of the template molecules.

After the binding process, the template molecules were extracted off by exhaustive soxhlet extraction EtOAc and use this concentration to calculate the binding capacity:

$$\left(\frac{Q_e}{Q_i}\right) \times 100\% \quad (3)$$

Where Q_i ($\mu\text{mol/g}$) is the initial amount of template molecules in solution used to prepare MIPs before the binding experiment, and Q_e ($\mu\text{mol/g}$) is the amount of template molecules in solution obtained from exhaustive extraction at the end of the binding process.

During the binding experiment, the concentrations of the sampled pyrene solutions in the presence of pyrene-MIPs were not much different from those of NIPs (**Figure 3.1**). The C_e value was taken from the average of the fluctuated values during 2-12 h which were regarded as the equilibrium region for the pyrene-MIPs binding experiment. The same region was used for the NIPs. The calculation (**Appendix B**) yielded the specific adsorption value (ΔQ) of pyrene molecules bound to the MIPs to be only $7.99 \mu\text{mol/g}$. This rather small value for pyrene differential binding indicated the failure to induce specific binding cavities for pyrene by this process. However, it is possible that EtOAc was not quite suitable to extract off the pyrene after the templating step, and made the binding experiment ineffective. Therefore, MeOH was used for template extraction in another set of experiment (**Figure 3.2**).

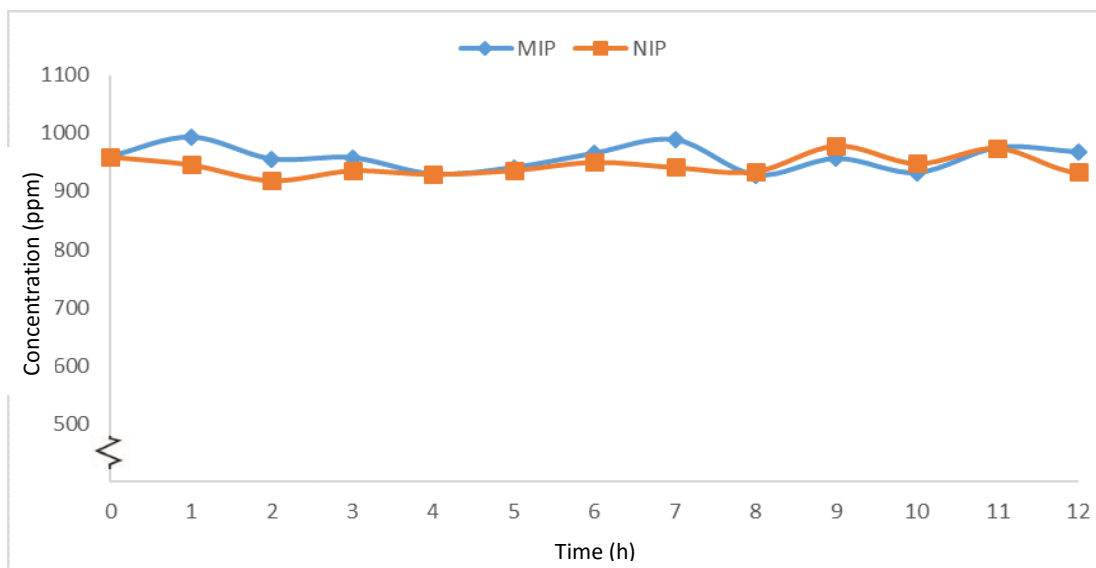


Figure 3.1 The concentrations of pyrene at various sampling times during binding process in the presence of pyrene-MIPs and NIPs, using EtOAc extraction off the template.

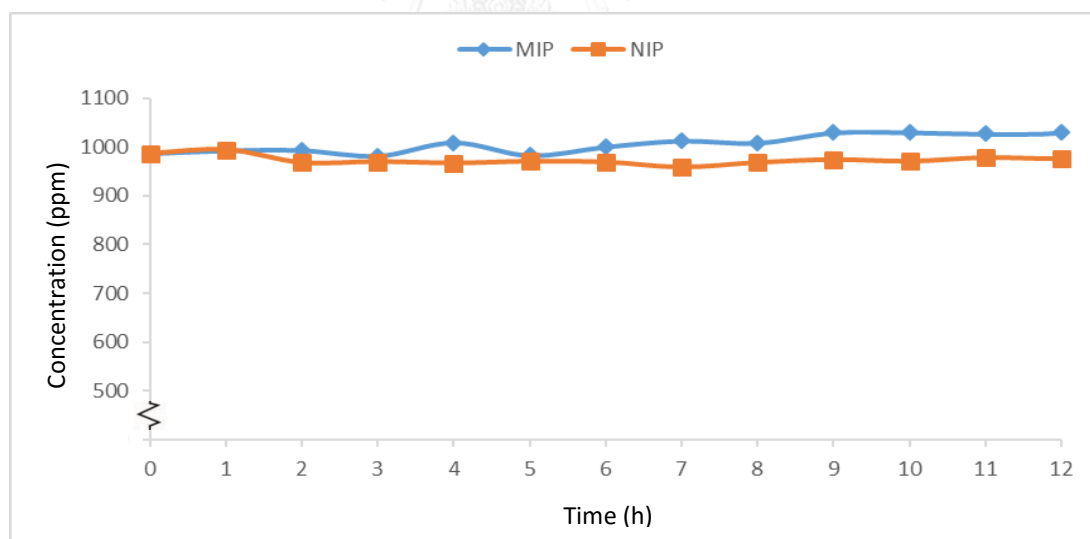
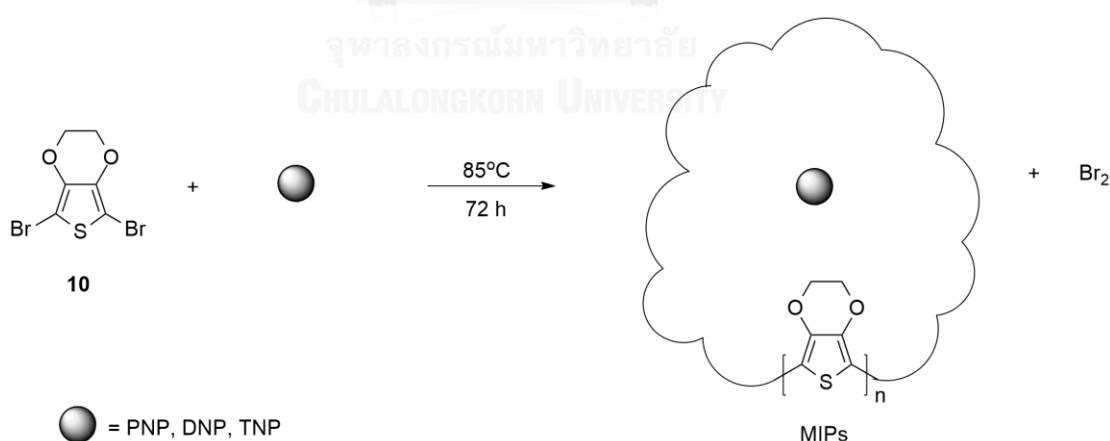


Figure 3.2 The concentrations of pyrene at various sampling times during binding process in the presence of pyrene-MIPs and NIPs, using MeOH extraction off the template.

The differential binding results of MIP and NIP with MeOH removal of template were still disappointingly not as pronounced as the previous one with EtOAc extraction. The concentrations of pyrene from MIPs slightly increased in later samplings, perhaps due to incomplete extraction of template by MeOH. The NIPs only slightly declined at the beginning and largely remained quite constant after 2 h. The average of those sampling values from 2 to 8 h were regarded as the equilibrium region for the binding experiment. The suspected data associated with the possible leach of the remaining pyrene template after 8 h samplings were omitted. The calculation (**Appendix B**) yielded the ΔQ value or the specific adsorption value of pyrene molecules bound to the MIPs to be $-120.53 \mu\text{mol/g}$, suggesting that pyrene, which is relatively non-polar, poorly interacted with the polymer and did not well distributed. Thus, the cavities were not sufficiently created during the MIPs preparation. Methanol was also not a suitable solvent to extract off the template, leading to the erroneous results

3.3.2 *p*-Nitrophenol molecularly imprinted polymers (PNP-MIPs)

PNP was first chosen as the template with polar functional groups. Its MIPs were prepared from SSP of **10** and PNP solid mixture (**Scheme 3.10**).



Scheme 3.10 Synthesis of MIPs with a template molecule

After the templating process, the template molecules were extracted by exhaustive soxhlet extraction with ethyl acetate (**Figure 3.3**).

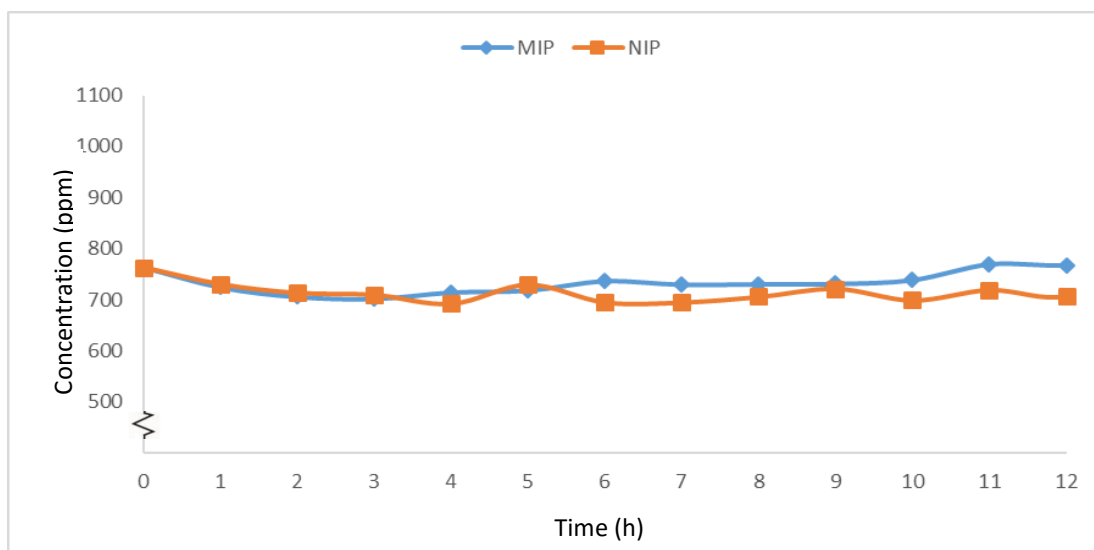


Figure 3.3 The concentrations of PNP at various sampling times during binding process in the presence of PNP-MIPs and NIPs, using EtOAc extraction off the template.

The concentrations of PNP solution in the presence of PNP-MIPs were not distinctive from those of NIPs. The C_e value was taken from the average of the fluctuated values during 2-12 h which were regarded as the equilibrium region for the binding experiment. The calculation (**Appendix B**) yielded the specific adsorption value (ΔQ) of PNP molecules bound to the MIPs to be $-64.86 \mu\text{mol/g}$. This rather small value for PNP template could be due to the unsuccessful imprinting process as had seen earlier for pyrene, or the template may not efficiently extracted. Thus, the solvent for template extraction was changed to methanol, which is more polar and expected to dissolve PNP better. The results from binding experiment of PNP-MIPs after MeOH extraction were shown in **Figure 3.4**.

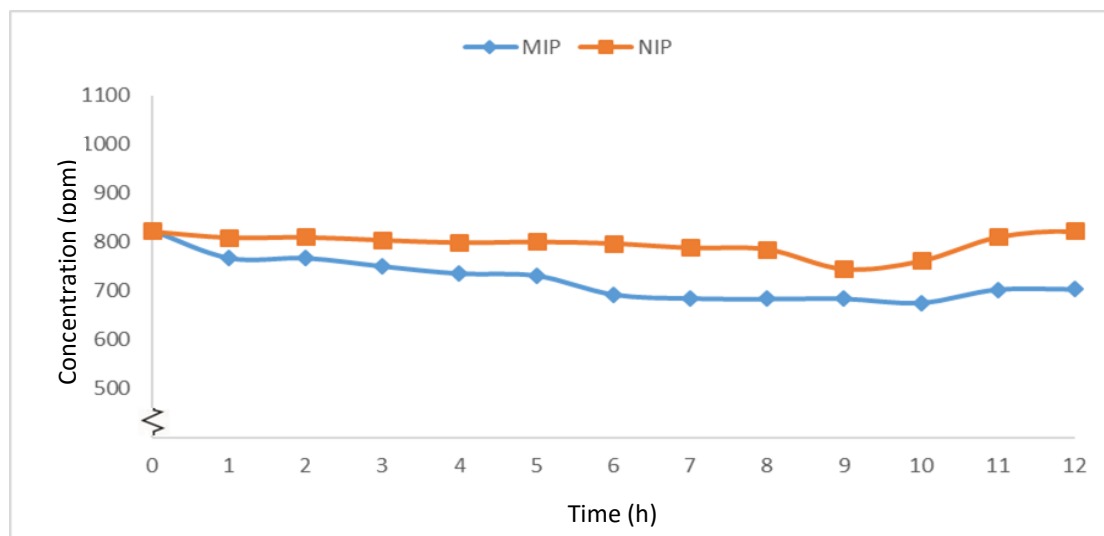


Figure 3.4 The concentrations of PNP at various sampling times during binding process in the presence of PNP-MIPs and NIPs, using MeOH extraction off the template.

The concentrations of PNP in this case for MIPs constantly declined from the beginning and became stable from 6 h onward until the end of the experiment. In contrast, the concentrations of PNP for NIPs remained relatively constant throughout the binding process with some fluctuations within a narrow range. The difference in concentrations of PNP between the two solutions after reaching equilibriums indicated the presence of differential adsorption of PNP into the polymer potentially induced from the inherent imprinting property of MIP. This result also helps explain the previous imprinting failure to be caused by the incapability of the less polar ethyl acetate to extract off the original PNP template during the MIP preparation.

In accordance with the current experiment with PNP, the C_e value was taken from the average of those sampling values from 6 h to 12 h which were regarded as the equilibrium region. The calculation (**Appendix B**) yielded the specific adsorption value (ΔQ) of PNP molecules bound to the MIPs to be $240.74 \mu\text{mol/g}$, indicating that the specific recognition sites were formed. It could be concluded that the attractive interactions between the template molecules (PNP) and the polymers are strong

enough to create such specific cavities. The rigid polymeric structure could also be maintained throughout the extraction process and remain effective for the rebinding of template. In other words, the template molecules were successfully imprinted into the polymeric structure of MIPs derived from SSP-PEDOT comparing to the non-specific background binding of NIPs. The rebinding capacities of the PNP-MIPs and NIPs were calculated to be 20.08% and 19.60%, respectively. The Δ binding capacities was only 0.48%.

3.3.3 2,4-Dinitrophenol molecularly imprinted polymers (DNP-MIPs)

DNP was next chosen as another polar template. Its MIPs were prepared from SSP of **10** and DNP solid mixture (**Scheme 3.10**). After the templating process, the template molecules were again extracted by exhaustive soxhlet extraction with either EtOAc or MeOH and subjected to the subsequent binding experiments with DNP.

The binding experiment indicated that the unsuccessful imprinting result was still observed for DNP-MIPs extracted off the template by ethyl acetate (**Figure 3.5**). The C_e value was taken from the average of the fluctuated values during 2-12 h which were regarded as the equilibrium region for the DNP-MIPs binding experiment, which were the same region as NIPs. The calculation (**Appendix B**) yielded the specific adsorption value (ΔQ) of DNP molecules bound to the MIPs to be $-32.75 \mu\text{mol/g}$. The incomplete extraction was again assumed to be the reason. Changing the extraction solvent to MeOH provided the results shown in **Figure 3.6**.

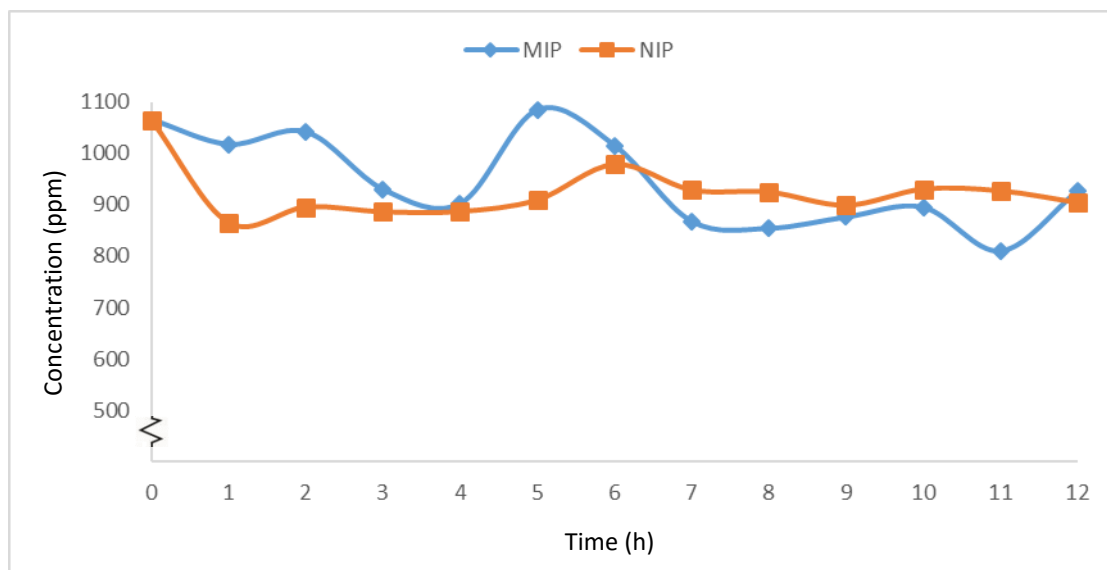


Figure 3.5 The concentrations of DNP at various sampling times during binding process in the presence of DNP-MIPs and NIPs, using EtOAc extraction off the template.

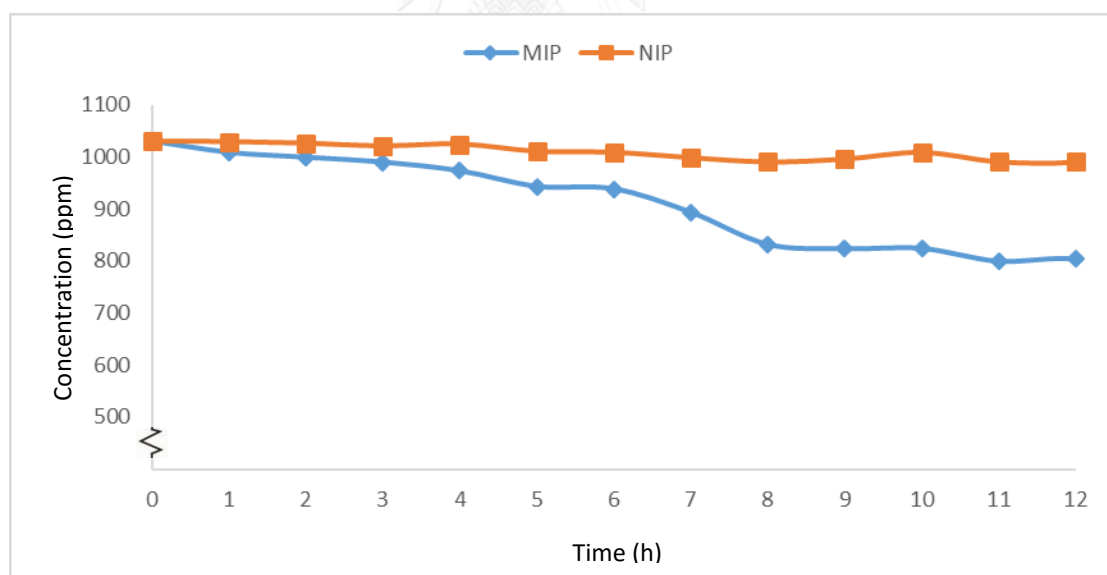


Figure 3.6 The concentrations of DNP at various sampling times during binding process in the presence of DNP-MIPs and NIPs, using MeOH extraction off the template.

The concentrations of DNP for MIPs constantly declined from the beginning and became stable from 8 h onward until the end of the experiment. In contrast, the concentrations of DNP with NIPs remained relatively constant throughout the binding process. The difference in concentrations of DNP between the two solutions after reaching equilibriums indicated the presence of similarly adsorption of DNP into the polymer potentially induced from the inherent imprinting property of MIP.

The C_e value was taken from the average of those sampling values from 8-12 h which were regarded as the equilibrium region. The calculation (**Appendix B**) yielded the specific adsorption value (ΔQ) of DNP molecules bound to the MIPs to be 486.68 $\mu\text{mol/g}$, indicating that better imprinting effect was achieved with this template, perhaps because of more polar groups. The rebinding capacities of the DNP-MIPs and NIPs were calculated to be 25.18% and 19.18%, respectively. The Δ binding capacities was 6.00%, much higher than the previous system with PNP template. Highly polar property of DNP could also be responsible for the difference in binding efficiency.

3.3.4 2,4,6-Trinitrophenol molecularly imprinted polymers (TNP-MIPs)

Another binding experiment was carried out to investigate the imprinting effect using TNP as the template molecules. (**Scheme 3.10**) In this experiment, only the polar MeOH was used as the extracting solvent for MIP preparations. For TNP-MIPs, the concentrations of TNP gradually decreased and reached equilibrium in 6 h. (**Figure 3.7**) The concentrations of TNP for NIPs also decreased and reached equilibrium in 6 h. The difference between the two samples was observed in this case as well as the report from the previous work.[30]

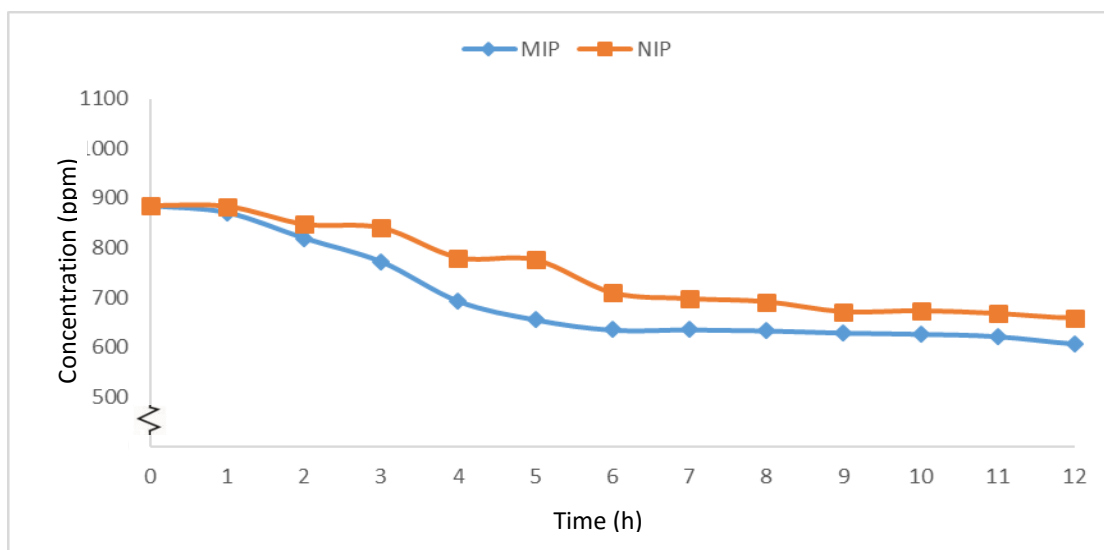
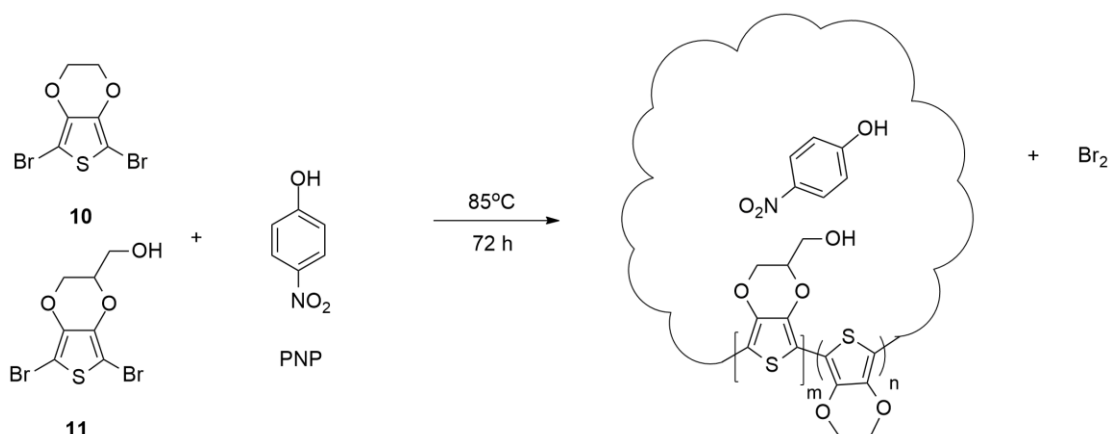


Figure 3.7 The concentrations of TNP at various sampling times during binding process in the presence of TNP-MIPs and NIPs.

The C_e value was taken from the average of the fluctuated values during 6-12 h which were regarded as the equilibrium region. The calculation (**Appendix B**) yielded the specific adsorption value (ΔQ) of TNP molecules bound to the MIPs to be $64.76 \mu\text{mol/g}$, which is quite close to the value obtained in the previous report ($63.76 \mu\text{mol/g}$). [30] The rebinding capacities of the TNP-MIPs and NIPs were calculated to be 79.20% and 73.89%, respectively. The Δ binding capacities was 5.31%. High capacities on both MIP and NIP may be arisen from large amount of non-specific interactions with such highly polar TNP template.

3.3.5 *p*-Nitrophenol molecularly imprinted copolymers (PNP-coMIPs)

The copolymers of PEDTM + PEDOT were prepared to incorporate more polar functional groups onto the polymer chain. Its coMIPs was obtained from SSP of solid mixtures of **10** and **11** in two different proportions (**Scheme 3.11**). Methanol was used as the solvent to extract off the templates in these cases.



Scheme 3.11 Synthesis of coMIPs with PNP as a template molecule

In the binding experiments with 20:80 PEDTM: PEDOT coMIPs (**Figure 3.8**), the concentrations of PNP for PNP-coMIPs gradually decreased and started to fluctuate and become steady after 12 h. The concentrations of PNP for coNIPs were instead reached equilibrium earlier at around 6 h. The C_e value was taken from the average of values during 12-15 h which were regarded as the equilibrium region for both coMIPs and coNIPs. The calculation (**Appendix B**) yielded the specific adsorption value (ΔQ) of PNP molecules bound to the coMIPs to be $270.95\ \mu\text{mol/g}$, which is higher than that from PNP-MIPs of SSP-PEDOT. The rebinding capacities of the PNP-20:80 PEDTM: PEDOT coMIPs and coNIPs were calculated to be 41.73% and 31.26%, respectively. The Δ binding capacities was 10.47%, which is also much higher than that from PNP-MIPs of SSP-PEDOT. These results support the idea that more polar groups on the MIPs help improve their imprinting ability with polar template.

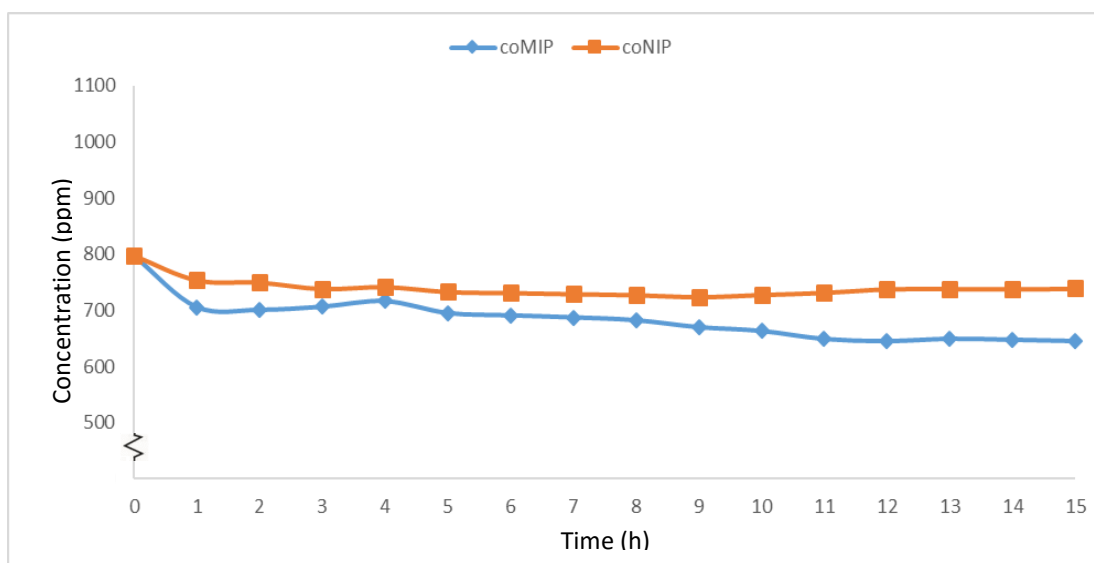


Figure 3.8 The concentrations of PNP at various sampling times during binding process in the presence of PNP-coMIPs and coNIPs.

Similar binding experiments were performed for PNP-coMIPs with 40:60 PEDTM: PEDOT and similar trend of the results was observed. The concentrations of PNP gradually decreased and reached equilibrium in 12 h while that for coNIPs was 8 h (**Figure 3.9**). Again, an obvious imprinting effect for PNP could also be noticed. The C_e value was taken from the results between 12-15 h as the equilibrium point. The calculation (**Appendix B**) yielded the specific adsorption value (ΔQ) of PNP molecules bound to the coMIPs to be 434.44 $\mu\text{mol/g}$. The rebinding capacities of the PNP-40:60 PEDTM: PEDOT coMIPs and coNIPs were calculated to be 33.80% and 17.81%, respectively. The Δ binding capacities was 15.99%, which is even higher than that from PNP-20:80 PEDTM: PEDOT coMIPs, emphasizing more polar groups on the MIPs would further improve their imprinting effect with polar template.

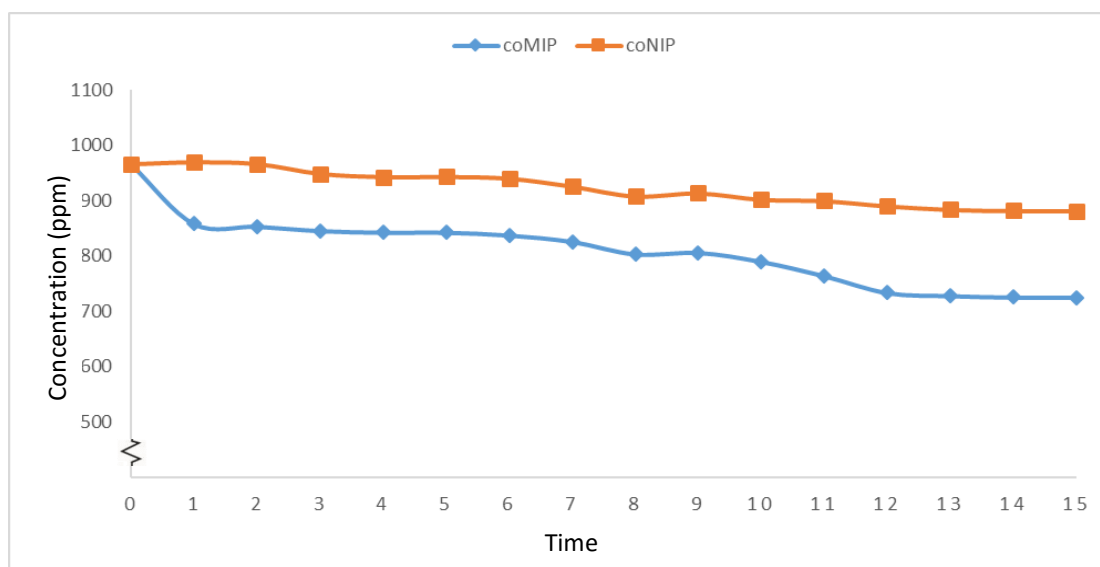
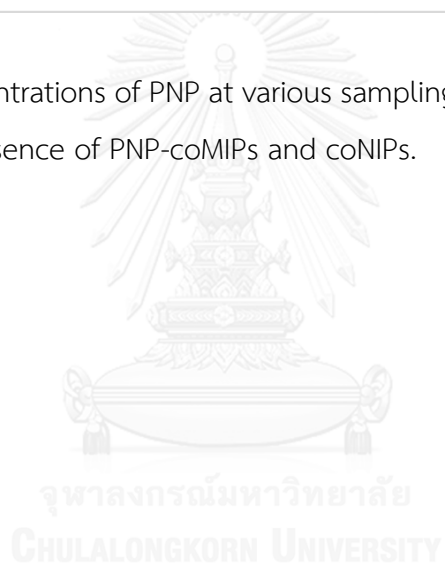


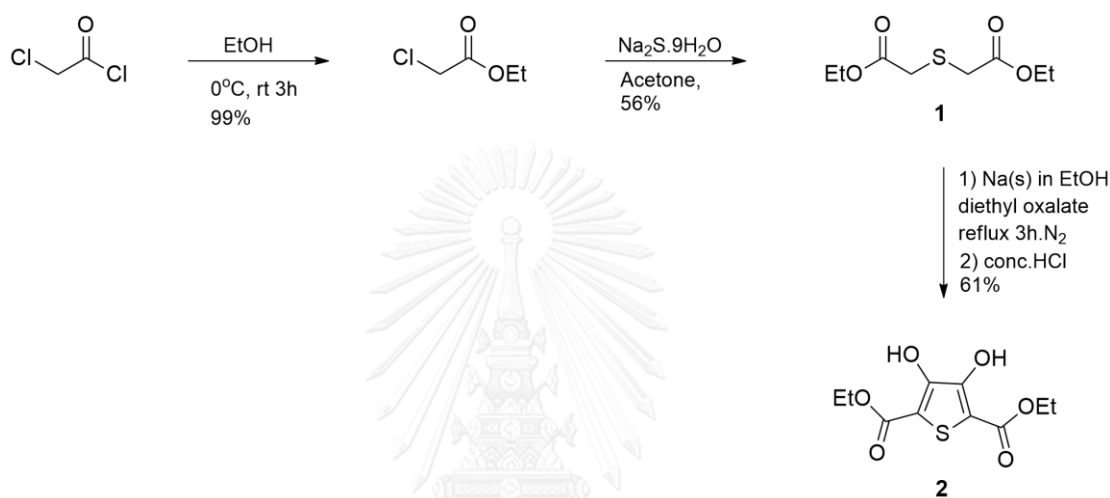
Figure 3.9 The concentrations of PNP at various sampling times during binding process in the presence of PNP-coMIPs and coNIPs.



CHAPTER IV

CONCLUSION

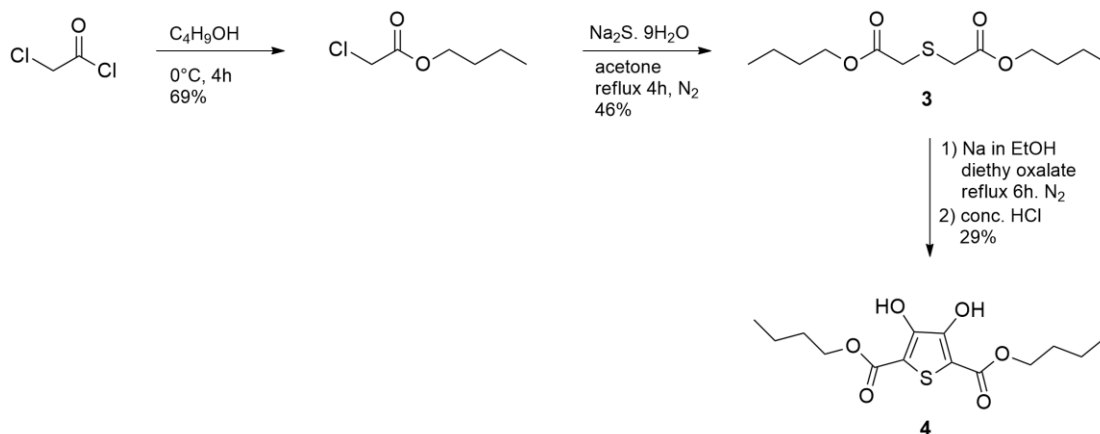
The synthesis of 3,4-dihydroxythiophene-2,5-dicarboxylate derivatives **2** were successfully carried out through the traditional synthetic route as shown in **Scheme 4.1**. [31, 32]



Scheme 4.1 Synthesis of compound **2**

Compound **1** was prepared from substitutions of ethyl chloroacetate with sodium sulfide nonahydrate (Na₂S·9H₂O) in 56% yield. Compound **1** was reacted with diethyl oxalate through Hinsberg reaction, resulting in the formation of compound **2** in 61% yield.

Similar to ethyl chloroacetate, butyl chloroacetate was prepared from chloroacetyl chloride and *n*-BuOH in 69% yield. Substitutions of butyl chloroacetate with Na₂S·9H₂O yielded compound **3** in 46%. Compound **4** was also obtained via Hinsberg reaction of compound **3** and diethyl oxalate in approximately 29.7%. Unfortunately, compound **4** could not be satisfactorily purified for the subsequent reactions. (**Scheme 4.2**)

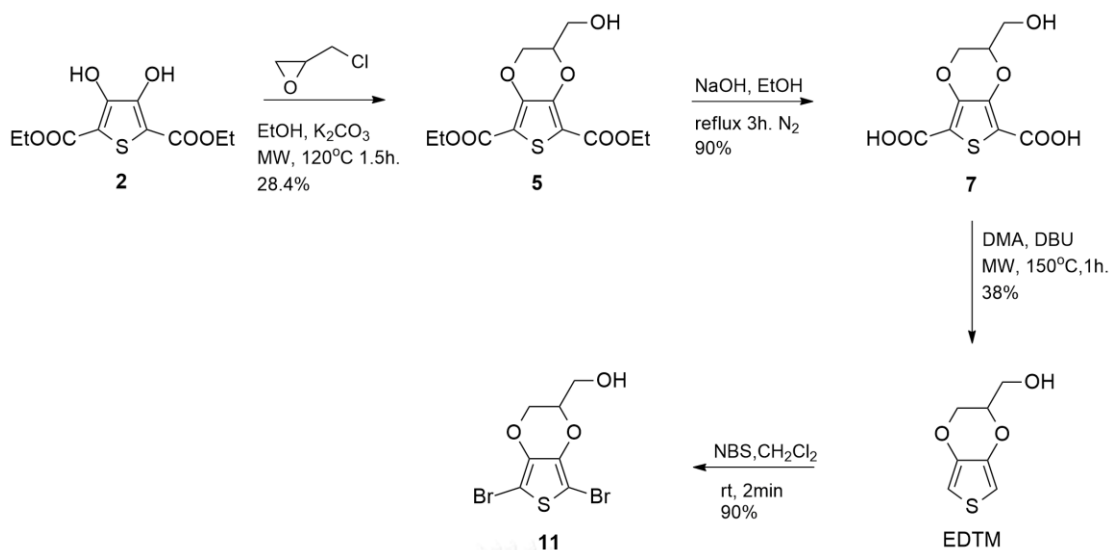


Scheme 4.2 Synthesis of compound **4**

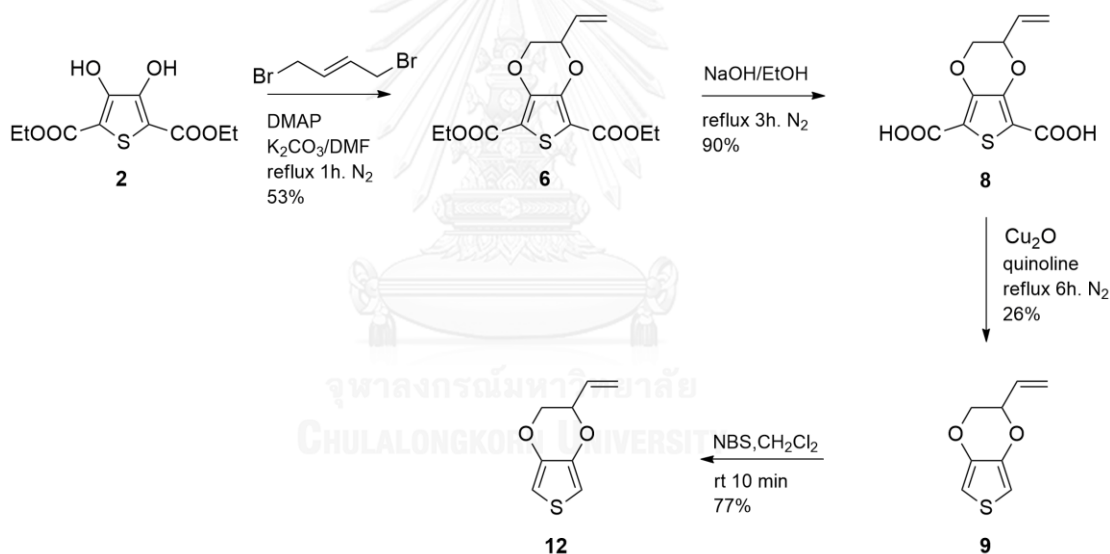
Compound **2** was used as the starting material for the synthesis of 2,5-dibromo-3,4-ethylenedioxythiophene derivatives **11** as shown in **Scheme 4.3**. [40-42] Compound **5** was synthesized from compound **2** and epichlorohydrin in 28.4%. Up to 80% yield from hydrolysis of diethylester derivatives **5** was achieved to get compound **7**. The diacids **7** was decarboxylated to obtain EDTM in 38%.

Compound **6** was prepared from compound **2** and trans-1,4-dibromo-2-butene through double nucleophilic substitutions in 53.2%. The hydrolysis of compound **6** was obtained compound **8** in 90% yield. The compound **8** was decarboxylated to obtain compound **9** in 26%.

Brominations of EDOT with NBS gave the corresponding dibromothiophene derivatives **10** in 98% yield, **11** in 77 % yield (**Scheme 4.3**) and **12** in 90% yield (**Scheme 4.4**).



Scheme 4.3 Synthesis of compound **11**



Scheme 4.4 Synthesis of compound **12**

The facile solid state polymerization (SSP) processes of monomer **10** surrounding the template molecules, PNP, DNP, TNP or pyrene, to obtain imprinted PEDOT have been achieved. After template removals, the binding experiments of these MIPs monitored by UV-Vis spectroscopy were accomplished by adding back the template molecules. The results exhibited that the specific adsorption values (ΔQ) that reflect the imprinting effect for PNP-MIPs, DNP-MIPs, TNP-MIPs and pyrene-MIPs as

compared to their corresponding NIPs and the rebinding capacities of the PNP-MIPs, DNP-MIPs, TNP-MIPs and Pyrene-MIPs were shown in **Table 4.1** and **Table 4.2**

Table 4.1 The specific adsorption values (ΔQ) of MIPs and NIPs

Template molecule	Extracted solvent	Q_{MIPs} ($\mu\text{mol/g}$)	Q_{NIPs} ($\mu\text{mol/g}$)	ΔQ ($\mu\text{mol/g}$)
Pyrene	EtOAc	24.26	19.27	7.99
	MeOH	-159.72	0.22	-120.53
PNP	EtOAc	90.41	155.31	-64.86
	MeOH	323.88	83.14	240.74
DNP	EtOAc	361.65	394.40	-32.75
	MeOH	576.74	90.06	486.68
TNP	MeOH	324.33	259.57	64.76

Table 4.2 The rebinding capacities of MIPs and NIPs

Template molecule	Solvent extracted	Binding capacities of MIPs (%)	Binding capacities of NIPs (%)	Δ Binding capacities (%)
PNP	MeOH	20.08	19.60	0.48
DNP	MeOH	25.18	19.18	6.00
TNP	MeOH	79.20	73.89	5.31

The SSP processes on the mixtures of monomers **10** and **11** surrounding PNP template molecules to obtain the unprecedented PNP imprinted PEDTM+PEDOT copolymers have been achieved. After template removals, the binding experiments of these coMIPs with added template molecules exhibited the specific adsorption values (ΔQ) for 20:80 PEDTM: PEDOT co-MIPs and 40:60 PEDTM: PEDOT co-MIPs as compared to NIPs. The adsorption values and the rebinding capacities were calculated and shown in **Table 4.3** and **Table 4.4**, respectively.

Table 4.3 the specific adsorption values (ΔQ) for PNP-MIPs and coMIPs.

PNP-MIPs	Q_{MIPs} ($\mu\text{mol/g}$)	Q_{NIPs} ($\mu\text{mol/g}$)	ΔQ ($\mu\text{mol/g}$)
PEDOT	326.48	96.44	230.04
20:80 PEDTM:PEDOT	439.42	168.47	270.95
40:60 PEDTM:PEDOT	668.48	234.04	434.44

Table 4.4 The rebinding capacities of PNP-MIPs and coMIPs.

PNP-MIPs	Binding capacities of MIPs (%)	Binding capacities of NIPs (%)	Δ Binding capacities (%)
PEDOT	20.08	19.60	0.48
20:80 PEDTM:PEDOT	41.73	31.26	10.47
40:60 PEDTM:PEDOT	33.80	17.81	15.99

The results indicated that PEDOT prepared by SSP could be imprinted and recognized its template molecules with high capacity for the relatively polar template, which exhibited more promising sensitivity and specificity in template detection than MIPs of non-polar pyrene. The co-MIPs prepared with PEDTM by SSP could be imprinted and even better recognized the template molecules with improved rebinding specificity and capacity. These results suggested that SSP-PEDOT and its PEDTM copolymer could be developed further into specific sensors for polar template molecules.

REFERENCES



REFERENCES

- [1] Wulff, G., Sarhan, A., and Zabrocki, K. Enzyme-analogue built polymers and their use for the resolution of racemates. Tetrahedron Letter 44 (1973): 4329-4332.
- [2] Arshady, R. and Mosbach, K. Synthesis of substrate-selective polymers by host-guest polymerization. Die Makromolekulare Chemie 182 (1981): 687-692.
- [3] Alexander, C., et al. Molecular imprinting science and technology: a survey of the literature for the years up to and including 2003. Journal of Molecular Recognition 19(2) (2006): 106-80.
- [4] Mahony, J.O., Nolan, K., Smyth, M.R., and Mizaikoff, B. Molecularly imprinted polymers—potential and challenges in analytical chemistry. Analytica Chimica Acta 534(1) (2005): 31-39.
- [5] Mayes, A.G. and Whitcombe, M.J. Synthetic strategies for the generation of molecularly imprinted organic polymers. Advanced Drug Delivery Reviews 57(12) (2005): 1742-78.
- [6] Shea, K.J. and Sasaki, D.Y. An analysis of small-molecule binding to functionalized synthetic polymers by ¹³C CP/MAS NMR and FT-IR spectroscopy. Journal of American Chemical Society 113 (1991): 4109-4120.
- [7] Whitcombe, M.J., Kirsch, N., and Nicholls, I.A. Molecular imprinting science and technology: a survey of the literature for the years 2004-2011. Journal of Molecular Recognition 27(6) (2014): 297-401.
- [8] Wulff, G., Best, W., and Akelah, A. Enzyme-analogue built polymers: Investigations on the racemic resolution of amino acids. Reactive Polymers, Ion Exchangers, Sorbents 2(3) (1984): 167-174.
- [9] Yan, M. Molecularly imprinted materials: science and technology. New York: CRC press, 2004.
- [10] Vasapollo, G., et al. Molecularly imprinted polymers: present and future perspective. International Journal of Molecular Sciences 12(9) (2011): 5908-45.
- [11] Pichon, V. Selective sample treatment using molecularly imprinted polymers. Journal of Chromatography A 1152 (2007): 41-53.

- [12] Urraca, J.L., Hall, A.J., Moreno-Bondi, M.C., and Sellergren, B. A stoichiometric molecularly imprinted polymer for the class-selective recognition of antibiotics in aqueous media. Angewandte Chemie International 45(31) (2006): 5158-61.
- [13] Sellergren, B. Polymer- and template-related factors influencing the efficiency in molecularly imprinted solid-phase extractions. Trends in Analytical Chemistry 18 (1999): 164-174.
- [14] Komiyama, M., Takeuchi, T., Mukawa, T., and Asanuma, H. Molecular imprinting: from fundamentals to applications. Weinheim: Wiley-VCH, 2003.
- [15] Meng, H., et al. Solid-state synthesis of a conducting polythiophene via an unprecedented heterocyclic coupling reaction. Journal of American Chemical Society 125(49) (2003): 15151-15162.
- [16] Groenendaal, L.B., Jonas, F., Freitag, D., Pielartzik, H., and Reynolds, J.R. Poly(3,4-ethylenedioxythiophene) and its derivatives: past, present, and future. Advanced Materials 12 (2000): 481-494.
- [17] Gulprasertrat, N., Chapromma, J., Aree, T., and Sritana-anant, Y. Synthesis of functionalizable derivatives of 3,4-ethylenedioxythiophene and their solid-state polymerizations. Journal of Applied Polymer Science 132(28) (2015): 42233. จุฬาลงกรณ์มหาวิทยาลัย
- [18] Kim, Y.S., Park, J.H., Lee, S.-H., and Lee, Y. Polymer photovoltaic devices using highly conductive poly(3,4-ethylenedioxythiophene-methanol) electrode. Solar Energy Materials and Solar Cells 93(8) (2009): 1398-1403.
- [19] Yin, Y., Li, Z., Jin, J., Tusy, C., and Xia, J. Facile synthesis of poly(3,4-ethylenedioxythiophene) by acid-assisted polycondensation of 5-bromo-2,3-dihydro-thieno[3,4-b][1,4]dioxine. Synthetic Metals 175 (2013): 97-102.
- [20] Kubo, H., Yoshioka, N., and Takeuchi, T. Fluorescent imprinted polymers prepared with 2-acrylamidoquinoline as a signaling monomer. Journal of American Chemical Society 7 (2005): 359-362.
- [21] Pardieu, E., et al. Molecularly imprinted conducting polymer based electrochemical sensor for detection of atrazine. Analytica Chimica Acta 649(2) (2009): 236-45.

- [22] Yeh, W.-M. and Ho, K.-C. Amperometric morphine sensing using a molecularly imprinted polymer-modified electrode. *Analytica Chimica Acta* 542(1) (2005): 76-82.
- [23] Chen, L., Jin, J., Shu, X., and Xia, J. Solid state synthesis of poly(3,4-ethylenedioxythiophene) as counter electrode for dye-sensitized solar cell. *Journal of Power Sources* 248 (2014): 1234-1240.
- [24] Tiu, B.D.B., Krupadam, R.J., and Advincula, R.C. Pyrene-imprinted polythiophene sensors for detection of polycyclic aromatic hydrocarbons. *Sensors and Actuators B: Chemical* 228 (2016): 693-701.
- [25] Roy, A.C., Nisha, V.S., Dhand, C., Ali, M.A., and Malhotra, B.D. Molecularly imprinted polyaniline-polyvinyl sulphonic acid composite based sensor for para-nitrophenol detection. *Analytica Chimica Acta* 777 (2013): 63-71.
- [26] Jing, T., et al. Determination of trace 2,4-dinitrophenol in surface water samples based on hydrophilic molecularly imprinted polymers/nickel fiber electrode. *Biosens Bioelectron* 26(11) (2011): 4450-6.
- [27] Guo, Z., et al. 1,3,5-Trinitrotoluene detection by a molecularly imprinted polymer sensor based on electropolymerization of a microporous-metal-organic framework. *Sensors and Actuators B: Chemical* 207 (2015): 960-966.
- [28] Riskin, M., Tel-Vered, R., Bourenko, T., Granot, E., and Willner, I. Imprinting of molecular recognition sites through electropolymerization of functionalized Au nanoparticles: development of an electrochemical TNT sensor based on pi-donor-acceptor interactions. *Journal of American Chemical Society* 130(30) (2008): 9726-33.
- [29] Xu, S., et al. Dummy molecularly imprinted polymers-capped CdTe quantum dots for the fluorescent sensing of 2,4,6-trinitrotoluene. *ACS Applied Materials & Interfaces* 5(16) (2013): 8146-54.
- [30] Sukrakarn, S. *Synthesis of molecularly imprinted polythiophen*. Science Chulalongkorn University, 2013.
- [31] Overberger, C.G., Mallon, H.J., and Fine, R. Cyclic Sulfoxes. II. The Polymerization of Styrene in the Presence of 3,4-Diphenylthiophene-1-dioxide

- and 3,4-Di-(p-chlorophenyl)-thiophene-1-dioxide. Journal of American Chemical Society 72 (1950): 4958-4961.
- [32] Wynberg, H. and Kooreman, H. The Mechanism of the Hinsberg Thiophene Ring Synthesis^{1, 2}. Journal of the American Chemical Society 87(8) (1965): 1739-1742.
- [33] Lima, A., Schottland, P., Sadki, S., and Chevrot, C. Electropolymerization of 3, 4-ethylenedioxythiophene and 3, 4-ethylenedioxythiophene methanol in the presence of dodecylbenzenesulfonate. Synthetic Metals 93(1) (1998): 33-41.
- [34] Fager, E.W. Some derivatives of 3,4-dioxythiophene. Journal of the American Chemical Society 67(12) (1945): 2217-2218.
- [35] Kellogg, R.M., Schaap, A.P., Harper, E.T., and Wynbert, H. Acid-catalyzed brominations, deuterations, rearrangements, and debrominations of thiophenes under mild conditions. The Journal of Organic Chemistry 33(7) (1968): 2902-2909.
- [36] Srinivasan, P., Gunasekaran, M., Kanagasekaran, T., Gopalakrishnan, R., and Ramasamy, P. 2,4,6-trinitrophenol (TNP): An organic material for nonlinear optical (NLO) applications. Journal of Crystal Growth 289(2) (2006): 639-646.
- [37] He, J.-f., Zhu, Q.-h., and Deng, Q.-y. Investigation of imprinting parameters and their recognition nature for quinine-molecularly imprinted polymers. Spectrochimica Acta Part A: Molecular and Biomolecular Spectroscopy 67(5) (2007): 1297-1305.
- [38] Yoon, S.-D. and Byun, H.-S. Molecularly imprinted polymers for selective separation of acetaminophen and aspirin by using supercritical fluid technology. Chemical Engineering Journal 226 (2013): 171-180.
- [39] Allen, D., Callaghan, O., Cordier, F. L., Dobson, D. R., Harris, J. R., Hotten, T. M., Owton, W. M., Rathmell, R. E. and Wood, V. A. An improved synthesis of substituted benzo[b]thiophenes using microwave irradiation. Tetrahedron Letters 45 (2004) 9645-9647
- [40] Li, Li., Xue-yong, L., Ying, H. Synthesis of n-butyl chloroacetate catalyzed by sodium bisulfate under microwave irradiation. Bohai Daxue Xuebao, Ziran Kexueban 29 (2008): 134-137.

- [41] Wan, A. S., Ngiam, T. L., Leung, S. L., Go, M. L., Francisco, C. G., Freire, R., Hernandez, R., Salazar, J. A., Suarez, E., Garcia, G. A. Long-acting contraceptive agents: levonorgestrel esters of unsaturated acids. Steroids 41 (1983): 39-48.
- [42] Yu, Y. H., Chen, Y. C.; Hsu, K. M. Manufacture of high-purity 3,4-ethylenedioxythiophene as monomer for conductive polymers. Japaness. Kokai Tokkyo Koho (2009).





APPENDICES

จุฬาลงกรณ์มหาวิทยาลัย
CHULALONGKORN UNIVERSITY

APPENDIX A

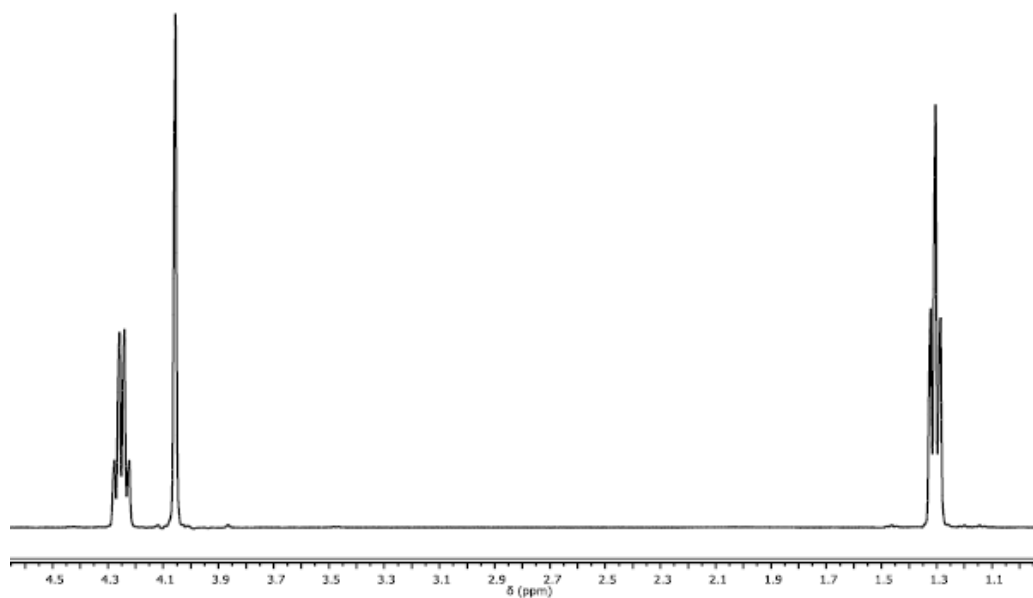


Figure A.1 ^1H NMR (CDCl_3) spectrum of ethyl chloroacetate

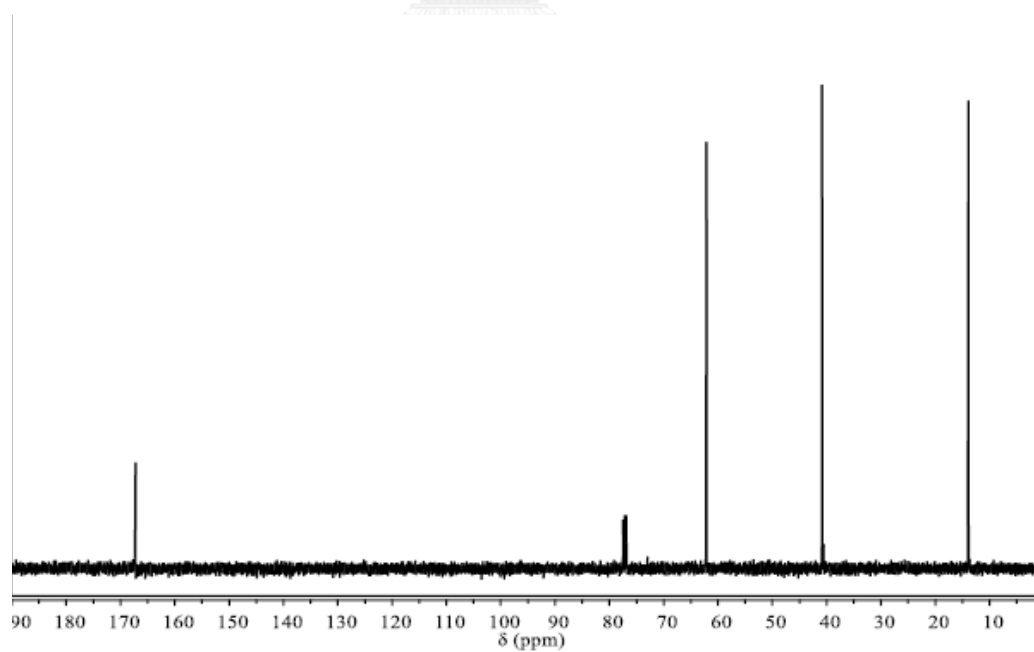


Figure A.2 ^{13}C NMR (CDCl_3) spectrum of ethyl chloroacetate

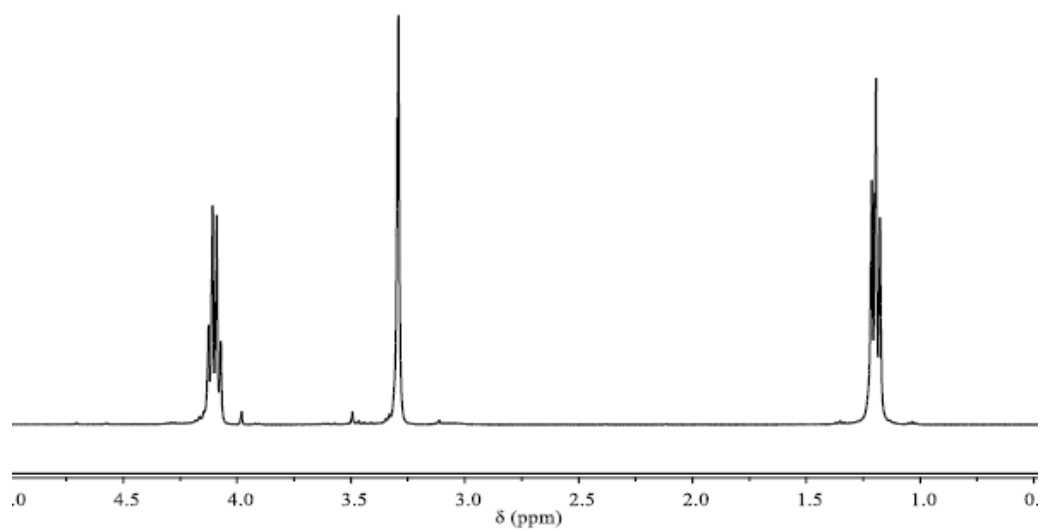


Figure A.3 ^1H NMR (CDCl_3) spectrum of compound **1**

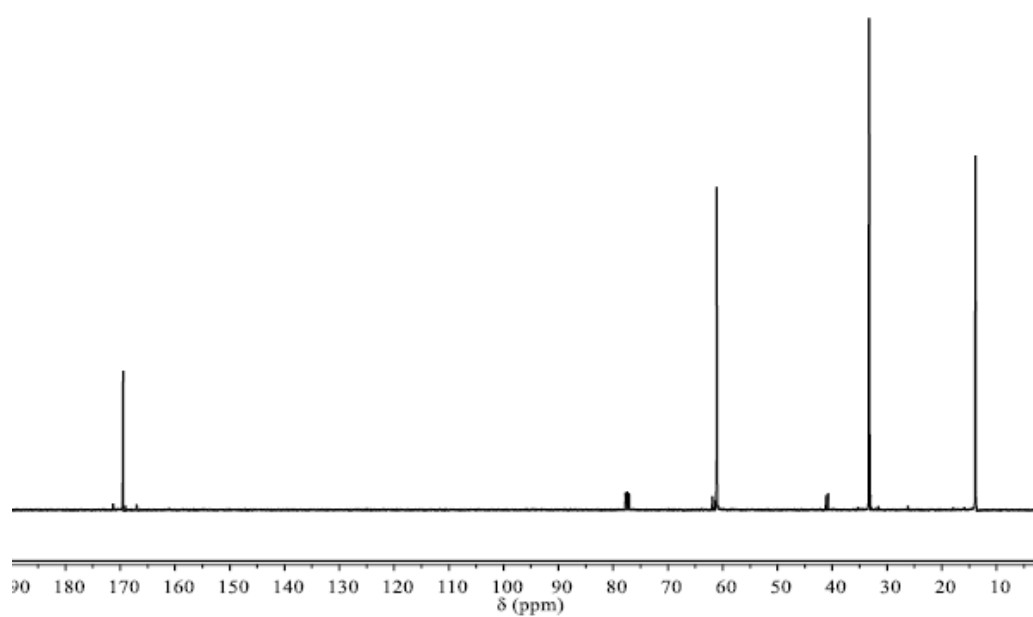


Figure A.4 ^{13}C NMR (CDCl_3) spectrum of compound **1**

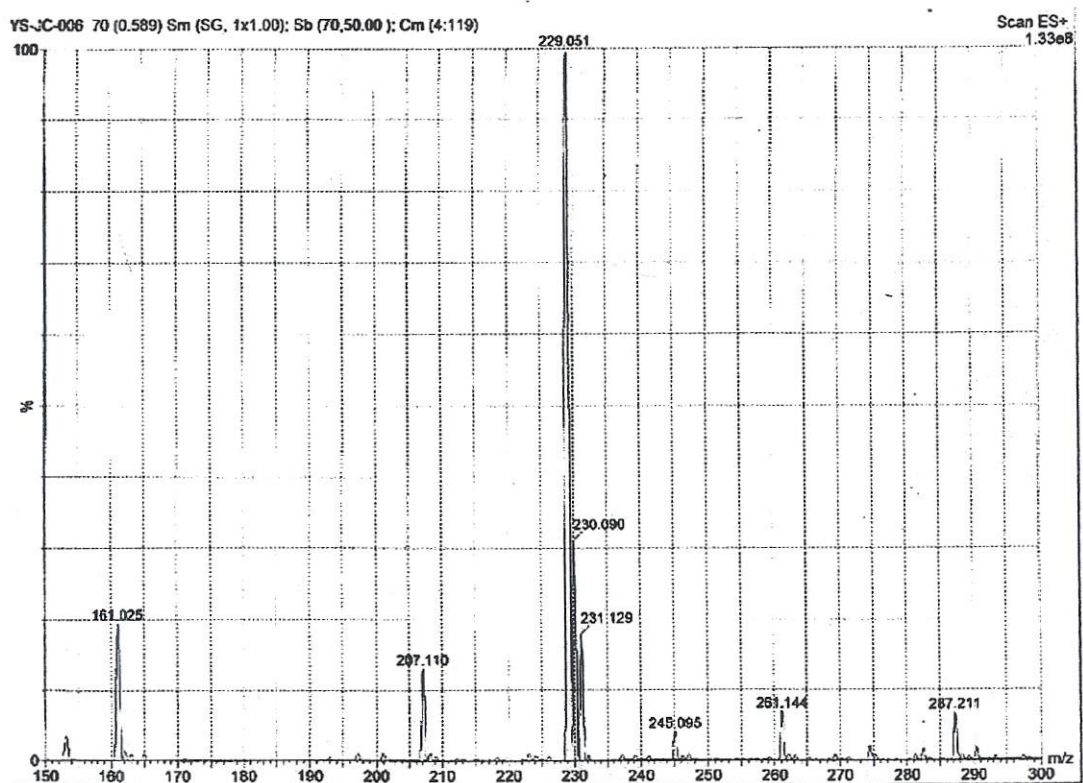


Figure A.5 Mass spectrum of compound 1

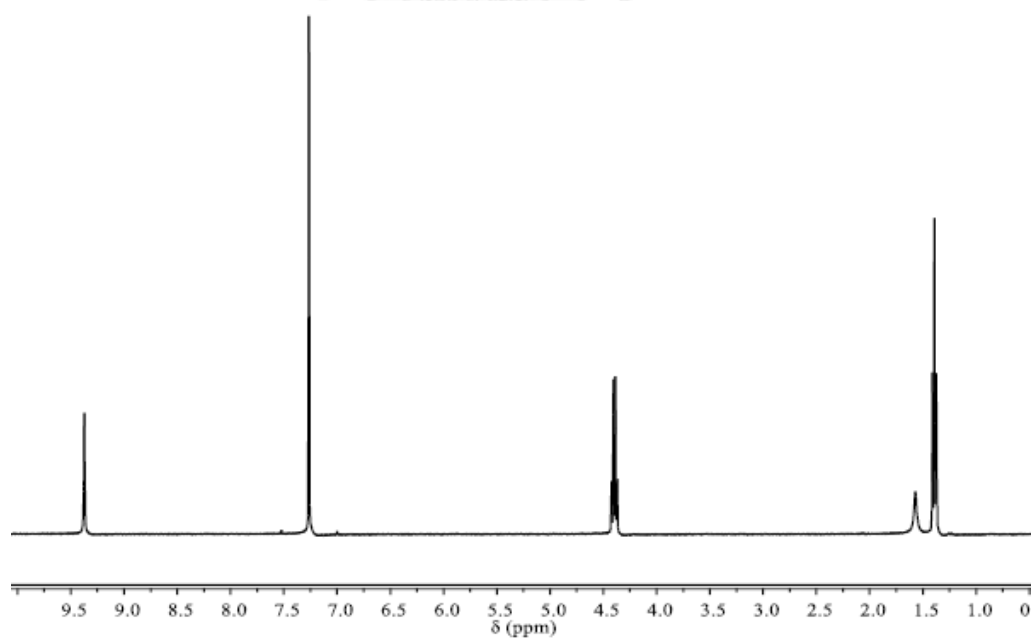


Figure A.6 ^1H NMR (CDCl_3) spectrum of compound 2

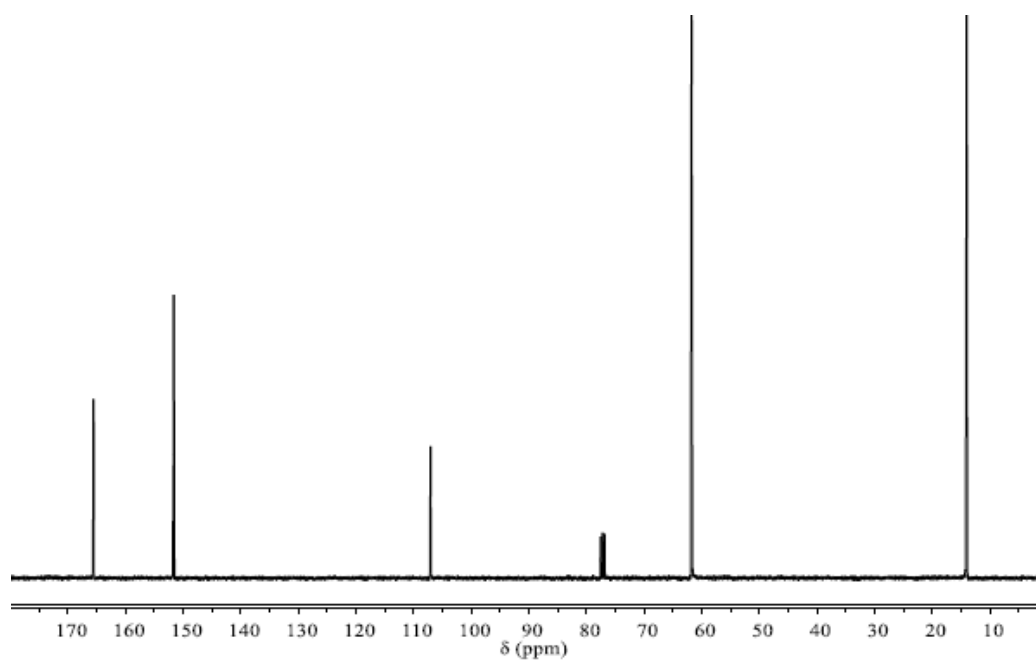


Figure A.7 ^{13}C NMR (CDCl_3) spectrum of compound 2

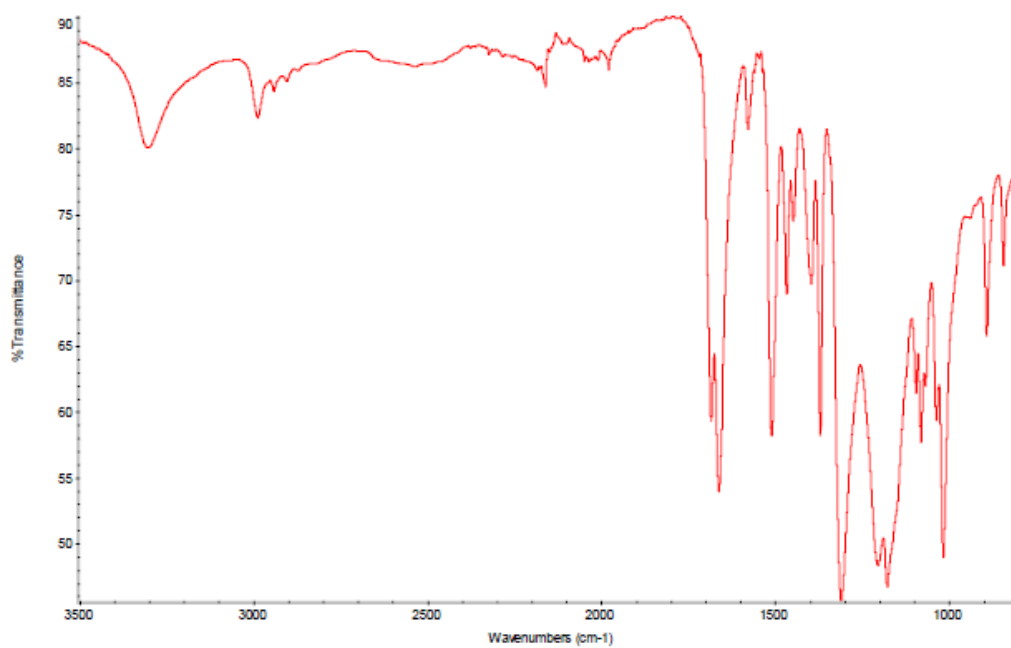


Figure A.8 IR spectrum of compound 2

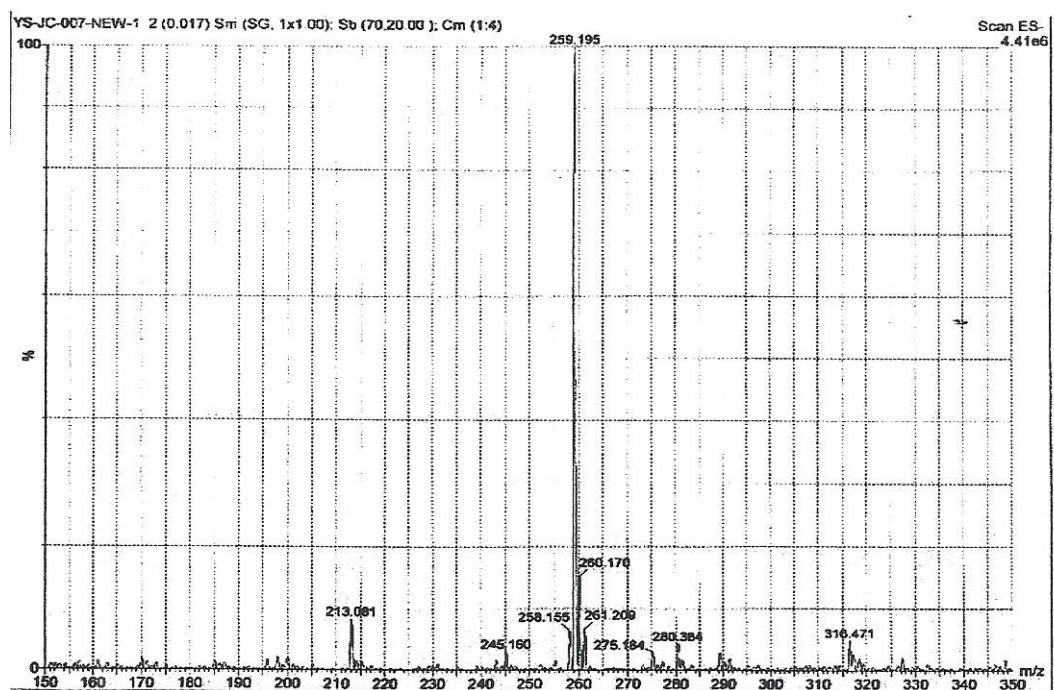


Figure A.9 Mass spectrum of compound 2

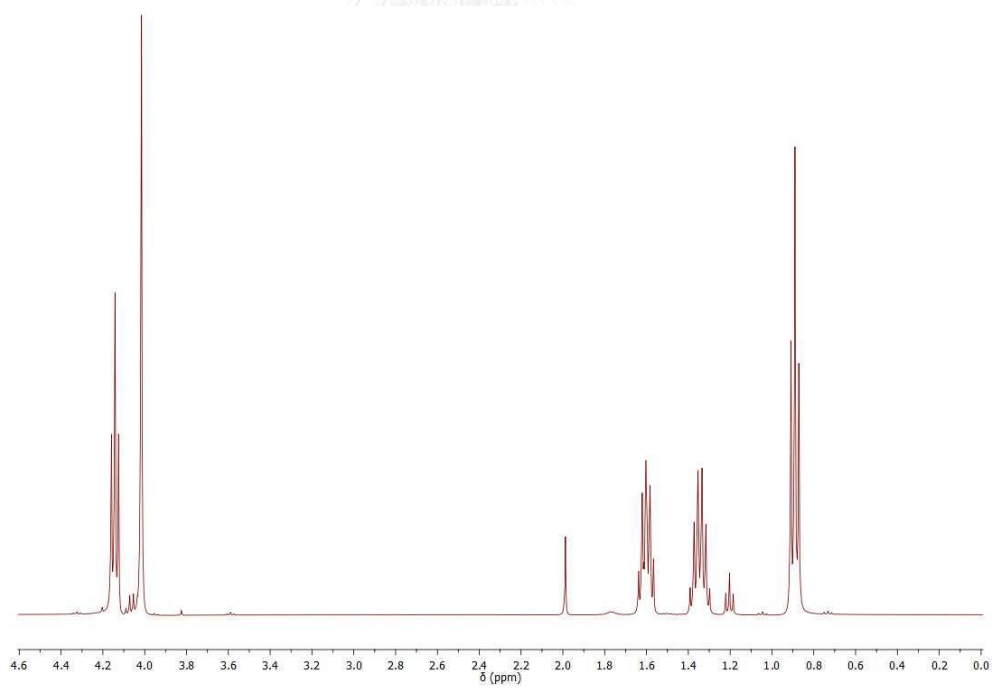


Figure A.10 ^1H NMR (CDCl_3) spectrum of butyl chloroacetate

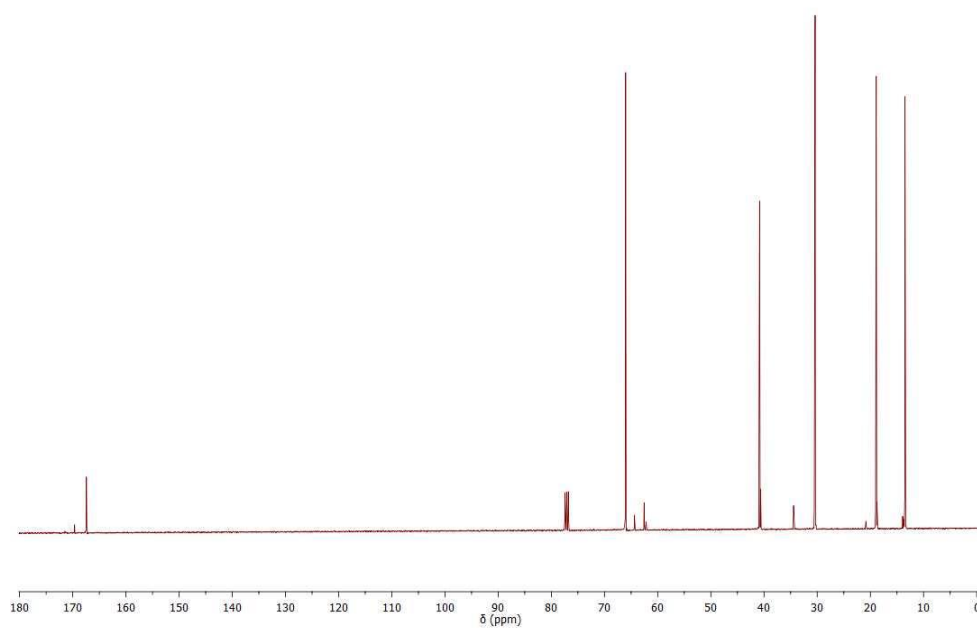


Figure A.11 ^{13}C NMR (CDCl_3) spectrum of butyl chloroacetate

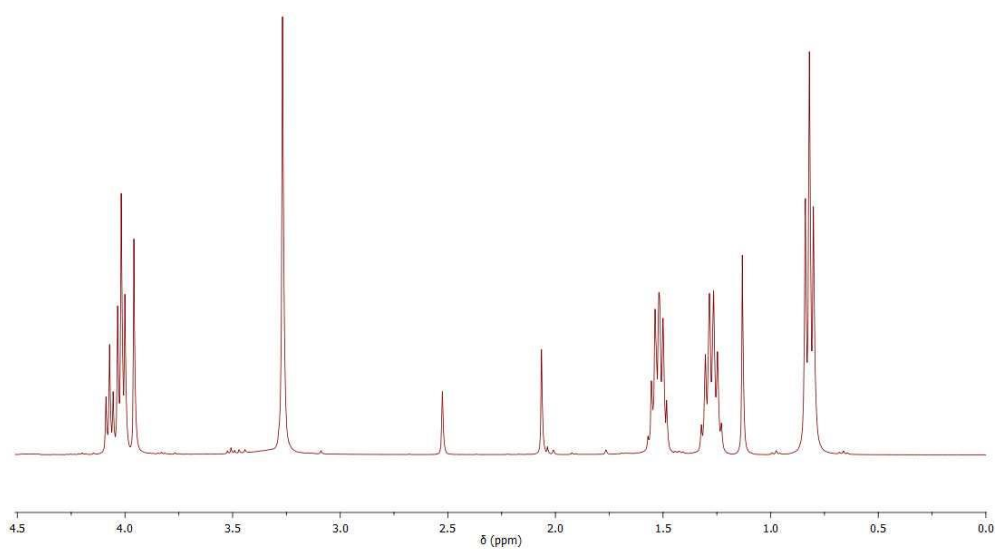


Figure A.12 ^1H NMR (CDCl_3) spectrum of compound 3

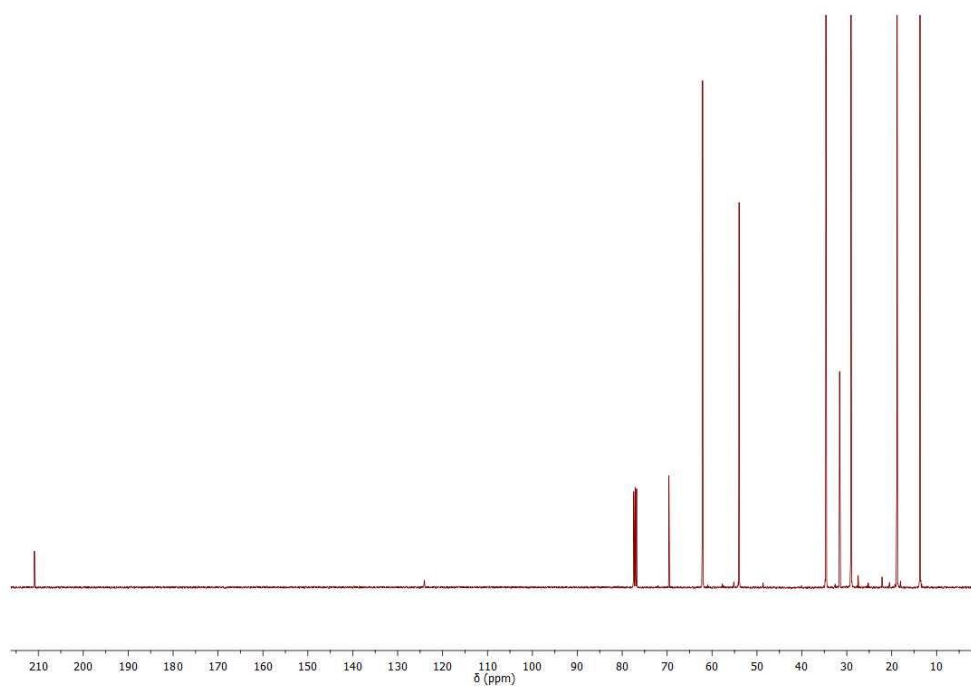


Figure A.13 ^{13}C NMR (CDCl_3) spectrum of compound 3

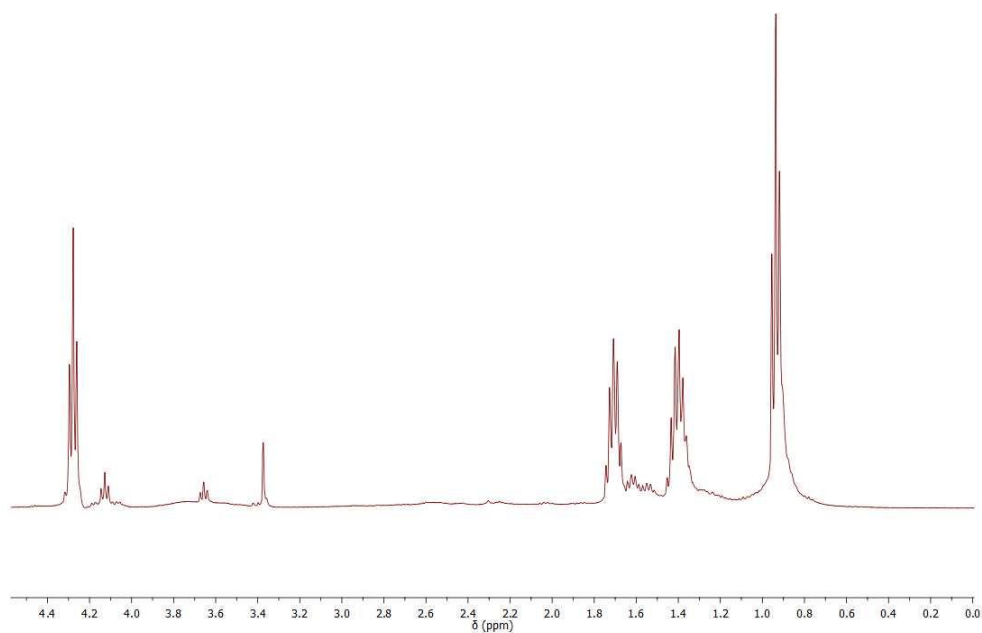


Figure A.14 ^1H NMR (CDCl_3) spectrum of compound 4

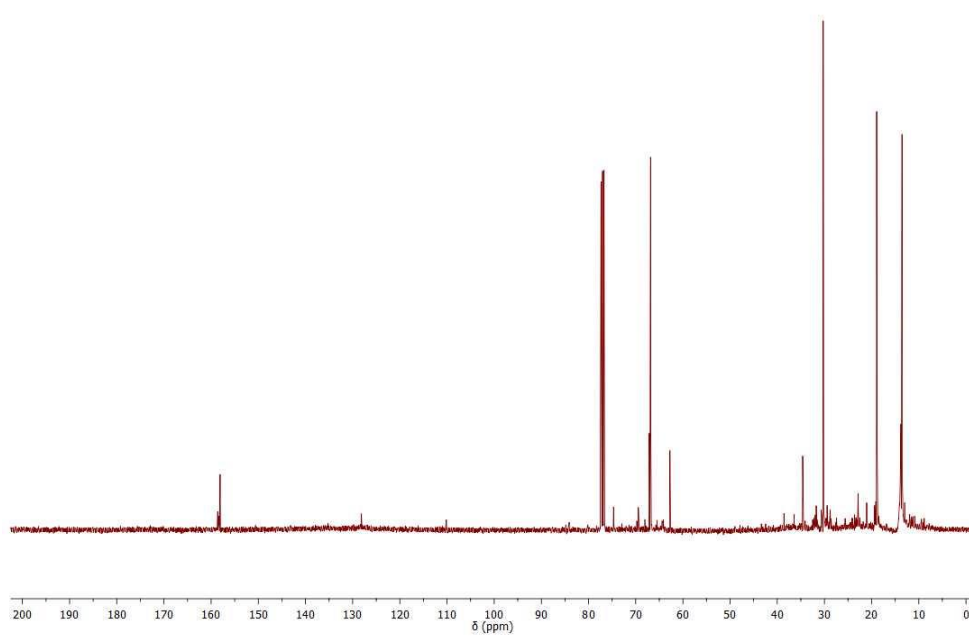


Figure A.15 ^{13}C NMR (CDCl_3) spectrum of compound 4

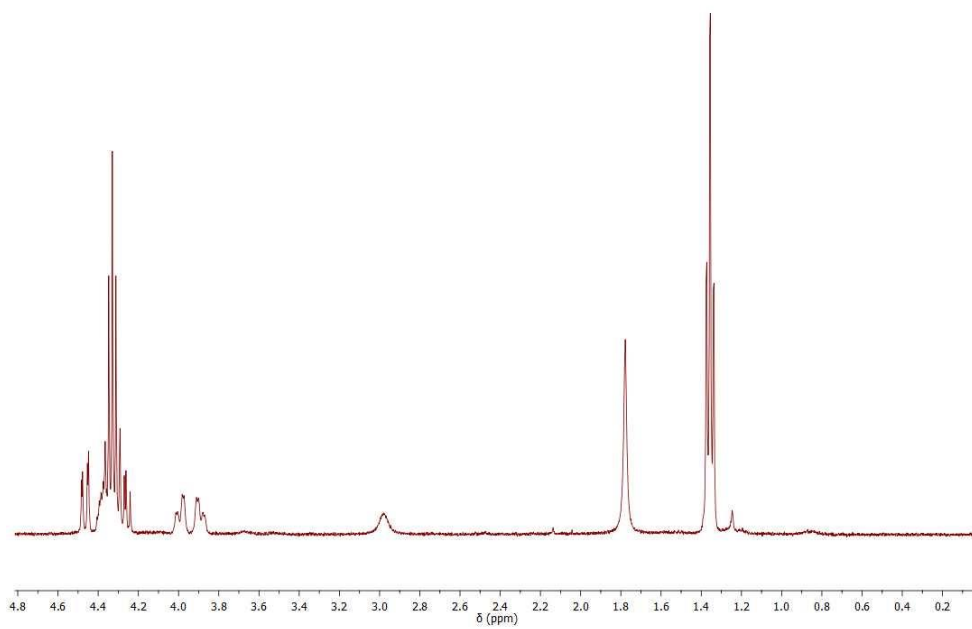


Figure A.16 ^1H NMR (CDCl_3) spectrum of compound 5

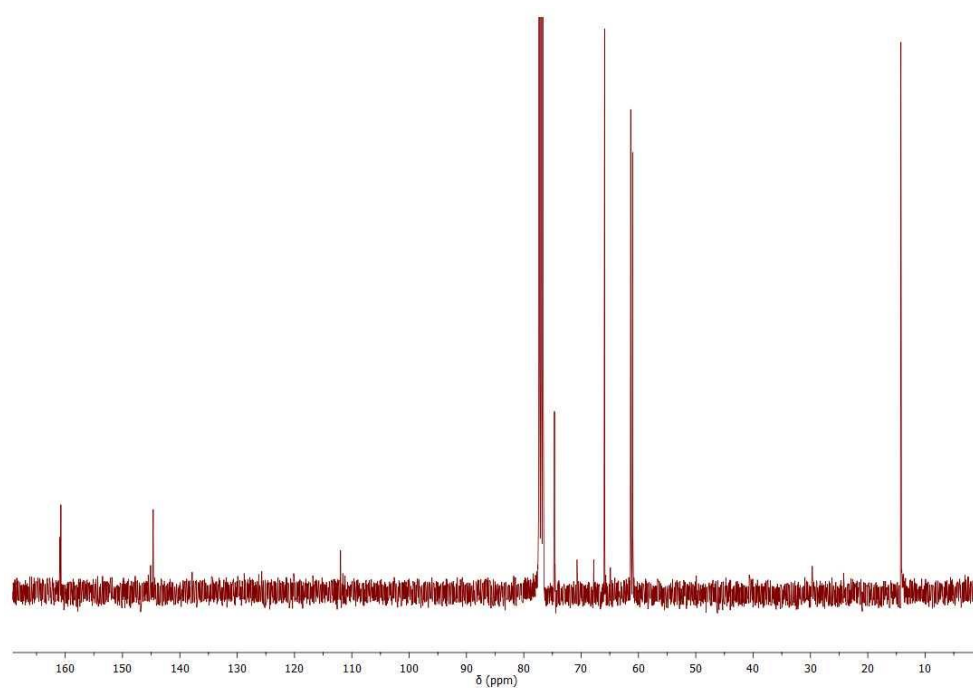


Figure A.17 ^{13}C NMR (CDCl_3) spectrum of compound 5

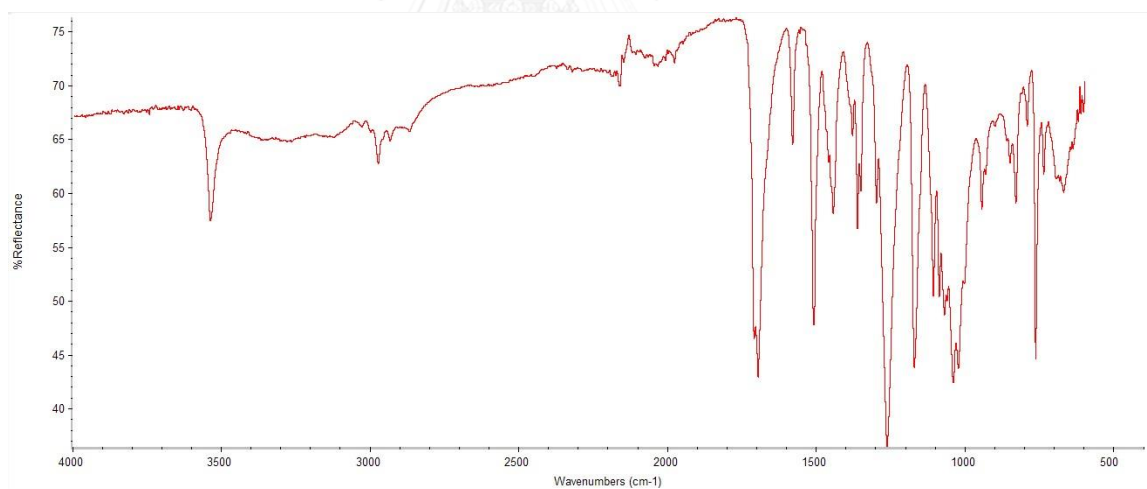


Figure A.18 IR spectrum of compound 5

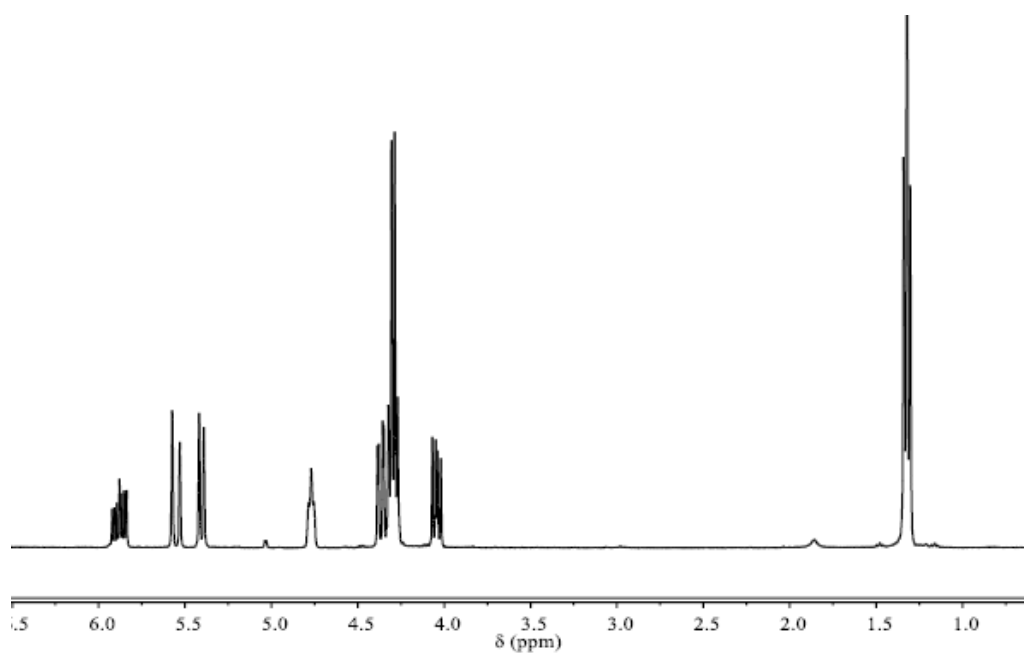


Figure A.19 ^1H NMR (CDCl_3) spectrum of compound 6

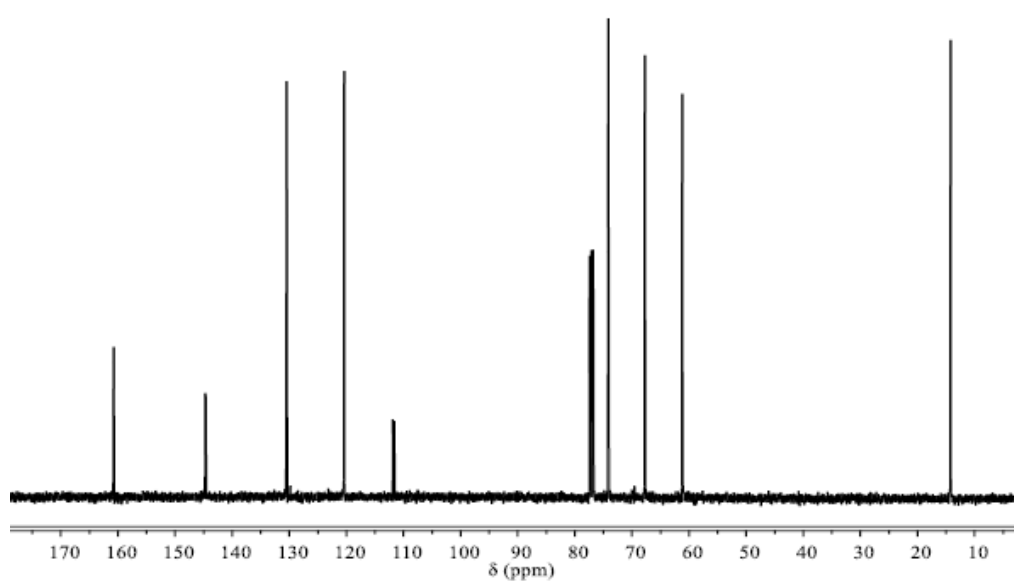


Figure A.20 ^{13}C NMR (CDCl_3) spectrum of compound 6

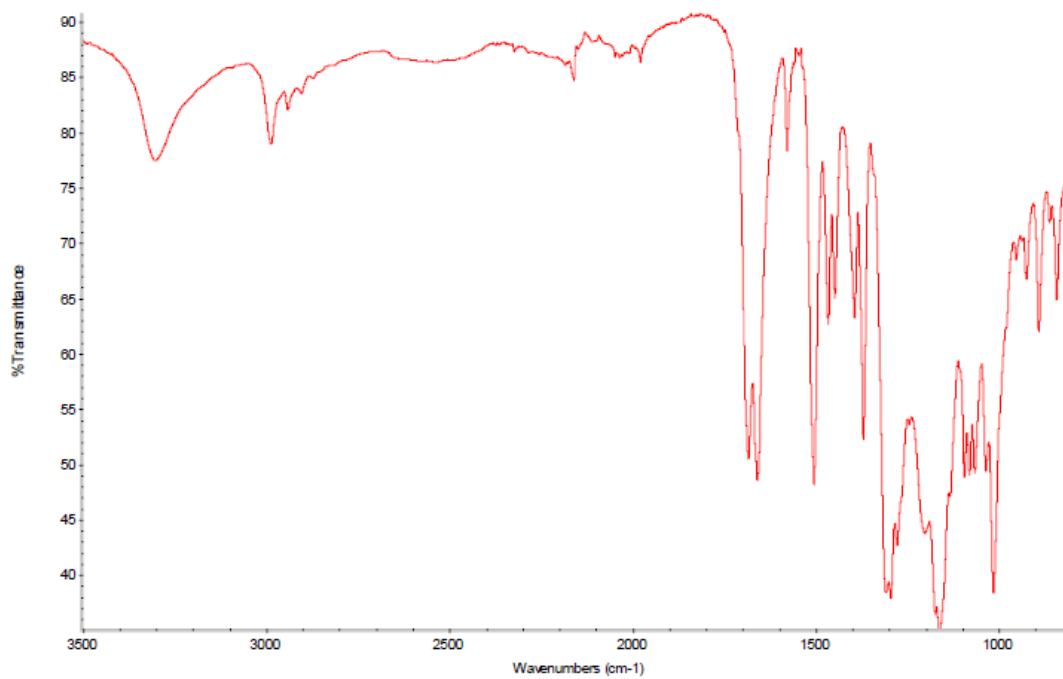


Figure A.21 IR spectrum of compound 6

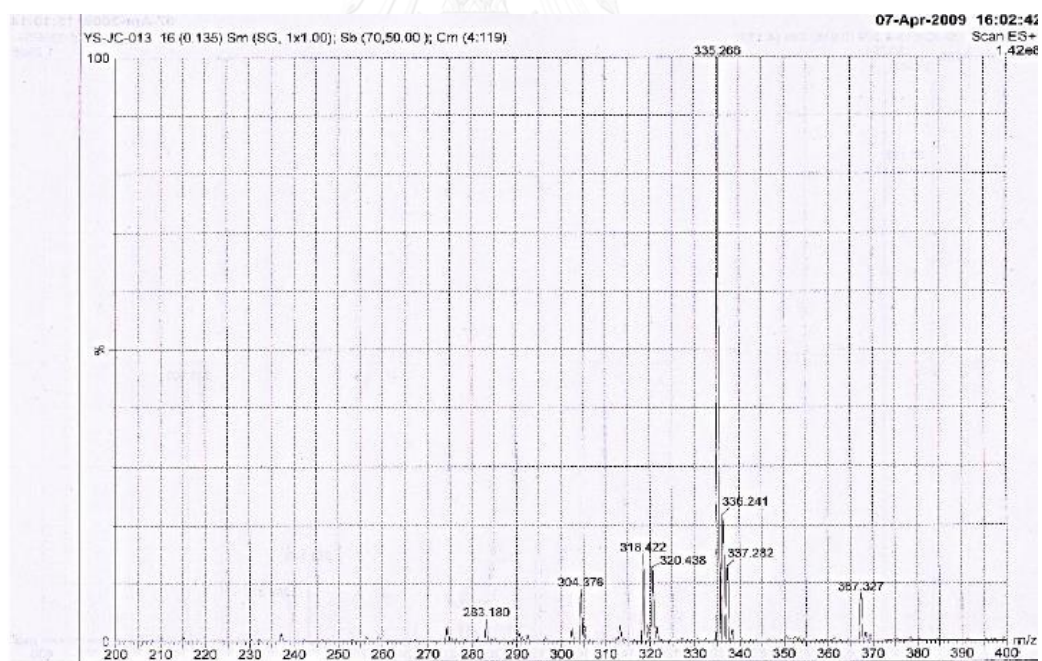


Figure A.22 Mass spectrum of compound 6

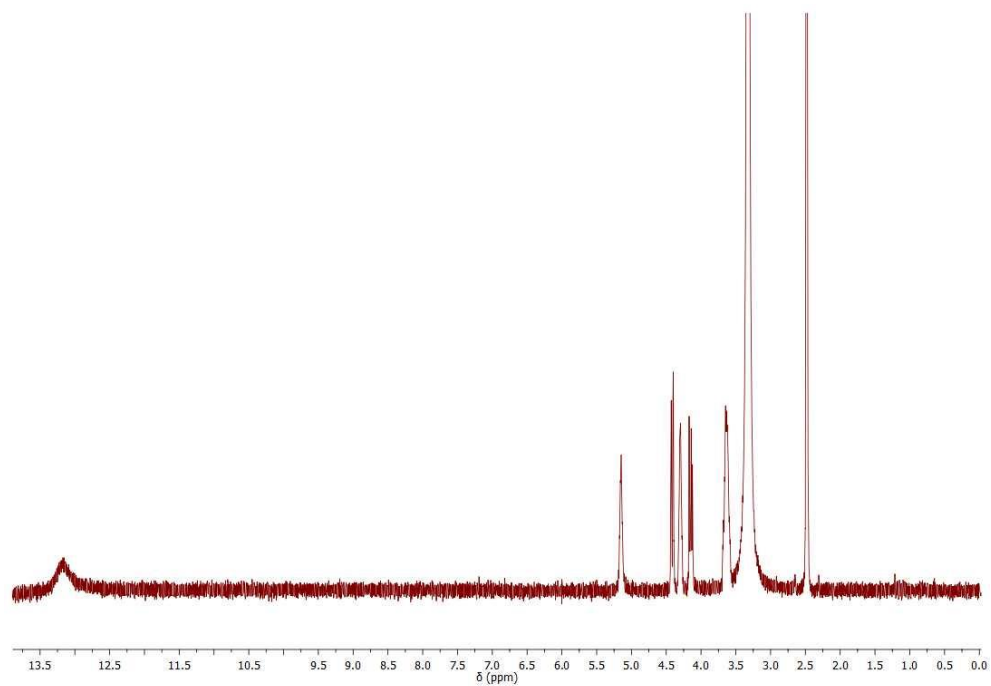


Figure A.23 ^1H NMR ($\text{DMSO-}d_6$) spectrum of compound 7

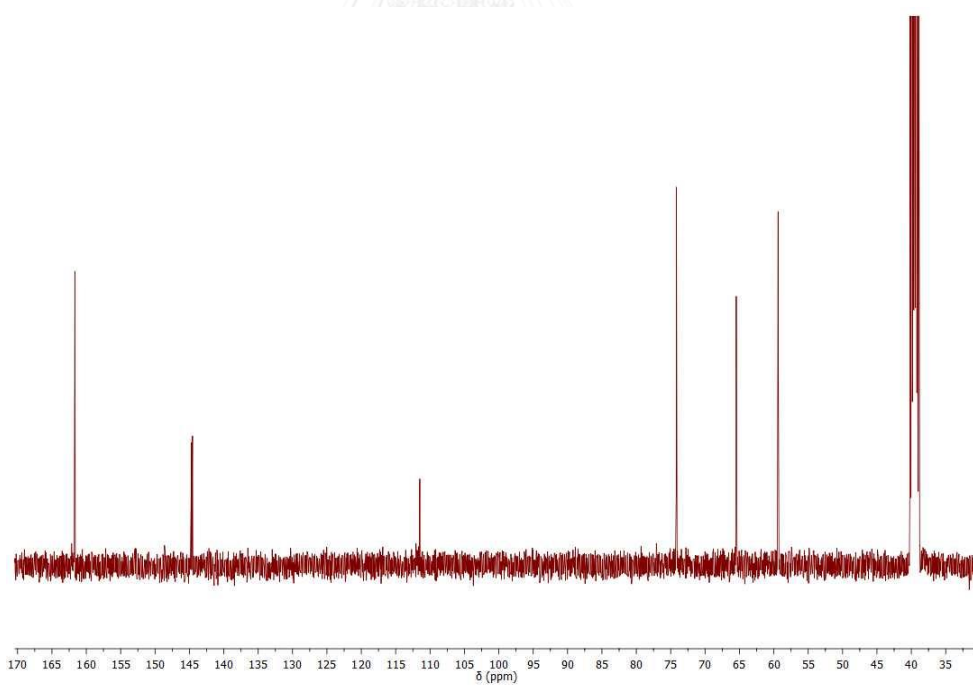


Figure A.24 ^{13}C NMR ($\text{DMSO-}d_6$) spectrum of compound 7

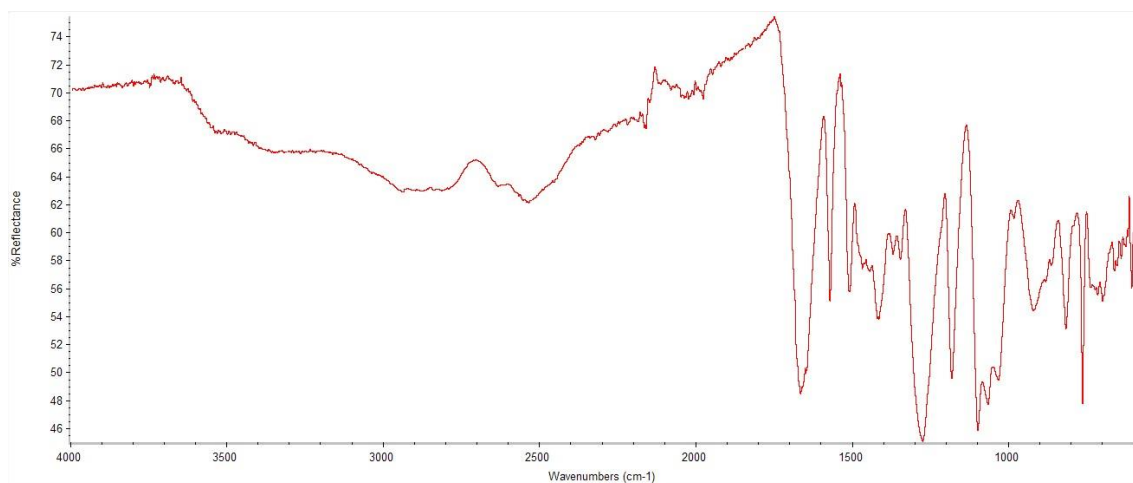


Figure A.25 IR spectrum of compound 7

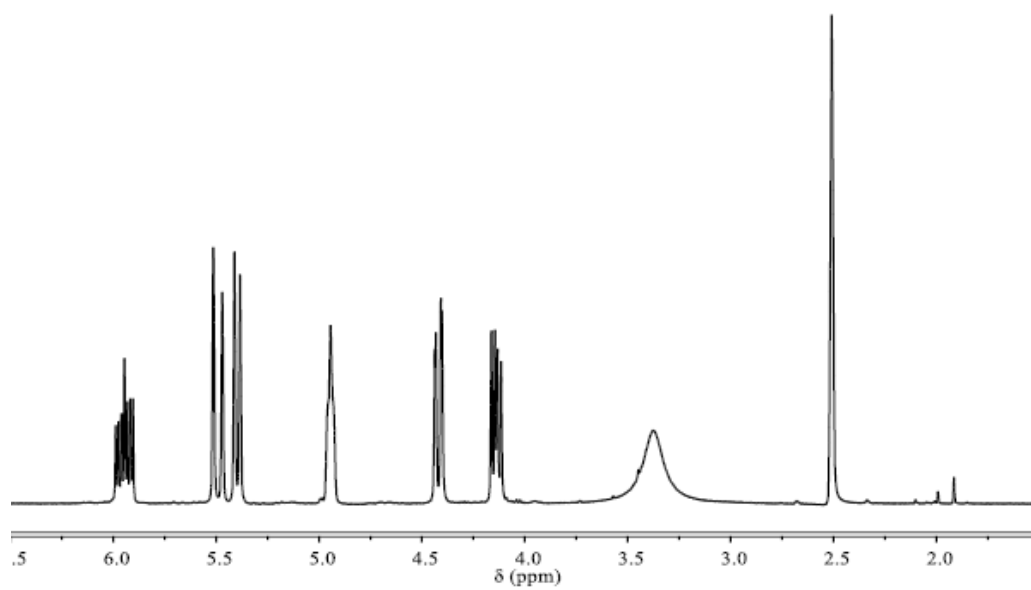


Figure A.26 ¹H NMR (DMSO-*d*₆) spectrum of compound 8

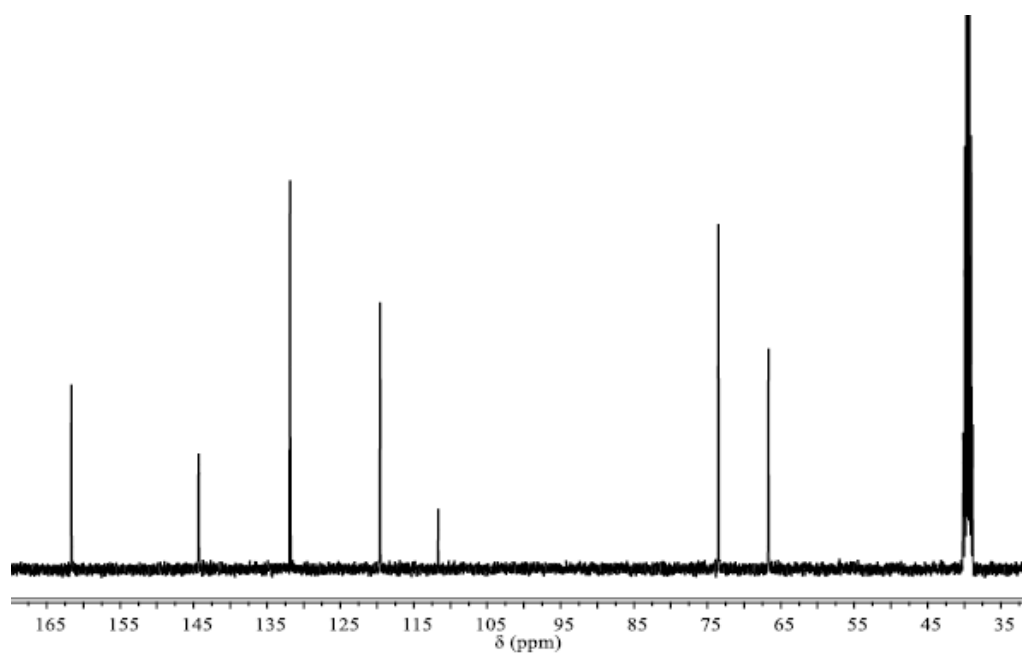


Figure A.27 ^{13}C NMR ($\text{DMSO-}d_6$) spectrum of compound **8**

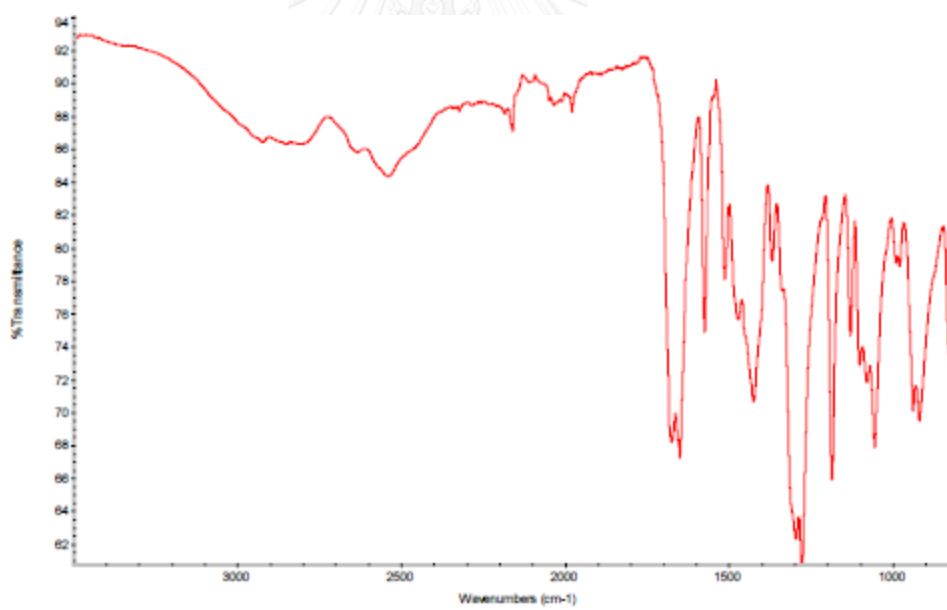


Figure A.28 IR spectrum of compound **8**

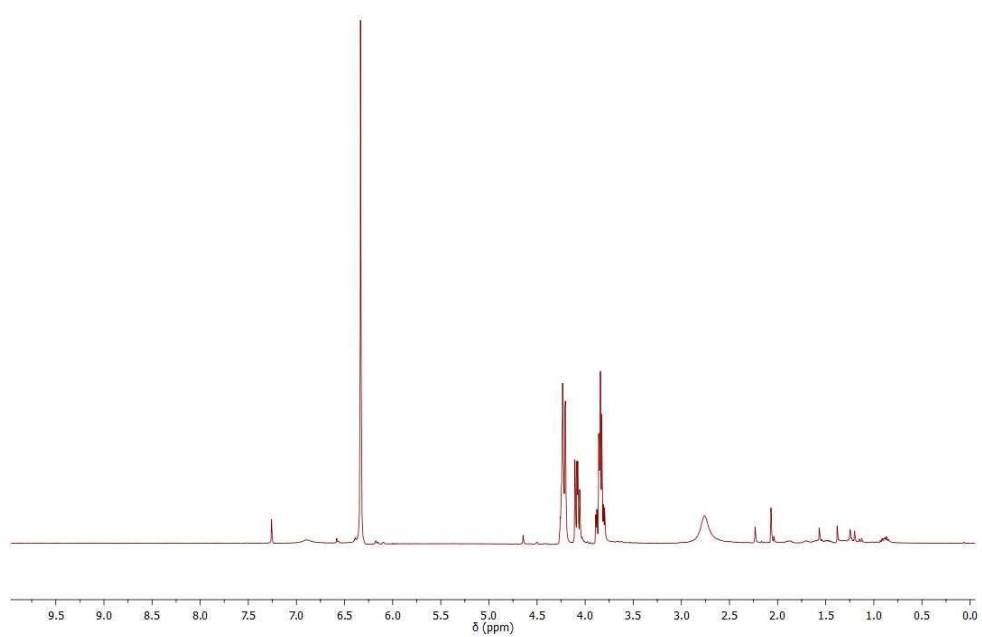


Figure A.29 ^1H NMR (CDCl_3) spectrum of EDTM

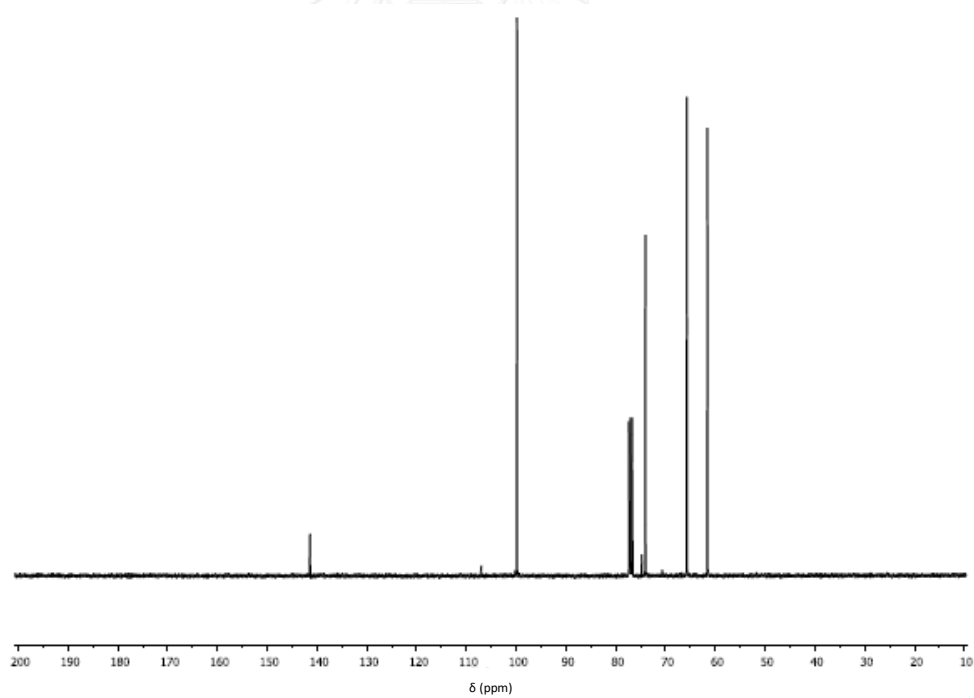


Figure A.30 ^{13}C NMR (CDCl_3) spectrum of EDTM

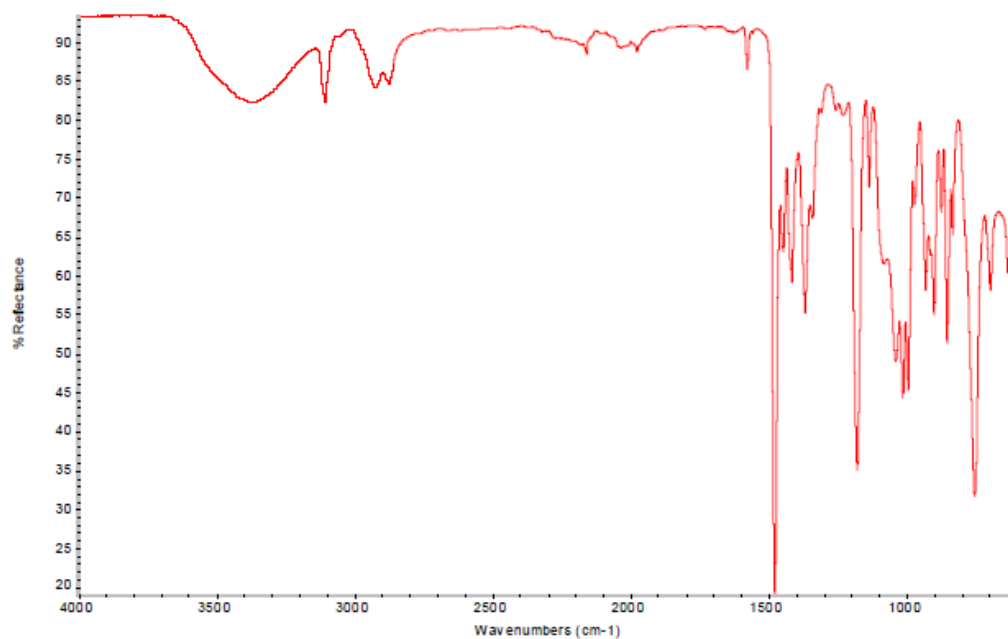


Figure A.31 IR spectrum of EDTM

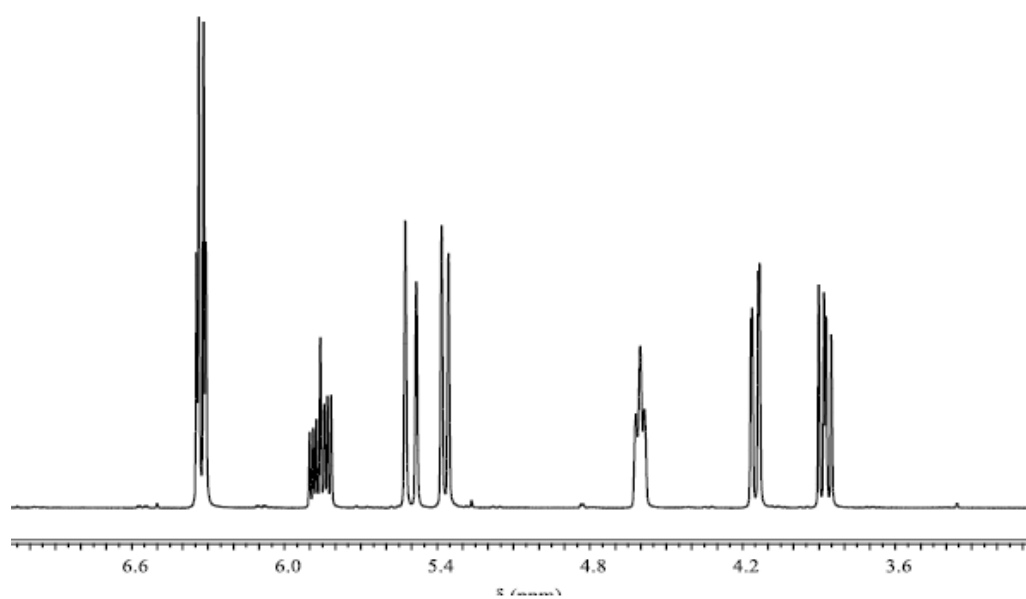


Figure A.32 ¹H NMR (CDCl₃) spectrum of compound 9

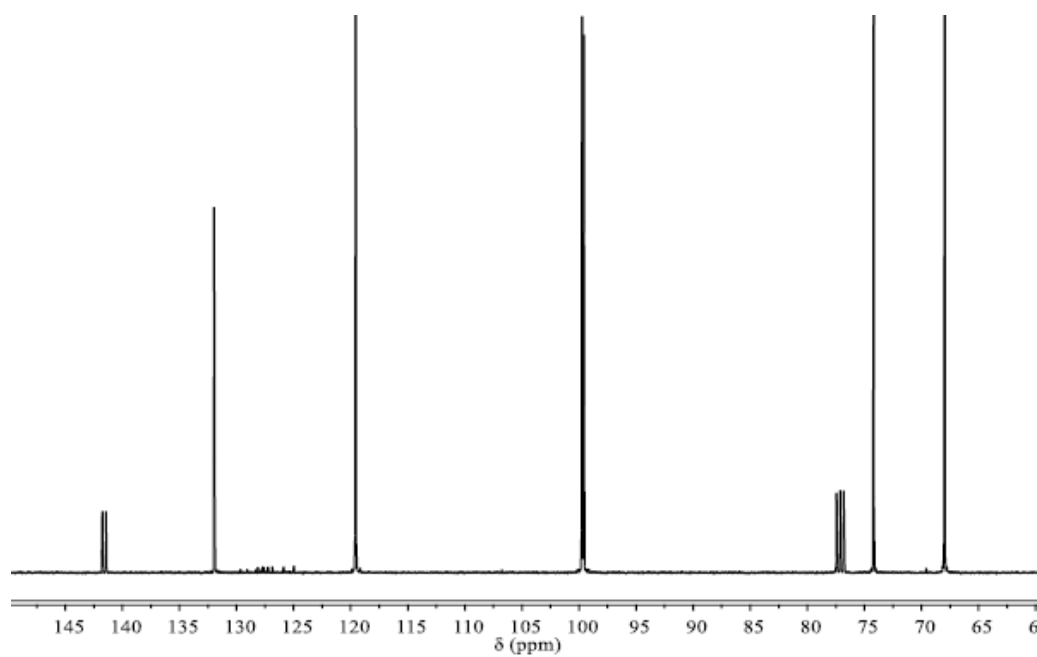


Figure A.33 ^{13}C NMR (CDCl_3) spectrum of compound 9

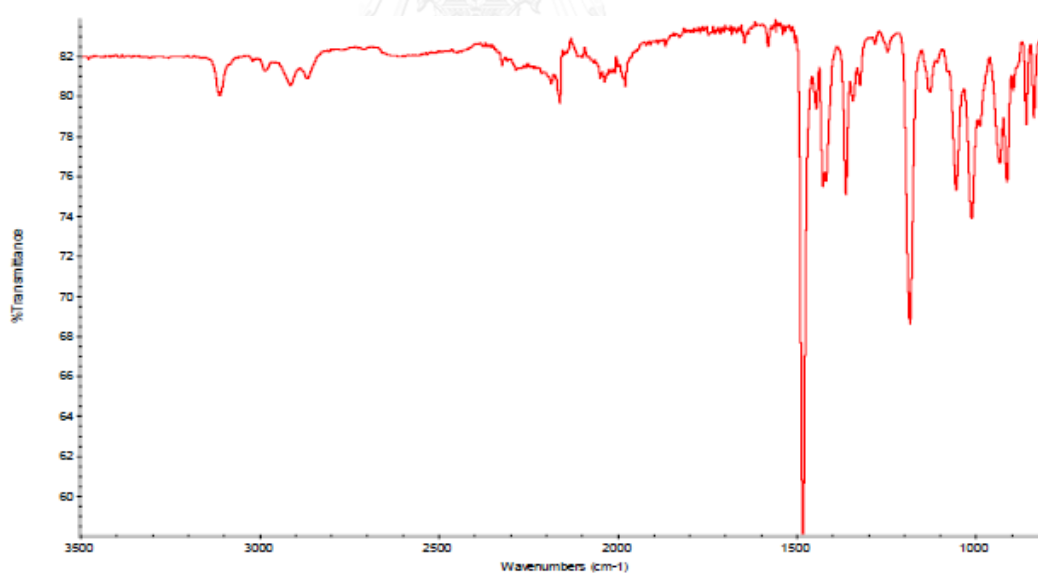


Figure A.34 IR spectrum of compound 9

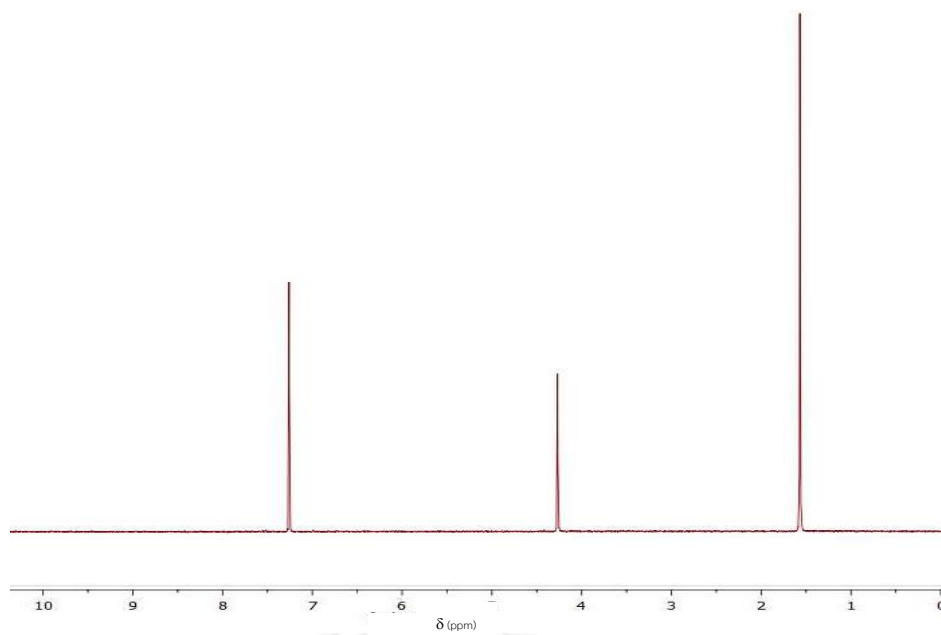


Figure A.35 ^1H NMR (CDCl_3) spectrum of compound **10**

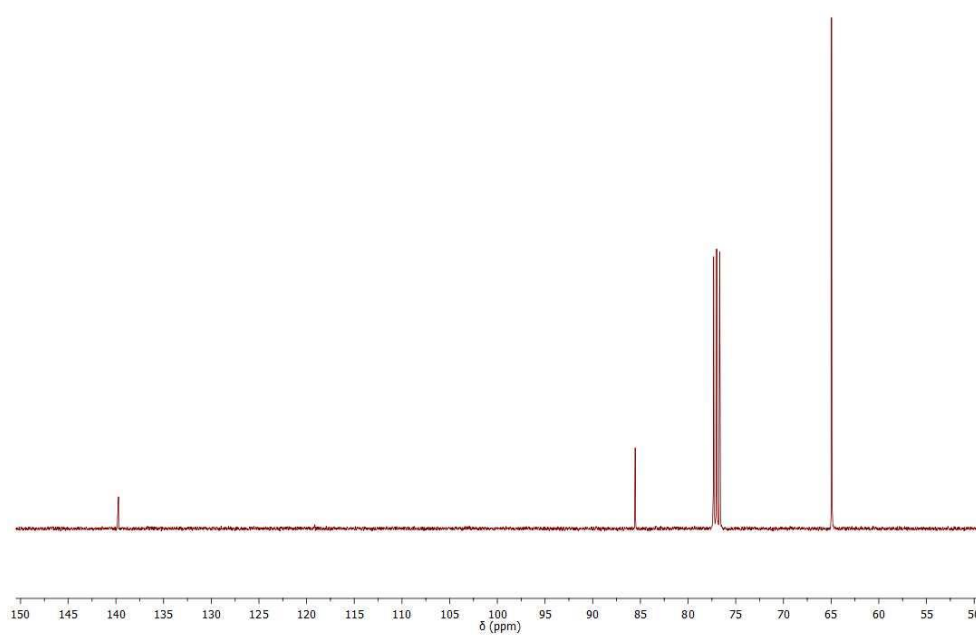


Figure A.36 ^{13}C NMR (CDCl_3) spectrum of compound **10**

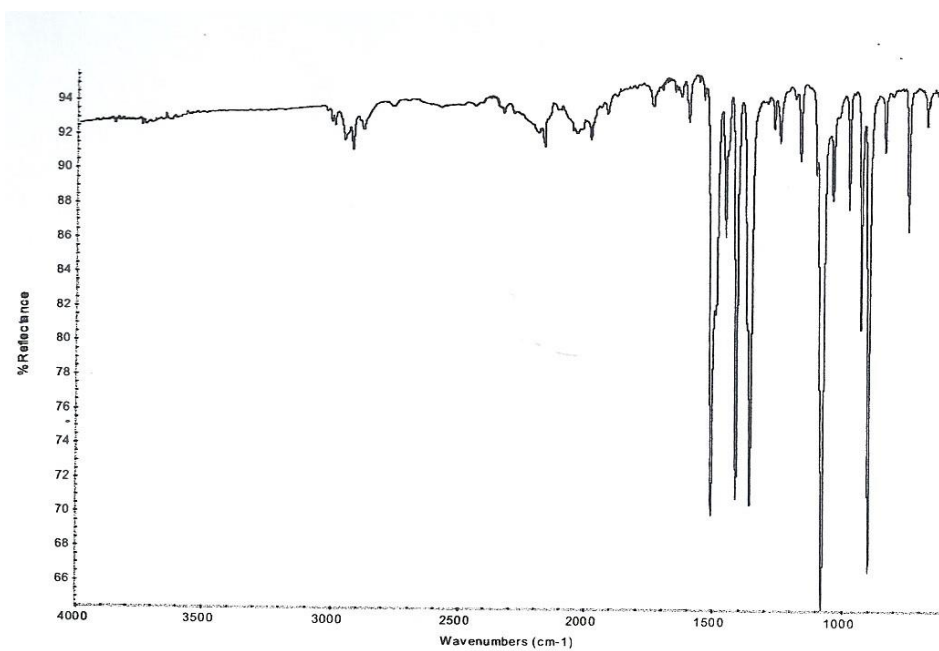


Figure A.37 IR spectrum of compound 10

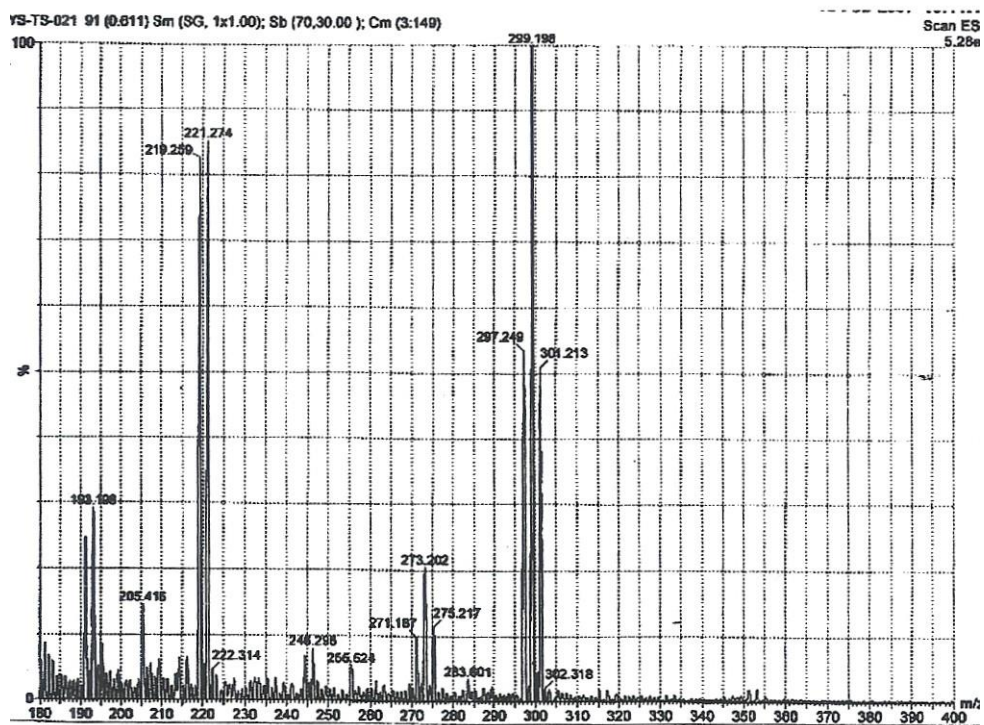


Figure A.38 Mass spectrum of compound 10

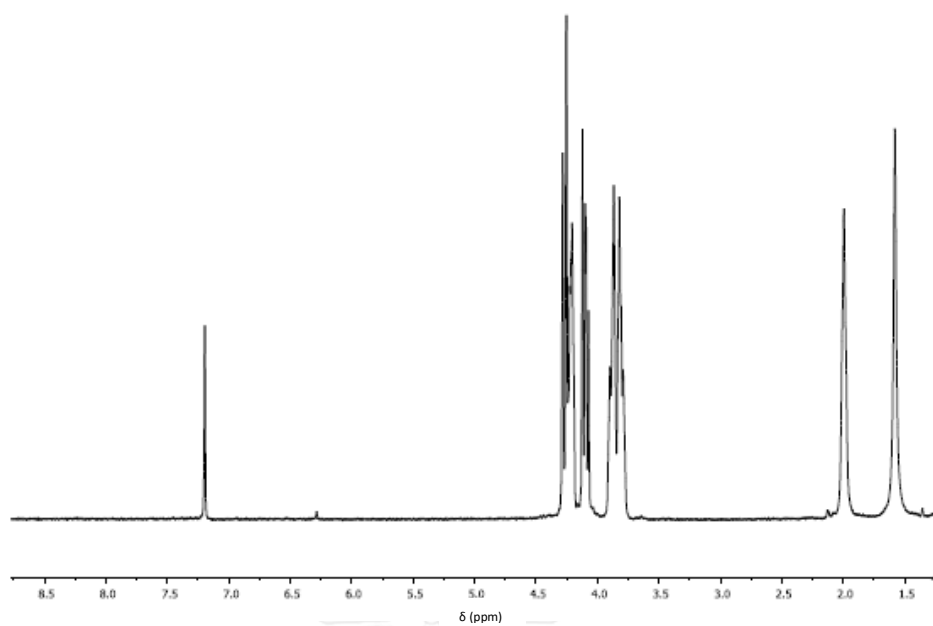


Figure A.39 ^1H NMR (CDCl_3) spectrum of compound 11

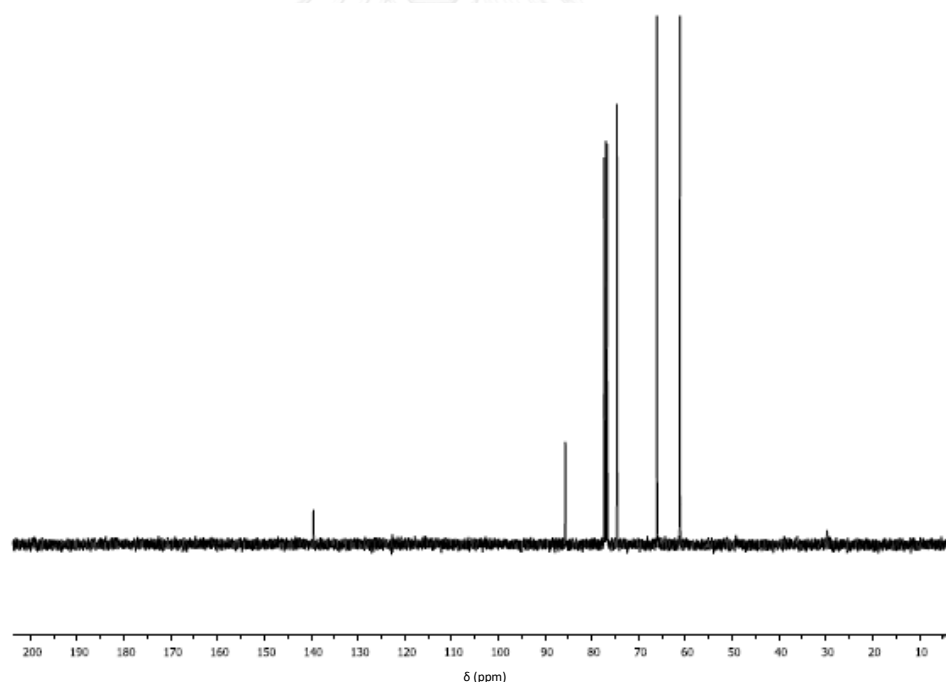


Figure A.40 ^{13}C NMR (CDCl_3) spectrum of compound 11

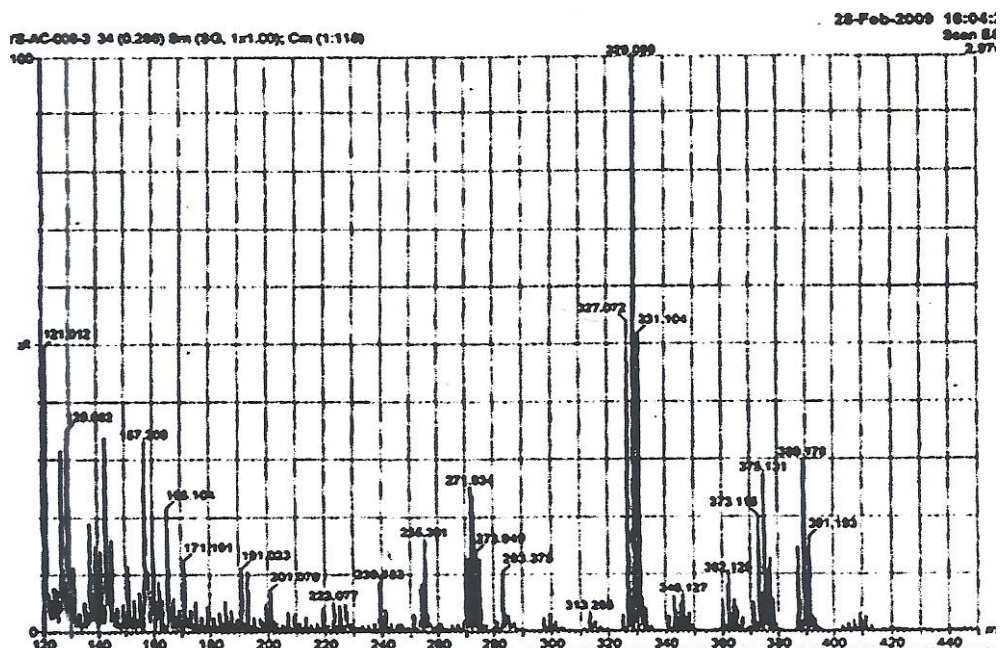


Figure A.41 Mass spectrum of compound 11

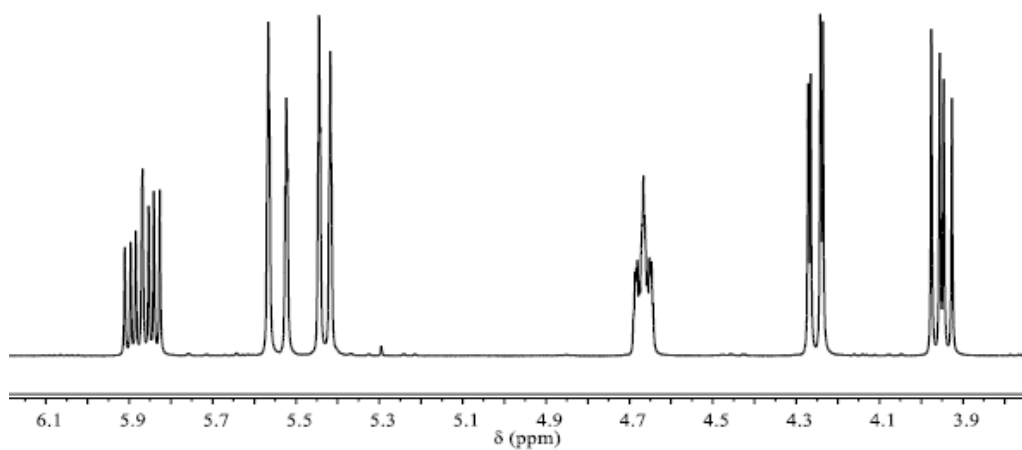


Figure A.42 ^1H NMR (CDCl_3) spectrum of compound 12

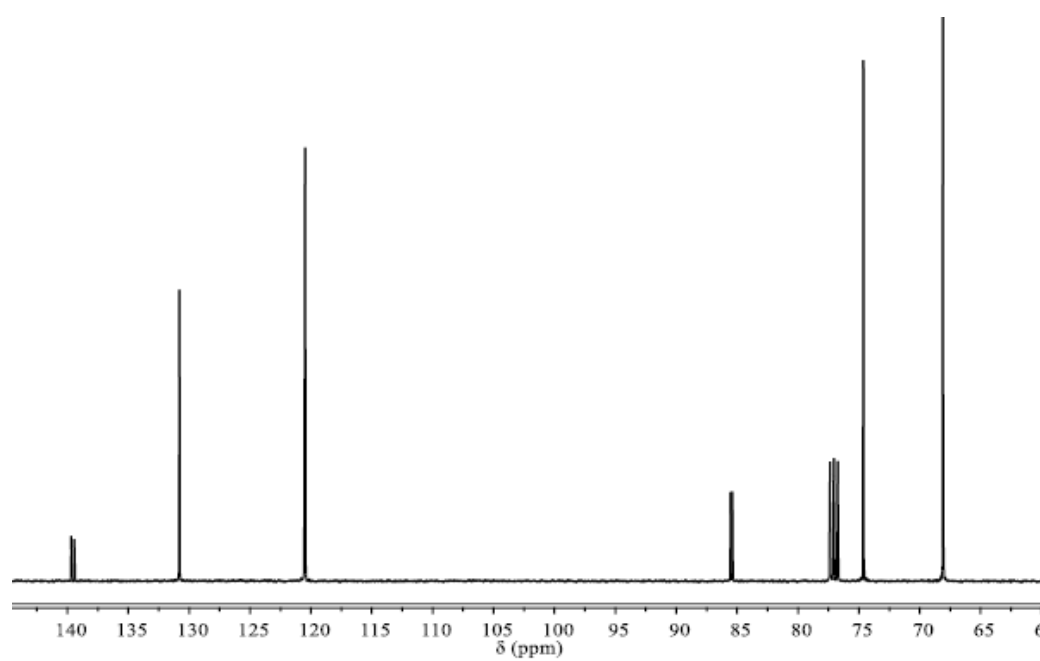


Figure A.43 ^{13}C NMR (CDCl_3) spectrum of compound 12

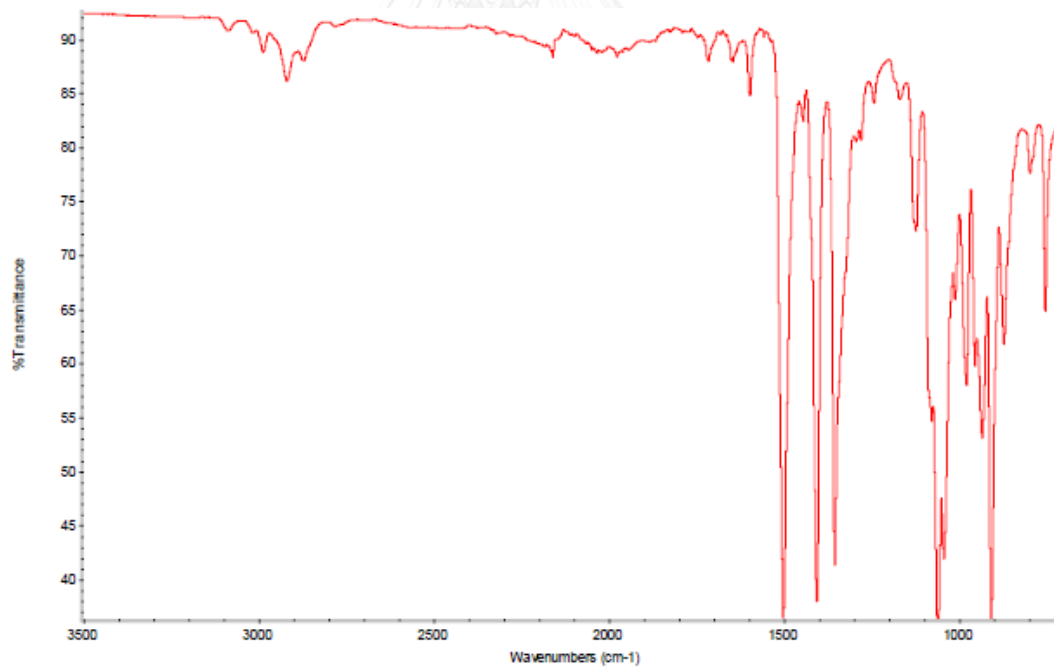


Figure A.44 IR spectrum of compound 12

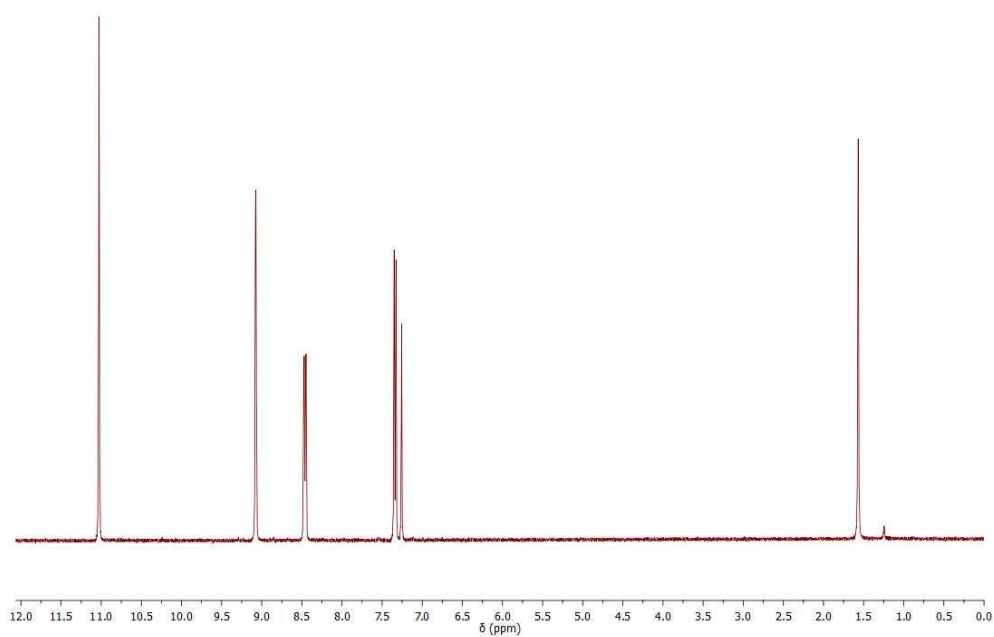


Figure A.45 ^1H NMR (CDCl_3) spectrum of DNP

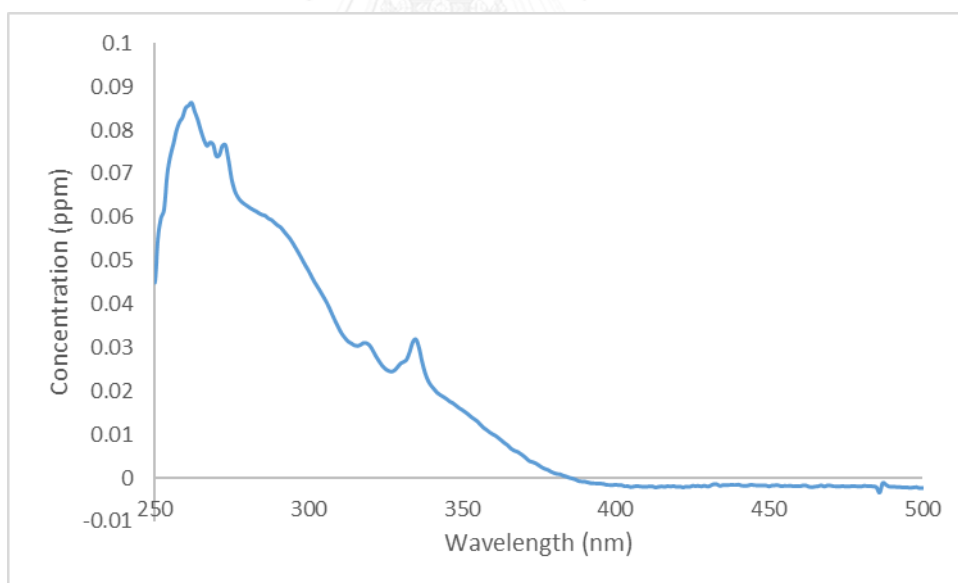


Figure A.46 UV-vis spectrum of DNP ($\lambda_{\text{max}} = 262$ nm)

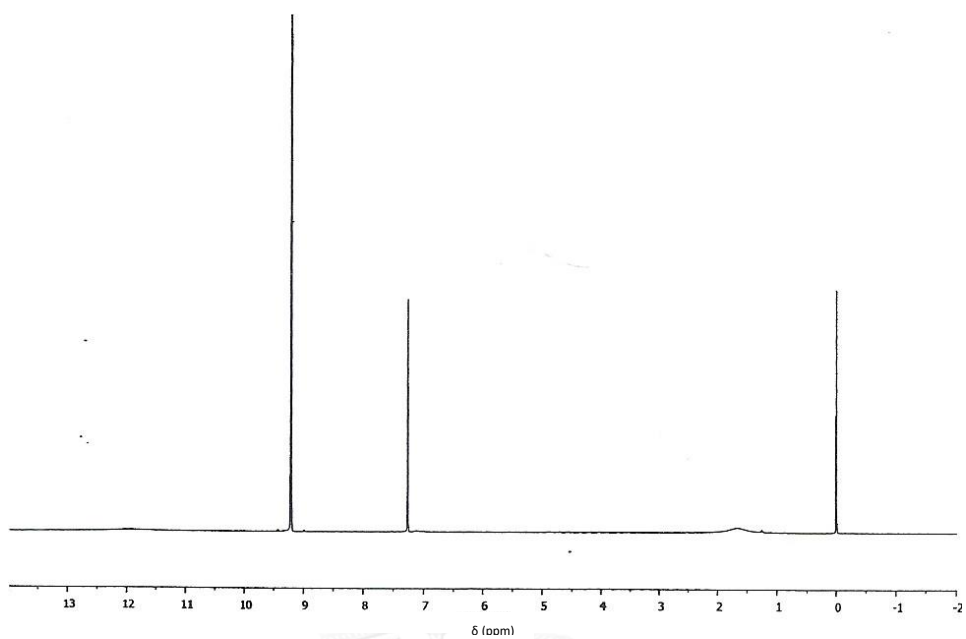


Figure A.47 ^1H NMR (CDCl_3) spectrum of TNP

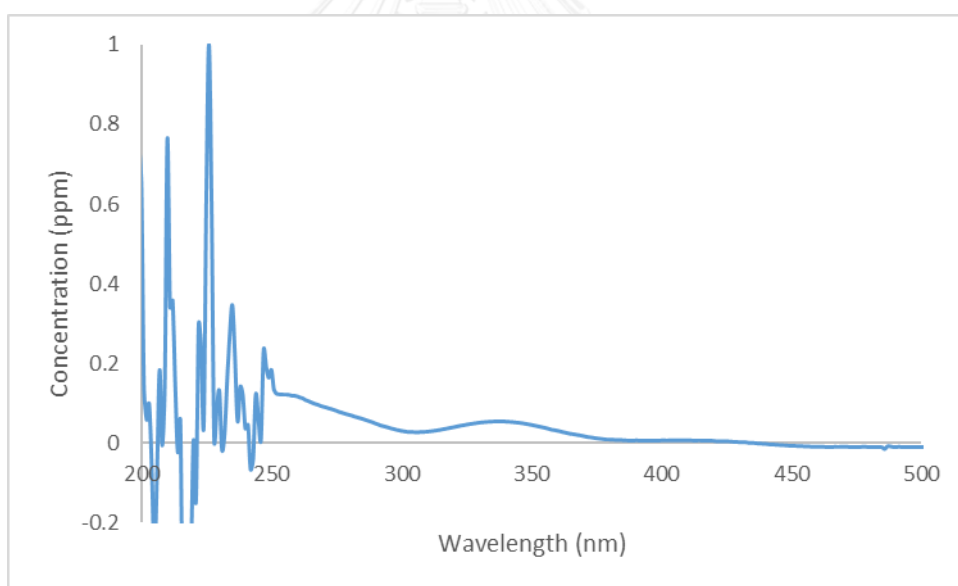


Figure A.48 UV-vis spectrum of TNP ($\lambda_{\text{max}} = 254 \text{ nm}$)

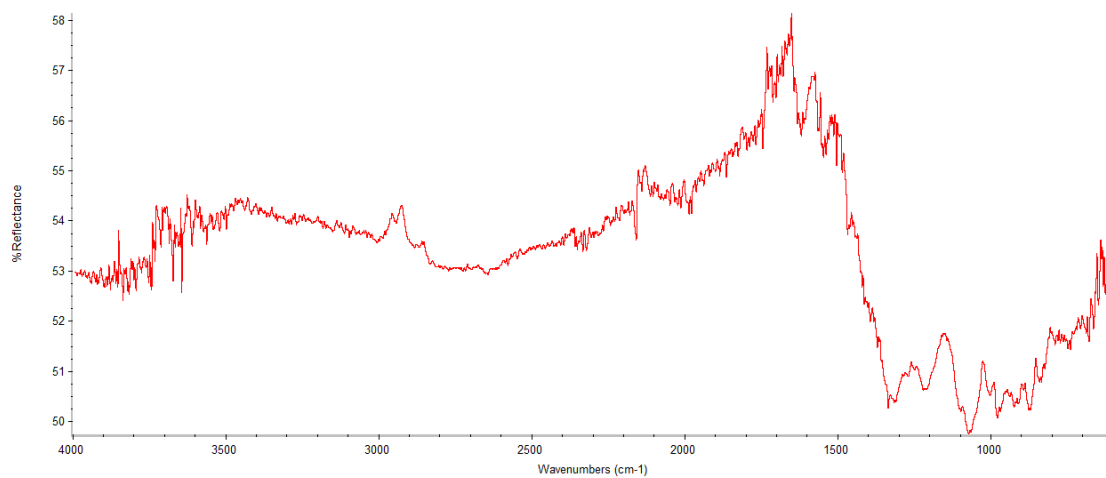


Figure A.49 IR spectrum of PEDOT

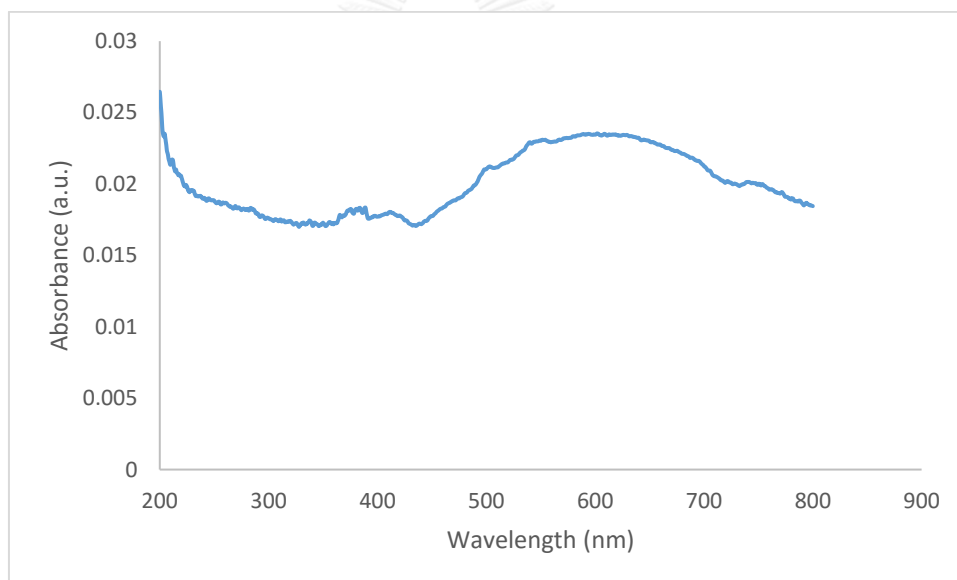


Figure A.50 UV-vis spectrum of PEDOT ($\lambda_{\text{max}} = 602 \text{ nm}$)

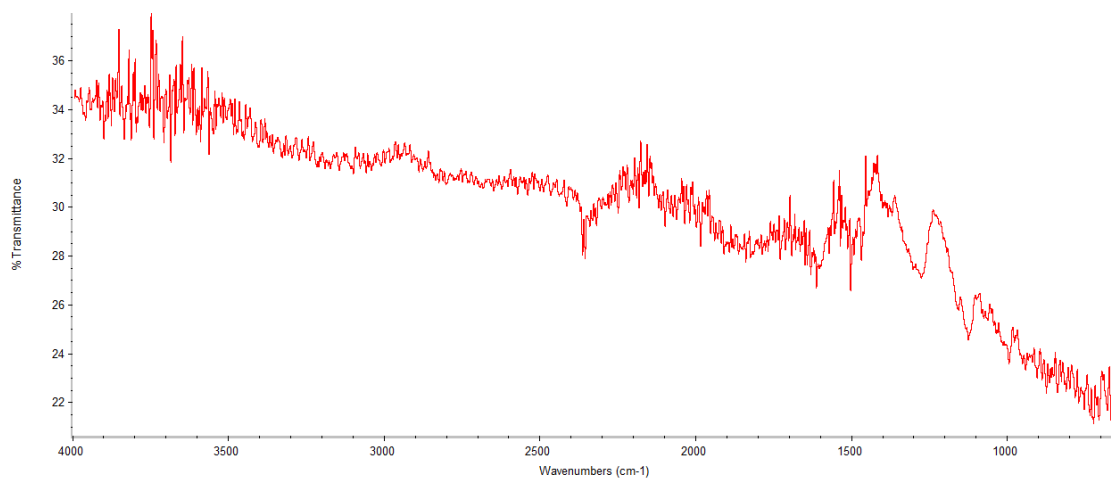


Figure A.51 IR spectrum of PEDTM:PEDOT

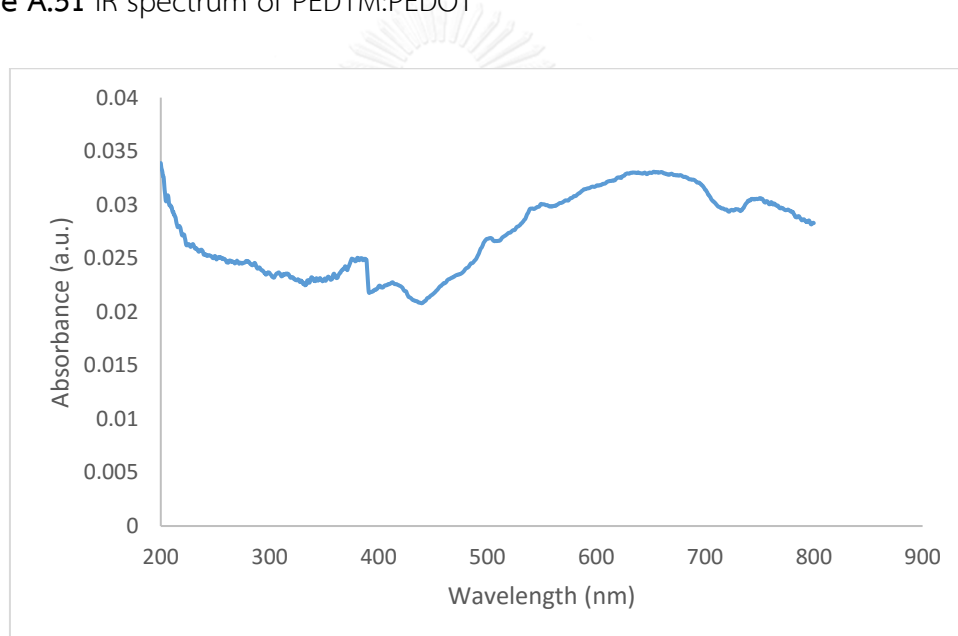


Figure A.52 UV-vis spectrum of PEDTM:PEDOT ($\lambda_{\text{max}} = 680 \text{ nm}$)

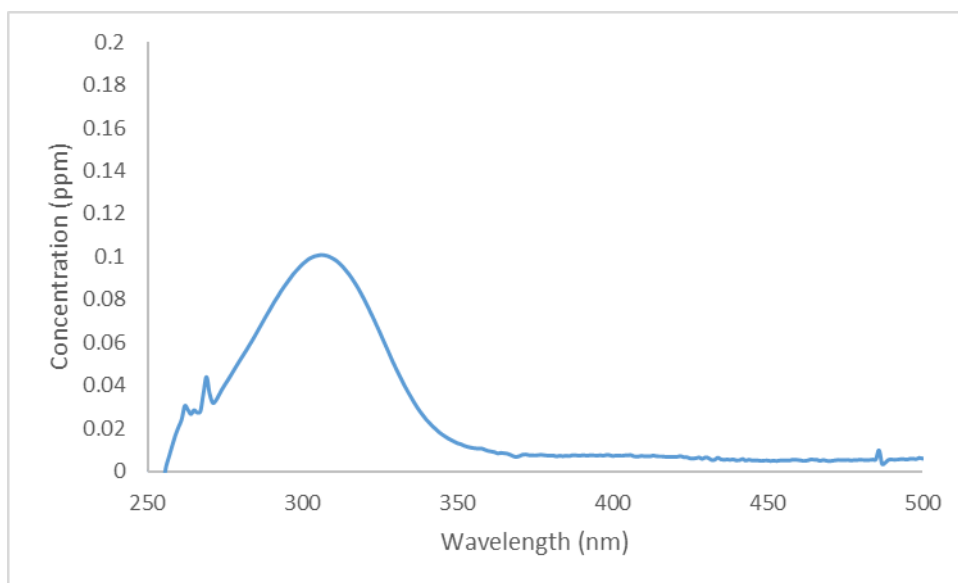


Figure A.53 UV-vis spectrum of PNP ($\lambda_{\text{max}} = 306 \text{ nm}$)

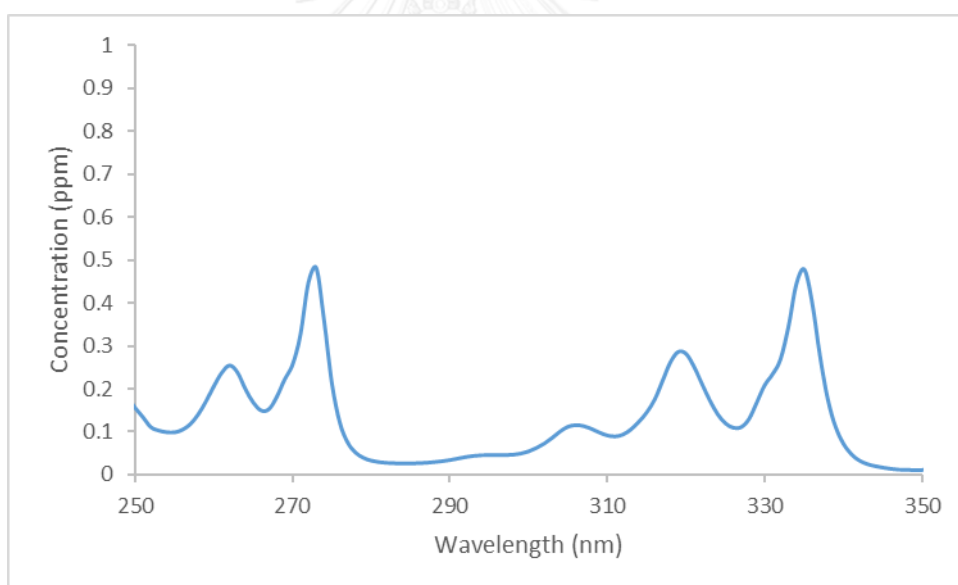


Figure A.54 UV-vis spectrum of pyrene ($\lambda_{\text{max}} = 273 \text{ and } 335 \text{ nm}$)

APPENDIX B

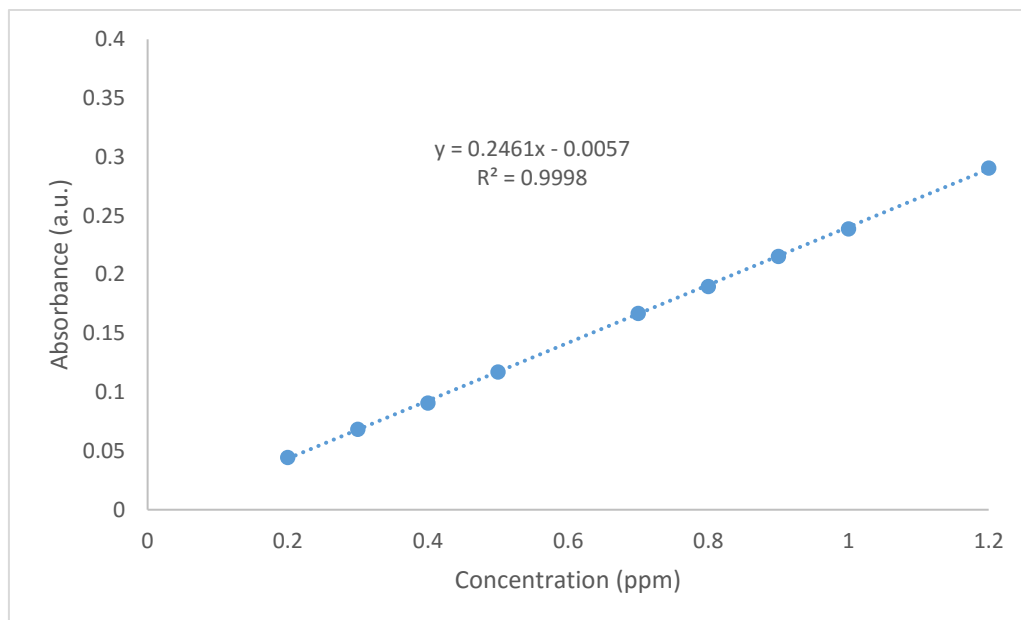


Figure B.1 Calibration curve of pyrene in ethyl acetate ($\lambda_{\max} = 273 \text{ nm}$)

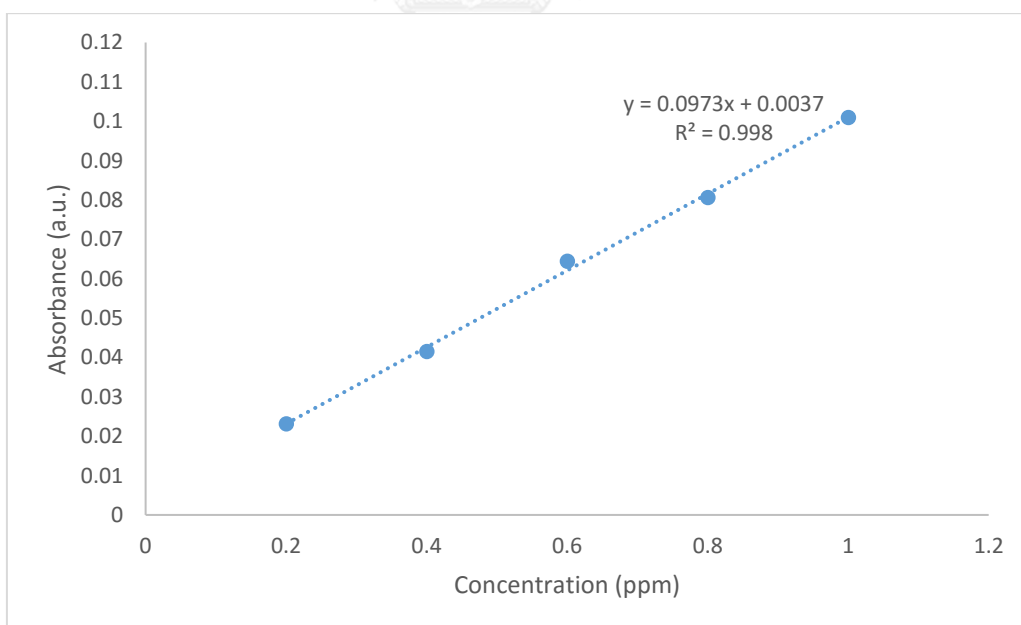


Figure B.2 Calibration curve of PNP in ethyl acetate ($\lambda_{\max} = 306 \text{ nm}$)

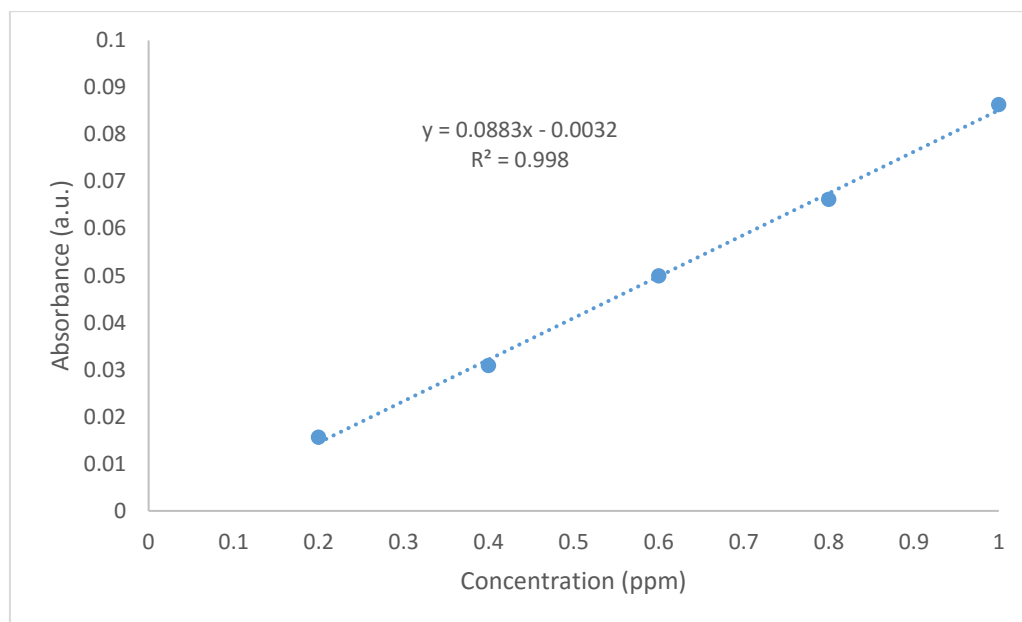


Figure B.3 Calibration curve of DNP in ethyl acetate ($\lambda_{\max} = 262$ nm)

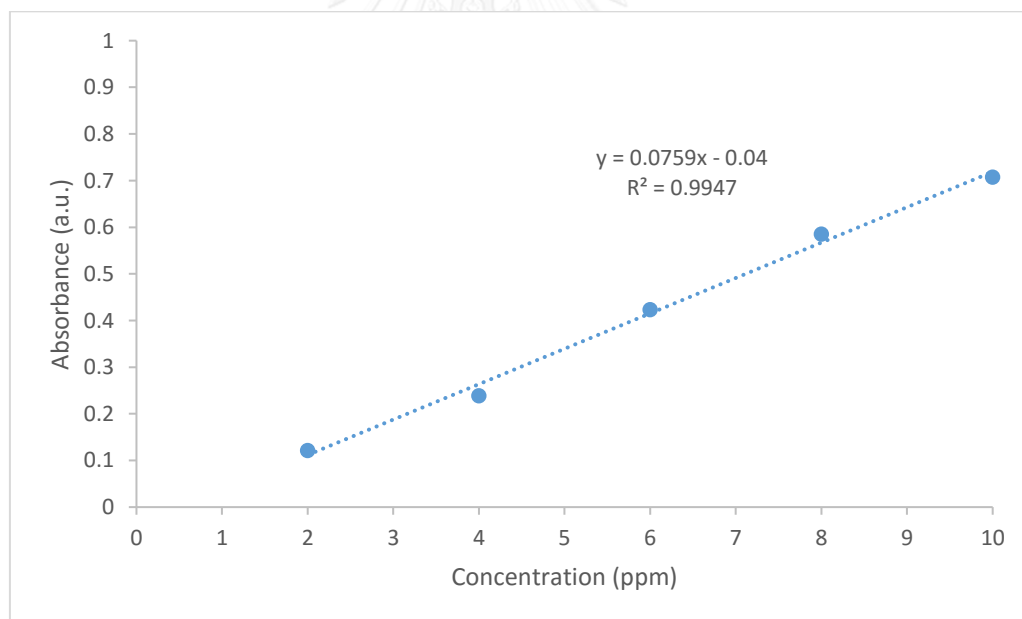


Figure B.4 Calibration curve of TNP in ethyl acetate ($\lambda_{\max} = 254$ nm)

- The calculation of QMIPs, QNIPs and ΔQ values of pyrene-MIPs binding experiment, using EtOAc extraction off the template.

Note: The weight of all dried pyrene-MIPs and NIPs used was 0.161 g.

From **Figure 3.1**, at 2-12 h.

From equation (2);

$$\begin{aligned} Q_{\text{MIPs}} (\mu\text{mol/g}) &= \left(\frac{C_i - C_e}{W \times MW} \right) \times V \\ &= \left(\frac{959.69 - 928.09}{0.161 \times 202.25} \right) \times 25 \\ &= 24.26 \mu\text{mol/g} \end{aligned}$$

From equation (2);

$$\begin{aligned} Q_{\text{NIPs}} (\mu\text{mol/g}) &= \left(\frac{C_i - C_e}{W \times MW} \right) \times V \\ &= \left(\frac{959.69 - 934.58}{0.161 \times 202.25} \right) \times 25 \\ &= 19.27 \mu\text{mol/g} \end{aligned}$$

From equation (1);

$$\begin{aligned} \Delta Q &= Q_{\text{MIPs}} - Q_{\text{NIPs}} \\ &= 24.26 - 19.27 \mu\text{mol/g} \\ &= 7.99 \mu\text{mol/g} \end{aligned}$$

- The calculation of QMIPs, QNIPs and ΔQ values of pyrene-MIPs binding experiment, using MeOH extraction off the template.

Note: The weight of all dried pyrene-MIPs and NIPs used was 0.161 g.

From **Figure 3.2**, at 2-12 h.

From equation (2);

$$\begin{aligned} Q_{\text{MIPs}} (\mu\text{mol/g}) &= \left(\frac{C_i - C_e}{W \times MW} \right) \times V \\ &= \left(\frac{986.50 - 1046}{0.161 \times 202.25} \right) \times 50 \\ &= -91.36 \mu\text{mol/g} \end{aligned}$$

From equation (2);

$$\begin{aligned} Q_{\text{NIPs}} (\mu\text{mol/g}) &= \left(\frac{C_i - C_e}{W \times MW} \right) \times V \\ &= \left(\frac{986.50 - 967.50}{0.161 \times 202.25} \right) \times 50 \\ &= 29.17 \mu\text{mol/g} \end{aligned}$$

From equation (1);

$$\begin{aligned}\Delta Q &= Q_{\text{MIPs}} - Q_{\text{NIPs}} \\ &= (-91.36) - 29.17 \text{ } \mu\text{mol/g} \\ &= -120.53 \text{ } \mu\text{mol/g}\end{aligned}$$

- The calculation of Q_{MIPs} , Q_{NIPs} and ΔQ values of PNP-MIPs binding experiment, using EtOAc extraction off the template.

Note: The weight of all dried PNP-MIPs and NIPs used was 0.125 g.

From **Figure 3.3**, at 2-12 h.

From equation (2);

$$\begin{aligned}Q_{\text{MIPs}} \text{ (}\mu\text{mol/g)} &= \left(\frac{C_i - C_e}{W \times MW} \right) \times V \\ &= \left(\frac{762.89 - 731.46}{0.125 \times 139.11} \right) \times 50 \\ &= 90.41 \text{ } \mu\text{mol/g}\end{aligned}$$

From equation (2);

$$\begin{aligned}Q_{\text{NIPs}} \text{ (}\mu\text{mol/g)} &= \left(\frac{C_i - C_e}{W \times MW} \right) \times V \\ &= \left(\frac{762.89 - 708.31}{0.125 \times 139.11} \right) \times 50 \\ &= 155.27 \text{ } \mu\text{mol/g}\end{aligned}$$

From equation (1);

$$\begin{aligned}\Delta Q &= Q_{\text{MIPs}} - Q_{\text{NIPs}} \\ &= 90.41 - 155.27 \text{ } \mu\text{mol/g} \\ &= -64.86 \text{ } \mu\text{mol/g}\end{aligned}$$

- The calculation of Q_{MIPs} , Q_{NIPs} and ΔQ values of PNP-MIPs binding experiment, using MeOH extraction off the template.

Note: The weight of all dried PNP-MIPs and NIPs used was 0.125 g.

From **Figure 3.4**, at 2-12 h.

From equation (2);

$$\begin{aligned}Q_{\text{MIPs}} \text{ (}\mu\text{mol/g)} &= \left(\frac{C_i - C_e}{W \times MW} \right) \times V \\ &= \left(\frac{822.09 - 709.45}{0.125 \times 139.11} \right) \times 50 \\ &= 323.88 \text{ } \mu\text{mol/g}\end{aligned}$$

From equation (2);

$$\begin{aligned} Q_{\text{NIPs}} (\mu\text{mol/g}) &= \left(\frac{C_i - C_e}{W \times MW} \right) \times V \\ &= \left(\frac{822.09 - 793.18}{0.125 \times 139.11} \right) \times 50 \\ &= 83.14 \mu\text{mol/g} \end{aligned}$$

From equation (1);

$$\begin{aligned} \Delta Q &= Q_{\text{MIPs}} - Q_{\text{NIPs}} \\ &= 323.88 - 83.14 \mu\text{mol/g} \\ &= 240.74 \mu\text{mol/g} \end{aligned}$$

- The calculation of Q_{MIPs} , Q_{NIPs} and ΔQ values of DNP-MIPs binding experiment, using EtOAc extraction off the template.

Note: The weight of all dried DNP-MIPs and NIPs used was 0.103 g.

From **Figure 3.5**, at 2-12 h.

From equation (2);

$$\begin{aligned} Q_{\text{MIPs}} (\mu\text{mol/g}) &= \left(\frac{C_i - C_e}{W \times MW} \right) \times V \\ &= \left(\frac{1065.13 - 927.97}{0.103 \times 184.10} \right) \times 50 \\ &= 361.65 \mu\text{mol/g} \end{aligned}$$

From equation (2);

$$\begin{aligned} Q_{\text{NIPs}} (\mu\text{mol/g}) &= \left(\frac{C_i - C_e}{W \times MW} \right) \times V \\ &= \left(\frac{1065.13 - 915.55}{0.103 \times 184.10} \right) \times 50 \\ &= 394.40 \mu\text{mol/g} \end{aligned}$$

From equation (1);

$$\begin{aligned} \Delta Q &= Q_{\text{MIPs}} - Q_{\text{NIPs}} \\ &= 361.65 - 394.40 \mu\text{mol/g} \\ &= -32.75 \mu\text{mol/g} \end{aligned}$$

- The calculation of Q_{MIPs} , Q_{NIPs} and ΔQ values of DNP-MIPs binding experiment, using MeOH extraction off the template.

Note: The weight of all dried DNP-MIPs and NIPs used was 0.103 g.

From **Figure 3.6**, at 8-12 h.

From equation (2);

$$\begin{aligned} Q_{MIPs} (\mu\text{mol/g}) &= \left(\frac{C_i - C_e}{W \times MW} \right) \times V \\ &= \left(\frac{1029.22 - 810.48}{0.103 \times 184.10} \right) \times 50 \\ &= 576.74 \mu\text{mol/g} \end{aligned}$$

From equation (2);

$$\begin{aligned} Q_{NIPs} (\mu\text{mol/g}) &= \left(\frac{C_i - C_e}{W \times MW} \right) \times V \\ &= \left(\frac{1029.22 - 995.06}{0.103 \times 184.10} \right) \times 50 \\ &= 90.06 \mu\text{mol/g} \end{aligned}$$

From equation (1);

$$\begin{aligned} \Delta Q &= Q_{MIPs} - Q_{NIPs} \\ &= 576.74 - 90.06 \mu\text{mol/g} \\ &= 486.68 \mu\text{mol/g} \end{aligned}$$

- The calculation of Q_{MIPs} , Q_{NIPs} and ΔQ values of TNP-MIPs binding experiment, using MeOH extraction off the template.

Note: The weight of all dried TNP-MIPs and NIPs used was 0.194 g.

From **Figure 3.7**, at 6-12 h.

From equation (2);

$$\begin{aligned} Q_{MIPs} (\mu\text{mol/g}) &= \left(\frac{C_i - C_e}{W \times MW} \right) \times V \\ &= \left(\frac{884.40 - 595.06}{0.194 \times 229.10} \right) \times 50 \\ &= 324.33 \mu\text{mol/g} \end{aligned}$$

From equation (2);

$$\begin{aligned} Q_{NIPs} (\mu\text{mol/g}) &= \left(\frac{C_i - C_e}{W \times MW} \right) \times V \\ &= \left(\frac{884.40 - 652.84}{0.194 \times 229.10} \right) \times 50 \end{aligned}$$

$$= 259.57 \mu\text{mol/g}$$

From equation (1);

$$\begin{aligned}\Delta Q &= Q_{\text{MIPs}} - Q_{\text{NIPs}} \\ &= 324.33 - 259.57 \mu\text{mol/g} \\ &= 64.76 \mu\text{mol/g}\end{aligned}$$

- The calculation of Q_{coMIPs} , Q_{coNIPs} and ΔQ values of PNP-coMIPs (20:80 PEDTM:PEDOT) binding experiment

Note: The weight of all dried pyrene-MIPs and NIPs used was 0.125 g.

From **Figure 3.8**, at 12-15 h.

From equation (2);

$$\begin{aligned}Q_{\text{MIPs}} (\mu\text{mol/g}) &= \left(\frac{C_i - C_e}{W \times MW} \right) \times V \\ &= \left(\frac{797.33 - 644.51}{0.125 \times 139.11} \right) \times 50 \\ &= 439.42 \mu\text{mol/g}\end{aligned}$$

From equation (2);

$$\begin{aligned}Q_{\text{NIPs}} (\mu\text{mol/g}) &= \left(\frac{C_i - C_e}{W \times MW} \right) \times V \\ &= \left(\frac{797.33 - 738.74}{0.125 \times 139.11} \right) \times 50 \\ &= 168.47 \mu\text{mol/g}\end{aligned}$$

From equation (1);

$$\begin{aligned}\Delta Q &= Q_{\text{MIPs}} - Q_{\text{NIPs}} \\ &= 439.42 - 168.47 \mu\text{mol/g} \\ &= 270.95 \mu\text{mol/g}\end{aligned}$$

- The calculation of Q_{coMIPs} , Q_{coNIPs} and ΔQ values of PNP-coMIPs (40:60 PEDTM:PEDOT) binding experiment

Note: The weight of all dried pyrene-MIPs and NIPs used was 0.129 g.

From **Figure 3.8**, at 12-15 h.

From equation (2);

$$\begin{aligned} Q_{\text{MIPs}} (\mu\text{mol/g}) &= \left(\frac{C_i - C_e}{W \times MW} \right) \times V \\ &= \left(\frac{966.18 - 725.33}{0.1259 \times 139.11} \right) \times 50 \\ &= 668.48 \mu\text{mol/g} \end{aligned}$$

From equation (2);

$$\begin{aligned} Q_{\text{NIPs}} (\mu\text{mol/g}) &= \left(\frac{C_i - C_e}{W \times MW} \right) \times V \\ &= \left(\frac{966.18 - 881.86}{0.129 \times 139.11} \right) \times 50 \\ &= 234.04 \mu\text{mol/g} \end{aligned}$$

From equation (1);

$$\begin{aligned} \Delta Q &= Q_{\text{MIPs}} - Q_{\text{NIPs}} \\ &= 668.48 - 234.04 \mu\text{mol/g} \\ &= 234.04 \mu\text{mol/g} \end{aligned}$$

- The calculation of binding capacities of PNP-MIPs, using MeOH extraction off the template.

From **Figure 3.4**;

The initial amount of PNP in ethyl acetate solution used to prepare MIPs before the binding experiment (Q_i) was 822.10 ppm or 2508.12 $\mu\text{mol/g}$.

The amount of PNP in ethyl acetate solution obtained from exhaustive extraction at the end of the binding process (Q_e) was 165.15 ppm or 503.85 $\mu\text{mol/g}$.

$$\begin{aligned} \text{The binding capacities of PNP-MIPs} &= \left(\frac{Q_e}{Q_i}\right) \times 100 \\ &= \left(\frac{503.85}{2508.12}\right) \times 100 \\ &= 20.08\% \end{aligned}$$

The initial amount of PNP in ethyl acetate solution used to prepare NIPs before the binding experiment (Q_i) was 822.10 ppm or 2508.12 $\mu\text{mol/g}$.

The amount of PNP in ethyl acetate solution obtained from exhaustive extraction at the end of the binding process (Q_e) was 161.17 ppm or 491.71 $\mu\text{mol/g}$.

$$\begin{aligned} \text{The binding capacities of PNP-MIPs} &= \left(\frac{Q_e}{Q_i}\right) \times 100 \\ &= \left(\frac{491.71}{2508.12}\right) \times 100 \\ &= 19.60\% \end{aligned}$$

$$\begin{aligned} \Delta \text{ binding capacities} &= 20.08 - 19.60\% \\ &= 0.48\% \end{aligned}$$

- The calculation of binding capacities of DNP-MIPs, using MeOH extraction off the template.

From **Figure 3.6**;

The initial amount of PNP in ethyl acetate solution used to prepare MIPs before the binding experiment (Q_i) was 1029.22 ppm or 2713.80 $\mu\text{mol/g}$.

The amount of PNP in ethyl acetate solution obtained from exhaustive extraction at the end of the binding process (Q_e) was 259.21 ppm or 683.47 $\mu\text{mol/g}$.

$$\begin{aligned} \text{The binding capacities of PNP-MIPs} &= \left(\frac{Q_e}{Q_i}\right) \times 100 \\ &= \left(\frac{683.47}{2713.80}\right) \times 100 \\ &= 25.18\% \end{aligned}$$

The initial amount of PNP in ethyl acetate solution used to prepare NIPs before the binding experiment (Q_i) was 1029.22 ppm or 2713.80 $\mu\text{mol/g}$.

The amount of PNP in ethyl acetate solution obtained from exhaustive extraction at the end of the binding process (Q_e) was 197.41 ppm or 520.52 $\mu\text{mol/g}$.

$$\begin{aligned} \text{The binding capacities of PNP-MIPs} &= \left(\frac{Q_e}{Q_i}\right) \times 100 \\ &= \left(\frac{520.52}{2713.80}\right) \times 100 \\ &= 19.18\% \end{aligned}$$

$$\begin{aligned} \Delta \text{ binding capacities} &= 25.18 - 19.18\% \\ &= 6.00\% \end{aligned}$$

- The calculation of binding capacities of TNP-MIPs, using MeOH extraction off the template.

From **Figure 3.7**;

The initial amount of PNP in ethyl acetate solution used to prepare MIPs before the binding experiment (Q_i) was 884.40 ppm or 991.36 $\mu\text{mol/g}$.

The amount of PNP in ethyl acetate solution obtained from exhaustive extraction at the end of the binding process (Q_e) was 700.46 ppm or 785.17 $\mu\text{mol/g}$.

$$\begin{aligned} \text{The binding capacities of PNP-MIPs} &= \left(\frac{Q_e}{Q_i}\right) \times 100 \\ &= \left(\frac{785.17}{991.36}\right) \times 100 \\ &= 79.20\% \end{aligned}$$

The initial amount of PNP in ethyl acetate solution used to prepare NIPs before the binding experiment (Q_i) was 884.40 ppm or 991.36 $\mu\text{mol/g}$.

The amount of PNP in ethyl acetate solution obtained from exhaustive extraction at the end of the binding process (Q_e) was 653.51 ppm or 732.54 $\mu\text{mol/g}$.

$$\begin{aligned} \text{The binding capacities of PNP-MIPs} &= \left(\frac{Q_e}{Q_i}\right) \times 100 \\ &= \left(\frac{732.54}{991.36}\right) \times 100 \\ &= 73.89\% \end{aligned}$$

$$\begin{aligned} \Delta \text{ binding capacities} &= 79.20 - 73.89\% \\ &= 5.31\% \end{aligned}$$

- The calculation of binding capacities of PNP-coMIPs (20:80 PEDTM:PEDOT)

From **Figure 3.8**;

The initial amount of PNP in ethyl acetate solution used to prepare MIPs before the binding experiment (Q_i) was 797.32 ppm or 2292.66 $\mu\text{mol/g}$.

The amount of PNP in ethyl acetate solution obtained from exhaustive extraction at the end of the binding process (Q_e) was 332.75 ppm or 956.80 $\mu\text{mol/g}$.

$$\begin{aligned} \text{The binding capacities of PNP-MIPs} &= \left(\frac{Q_e}{Q_i} \right) \times 100 \\ &= \left(\frac{956.80}{2292.66} \right) \times 100 \\ &= 41.73\% \end{aligned}$$

The initial amount of PNP in ethyl acetate solution used to prepare NIPs before the binding experiment (Q_i) was 797.32 ppm or 2292.66 $\mu\text{mol/g}$.

The amount of PNP in ethyl acetate solution obtained from exhaustive extraction at the end of the binding process (Q_e) was 249.31 ppm or 716.87 $\mu\text{mol/g}$.

$$\begin{aligned} \text{The binding capacities of PNP-MIPs} &= \left(\frac{Q_e}{Q_i} \right) \times 100 \\ &= \left(\frac{716.87}{2292.66} \right) \times 100 \\ &= 31.26\% \end{aligned}$$

$$\Delta \text{ binding capacities} = 41.73 - 31.26\%$$

$$= 10.47\%$$

- The calculation of binding capacities of PNP-coMIPs (40:60 PEDTM:PEDOT)

From **Figure 3.9**;

The initial amount of PNP in ethyl acetate solution used to prepare MIPs before the binding experiment (Q_i) was 966.18 ppm or 2681.65 $\mu\text{mol/g}$.

The amount of PNP in ethyl acetate solution obtained from exhaustive extraction at the end of the binding process (Q_e) was 318.92 ppm or 885.18 $\mu\text{mol/g}$.

$$\begin{aligned} \text{The binding capacities of PNP-MIPs} &= \left(\frac{Q_e}{Q_i} \right) \times 100 \\ &= \left(\frac{885.18}{2681.65} \right) \times 100 \\ &= 33.80\% \end{aligned}$$

The initial amount of PNP in ethyl acetate solution used to prepare NIPs before the binding experiment (Q_i) was 966.18 ppm or 2681.65 $\mu\text{mol/g}$.

The amount of PNP in ethyl acetate solution obtained from exhaustive extraction at the end of the binding process (Q_e) was 168.10 ppm or 466.58 $\mu\text{mol/g}$.

$$\begin{aligned} \text{The binding capacities of PNP-MIPs} &= \left(\frac{Q_e}{Q_i} \right) \times 100 \\ &= \left(\frac{466.58}{2681.65} \right) \times 100 \\ &= 17.81\% \end{aligned}$$

$$\Delta \text{ binding capacities} = 33.80 - 17.81\%$$

$$= 15.99\%$$

VITA

Miss Phatsaraporn Angkornram was born on December 10th, 1990 in Buriram, Thailand. She received a Bachelor's degree of science from Department of Chemistry, Faculty of Science, Naresuan University, Thailand in 2012. She was admitted to a Master's Degree Program in Chemistry, Faculty of Science, Chulalongkorn University and completed the program in 2015. Her address is 225 Moo 2, Samet sub-district, Meuang Buriram district, Buriram province 31000.



